

University of Montana

ScholarWorks at University of Montana

Graduate Student Theses, Dissertations, &
Professional Papers

Graduate School

2004

Conodont biostratigraphy and facies correlations in an Upper Triassic island arc Keku Strait southeast Alaska

Erik C. Katvala

The University of Montana

Follow this and additional works at: <https://scholarworks.umt.edu/etd>

Let us know how access to this document benefits you.

Recommended Citation

Katvala, Erik C., "Conodont biostratigraphy and facies correlations in an Upper Triassic island arc Keku Strait southeast Alaska" (2004). *Graduate Student Theses, Dissertations, & Professional Papers*. 7063.
<https://scholarworks.umt.edu/etd/7063>

This Thesis is brought to you for free and open access by the Graduate School at ScholarWorks at University of Montana. It has been accepted for inclusion in Graduate Student Theses, Dissertations, & Professional Papers by an authorized administrator of ScholarWorks at University of Montana. For more information, please contact scholarworks@mso.umt.edu.



**Maureen and Mike
MANSFIELD LIBRARY**

The University of
Montana

Permission is granted by the author to reproduce this material in its entirety, provided that this material is used for scholarly purposes and is properly cited in published works and reports.

****Please check "Yes" or "No" and provide signature****

Yes, I grant permission _____

No, I do not grant permission _____

Author's Signature: Maureen Mansfield

Date: May 18, 2004

Any copying for commercial purposes or financial gain may be undertaken only with the author's explicit consent.

**Conodont Biostratigraphy and Facies Correlations in an
Upper Triassic Island Arc, Keku Strait, Southeast Alaska**

by

Erik C. Katvala

B.Sc. University of Calgary, Alberta, Canada, 2000

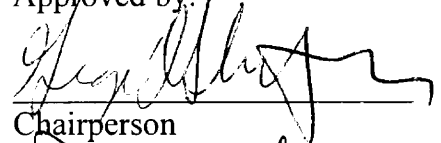
presented in partial fulfillment of the requirements for the degree of

Master of Science

The University of Montana

April 2004

Approved by:



Chairperson



Dean, Graduate School

5-20-04

Date

UMI Number: EP37864

All rights reserved

INFORMATION TO ALL USERS

The quality of this reproduction is dependent upon the quality of the copy submitted.

In the unlikely event that the author did not send a complete manuscript and there are missing pages, these will be noted. Also, if material had to be removed, a note will indicate the deletion.



UMI EP37864

Published by ProQuest LLC (2013). Copyright in the Dissertation held by the Author.

Microform Edition © ProQuest LLC.

All rights reserved. This work is protected against unauthorized copying under Title 17, United States Code



ProQuest LLC.
789 East Eisenhower Parkway
P.O. Box 1346
Ann Arbor, MI 48106 - 1346

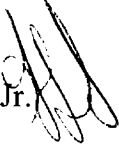
Abstract

Katvala, Erik C. M.S., February 2004

Geology

Conodont Biostratigraphy and Facies Correlations in an Upper Triassic Island Arc, Keku Strait, Southeast Alaska

Director: George D. Stanley, Jr.



Late Triassic rocks in the Keku Strait area of southeast Alaska record a variety of facies in an intra-arc setting. The Hyd Group consists of the Burnt Island Conglomerate, Keku sedimentary strata, Cornwallis Limestone, Hamilton Island Limestone, and the Hound Island Volcanics. The Burnt Island Conglomerate represents initial infill of the basin and underlies the Hamilton Island Limestone, which is coeval to the Cornwallis Limestone and Keku sedimentary strata. Volcanic and sedimentary rock of the Hound Island Volcanics overlie the entire area.

An improved biostratigraphic framework indicates deposition from Early Carnian through Late Norian time. Conodonts originating in the Late Carnian include *Metapolygnathus polygnathiformis*, *Metapolygnathus carpathicus*, *Metapolygnathus nodosus*, *Metapolygnathus* sp. cf. *M. reversus*, *Metapolygnathus* sp. aff. *M. zoeae*, *Metapolygnathus* sp. aff. *M. nodosus*, and *Metapolygnathus primitius*. Early Norian conodonts include *Epigondolella quadrata*, *Epigondolella* sp. aff. *E. quadrata*, *Epigondolella triangularis*, and the longer-ranging *Neogondolella* sp. and *Misikella longidentata*. Middle Norian conodonts include *Epigondolella spiculata*, *Epigondolella* sp. aff. *E. spatulata*, *Epigondolella* sp. aff. *E. transitia*, *Epigondolella* sp. aff. *E. matthewi*, *Epigondolella postera*, and *Neogondolella steinbergensis*. Late Norian conodonts include *Epigondolella bidentata*, *Epigondolella englandi*, *Epigondolella* sp. aff. *E. mosheri*, and *Epigondolella tozeri*.

This study resulted in three major accomplishments. Reworked Paleozoic conodonts in Late Triassic rocks, combined with geologic evidence, suggest major pre-Late Triassic uplift due to compressional tectonics. Late Carnian and Early Norian ages supports the correlation between the Keku sedimentary strata, shallow marine limestone of the Cornwallis Limestone, and deeper water limestone of the Hamilton Island Limestone. Precise conodont biostratigraphy establishes the base of the Hound Island Volcanics as late Early Norian, within the *Epigondolella triangularis* Zone.

Acknowledgements

Financially, I would first like to acknowledge the Robert and Leigh M. Besancon Fellowship and the Bertha Morton Scholarship awarded by the University of Montana, as they covered most of the costs associated with this thesis. George Stanley's National Science Foundation grants covered laboratory and most of the travel expenses associated with this study (EAR-9624501) and assisted with tuition in my final semester (EAR-0229795). In 2001, Mark Nay of the US Forest Service in Corvallis, Oregon granted use of their float house and boat in Kake. I would also like to thank the Department of Geology and the Graduate School, both of the University of Montana, and the Cordilleran Section of the Geological Society of America for travel support to conferences. Finally, I would like to thank the Subcommittee on Triassic Stratigraphy and IGCP project 467 for additional financial support and Tyler Beatty for providing lodging in Vancouver.

I greatly appreciate Robert Blodgett's and George Stanley's initial prompting to take on the Keku Strait field area as my Master's project. Adam Bender was a great field assistant who worked hard despite long hours of daylight. The people of Kake, Alaska, including the mayor Paul Reese, were very friendly and helpful. I specifically would like to thank the Organized Village of Kake, Mike and Edna Jackson, and Lonnie and Ellen Brumfield for their great interest, assistance, and facilities. The Kake Tribal Corporation and the United States Forest Service permitted access to land. Roy Pescador of the Electron Microscopy (EM) Facility, Division of Biological Sciences, University of Montana, provided electron microscopy services and resources. The EM Facility is supported, in part, by grant #RR-16455-01 from the National Center for Research

Resources (Biomedical Research Infrastructure Network program), National Institute of Health. Lori Suskin at the University of Oregon made the thin sections used in this study.

I would like to thank my supervisor, George Stanley, and the other members of my thesis committee, Marc Hendrix, and Eric Edlund, for their support on this project. Steve Sheriff and Marc Hendrix of Geology at the University of Montana also provided invaluable support through conversations of scientific and logistic matters. Mike Orchard, Chris McRoberts, Heinz Kozur, Leo Krystyn, and Norm Silberling provided assistance with the biostratigraphically significant fossil identifications. Mike Orchard in particular assisted me greatly with Late Triassic conodont taxonomy and helped review this thesis. Robert Blodgett, Sid Ash, Mike Sandy of the University of Dayton, and John Utting of the Geological Survey of Canada in Calgary all provided additional interest in examining fossil groups not covered by this project. Jim Mortenson of the Pacific Centre for Isotopic and Geochemical Research at the University of British Columbia provided valuable support with absolute age dates from rocks I collected from the Keku Volcanics. The Kake Medical Center assisted with George Stanley's acute appendicitis when we were in the field. I greatly appreciate Loreene Skeel, Christine Foster, and Brian Collins of the University of Montana for all their help and support. Michael Hofmann provided helpful stratigraphic and publication advice. Rebecca Kunz and Chris Hawkins were great friends throughout the course of my thesis. A further thanks to Andrew Caruthers, Craig Dugas, Robbi McKinney, Adam Bender, and Tim Wheeler for assistance in the paleontology and rock preparation labs at the University of Montana. And, of course, I would like to recognize the other graduate students at the University of Montana for being my peers in the experience and my family for their continued, sincere interest.

This thesis is intended for a Geological Society of America Special Publication based on the session “New Insights from Paleontology, Stratigraphy, and Sedimentology on Accreted Terranes of Western North America”, edited by Robert Blodgett and George Stanley at the Geological Society of America, 99th Annual Cordilleran Section Meeting in Puerto Vallarta, Mexico, April 2003.

Accordingly, the formatting within follows the publication guidelines set forth by the Geological Society of America.

Submitted for publication in June 2004

Table of Contents

Title Page	i
Abstract	ii
Acknowledgements	iii
Submitted for Publication	v
Table of Contents	vi
List of Figures	viii
List of Plates	xi
Introduction	1
Lithostratigraphy and Paleontology	14
Paleozoic Units	15
Triassic Units	
Burnt Island Conglomerate	17
Keku sedimentary strata	20
Cornwallis Limestone	27
Unnamed shallow water limestone	40
Hamilton Island Limestone	43
Hound Island Volcanics	52
Biostratigraphy	63
Middle Triassic	66
Early Carnian	67
Late Carnian	67
Late Carnian or Early Norian	70

Early Norian72
Middle Norian75
Late Norian76
Discussion	
Pre-Late Triassic Uplift77
Hyd Group Deposition79
Conclusions88
Taxonomic Notes90
References110
Appendix A: Table of Localities118
Appendix B: Biostratigraphic Fossil Occurrences121
Appendix C: Methods	
Field Work125
Laboratory Work126
Appendix D: Future Work128
Conodont Plates132

List of Figures and Tables

Figure 1.	Map of North America with position of Alexander and Wrangellia terranes . . .	2
Figure 2.	Map of southeast Alaska with Keku Strait area	3
Figure 3.	Map of Keku Strait area with generalized geologic units	5
Figure 4.	Generalized stratigraphic column of the Hyd Group	7
Figure 5.	Map of Keku Strait area with distributions of Paleozoic and Triassic outcrop, visited localities and areas of reference for Triassic rocks	10
Figure 6.	Larger scale maps of reference map areas in Figure 5 with Triassic units and visited localities	11-13
Figure 7.	Photograph of Burnt Island Conglomerate	18
Figure 8.	Photographs of Pybus clasts in the Burnt Island Conglomerate	19
Figure 9.	Stratigraphic section from southern Big Spruce Island	22
Figure 10.	Photograph of lithoclastic beds on Big Spruce Island	23
Figure 11.	Photograph of sedimentary scours on Big Spruce Island	23
Figure 12.	Photograph of Carboniferous limestone clast in sandstone beds on Big Spruce Island	24
Figure 13.	Photograph of neptunian dikes in the Keku sedimentary strata	24
Figure 14.	Photograph of fossils in a neptunian dike	26
Figure 15.	Photograph of reworked Permian brachiopod	26
Figure 16.	Photograph of massive, fossiliferous limestone from Big Spruce Island . . .	28
Figure 17.	Photograph of lithoclastic limestone from the eastern side of Kuiu Island .	28
Figure 18.	Photograph of ooids in thin section	29

Figure 19. Photograph of cross-bedded lithoclastic limestone from eastern side of Kuiu Island	31
Figure 20. Photograph of Flounder C�ve succession	31
Figure 21. Stratigraphic section from the Flounder Cove locality	32
Figure 22. Photograph of oncoidal limestone from the Flounder Cove locality	33
Figure 23. Photographs of shallow water fossils from the Cornwallis Limestone	35
Figure 24. Photographs of plant material from the Cornwallis Limestone	36
Figure 25. Photographs of vertebrate material from the Cornwallis Limestone	36
Figure 26. Photographs of microfossils from the Cornwallis Limestone	38-39
Figure 27. Photographs of lithoclastic limestone from Cape Bendel region	41
Figure 28. Photographs of oyster and lithoclastic limestone from Portage Pass	42
Figure 29. Stratigraphic section from northeast Hamilton Island	44
Figure 30. Photograph of slump fold on northeast Hamilton Island	45
Figure 31. Photograph of debris flow conglomerate from northeast Hamilton Island	45
Figure 32. Photograph of <i>Halobia</i> from Hamilton Island Limestone	47
Figure 33. Photograph of silicified branch from northeast Hamilton Island	49
Figure 34. Photograph of silicified <i>Halobia</i> from Portage Pass	49
Figure 35. Photographs of microfossils from the Hamilton Island Limestone	50-51
Figure 36. Photograph of debris flow breccia from western Hamilton Island	53
Figure 37. Photograph of pahoehoe from Cape Bendel region	53
Figure 38. Photograph of limestone draping pillow basalt from Hamilton Bay	54
Figure 39. Photograph of lensoid limestone from western Hound Island	54
Figure 40. Photograph of succession on eastern Hound Island	56

Figure 41. Photographs of trace fossils in sandstone from western Hound Island	57
Figure 42. Photograph of silicified fossil bed from Gil Harbor mudflat	59
Figure 43. Photographs of microfossils from the Hound Island Volcanics	60-61
Figure 44. Chart of Late Triassic biochronology with index fossils	64
Figure 45. Photograph of thrust fault in northern Keku Islets and corresponding map . .	82
Figure 46. Chronostratigraphic cross-section across northern part of study area	85
Figure 47. Chronostratigraphic cross-section across southern part of study area	86
Figure 48. Block diagram of Carnian to Early Norian facies correlations	87
Table 1. Table of Triassic macrofossils found in the Hyd Group	16

List of Plates

- Plate 1. Scanning Electron Microscope photographs of *Belodella triangularis*, *Panderodus* sp., *Polygnathus linguiformis*, *Palmatolepis* sp., *Polygnathus* sp., Pb elements, *Sweetognathus?* sp., and *Mesogondolella* sp.132
- Plate 2. Scanning Electron Microscope photographs of *Metapolygnathus polygnathiformis*, juvenile *Metapolygnathus* sp., juvenile *Metapolygnathus* sp. cf. *M. nodosus*, *Metapolygnathus carpathicus*, *Metapolygnathus* sp. cf. *M. reversus*, *Metapolygnathus nodosus*, *Metapolygnathus* sp. aff. *M. zoeae*, and *Metapolygnathus* sp. aff. *M. nodosus*134
- Plate 3. Scanning Electron Microscope photographs of *Metapolygnathus* sp. cf. *M. primitius*, *Metapolygnathus primitius*, *Neogondolella* sp., *Epigondolella quadrata*, and *Epigondolella* sp. aff. *E. quadrata*137
- Plate 4. Scanning Electron Microscope photographs of *Epigondolella* sp. aff. *E. quadrata*, *Epigondolella triangularis uniformis*, *Epigondolella triangularis triangularis*, juvenile *Epigondolella* sp., *Misikella longidentata*, *Epigondolella* sp. aff. *E. transitia*, and *Epigondolella* sp. aff. *E. spatulata*139
- Plate 5. Scanning Electron Microscope photographs of *Epigondolella spiculata*, subadult *Epigondolella* sp., *Epigondolella* sp. aff. *E. matthewi*, *Epigondolella* sp. cf. *E. postera*, *Neogondolella* sp. cf. *N. steinbergensis*, *Neogondoella* sp., juvenile *Neogondoella* sp., *Epigondolella bidentata*, *Epigondolella tozeri*, *Epigondolella englandi*, *Epigondolella* sp. aff. *E. mosheri*, and juvenile *Epigondolella* sp.141

Introduction

Alaska and the North American Cordillera are predominantly composed of allochthonous tectonostratigraphic terranes that accreted to the continental margin during the Mesozoic and Cenozoic (Coney *et al.*, 1980; Jones *et al.*, 1983). While a unique internal stratigraphy defines tectonostratigraphic terranes, tectonic processes shape them geographically, structurally, and depositionally (Coney *et al.*, 1980; Saleeby, 1983). The tectonic fragment known as the Alexander terrane encompasses most of southeast Alaska, as well as parts of western British Columbia, southwestern Yukon, and eastern Alaska (**Figure 1**) (Berg *et al.*, 1972; Jones *et al.*, 1972; Gehrels and Saleeby, 1987). The Alexander terrane is a displaced continental fragment that was a separate tectonic entity throughout much of the Phanerozoic (Wilson, 1968; Monger and Ross, 1971; Jones *et al.*, 1972; Monger *et al.*, 1972). Its distinctive foundation of late Proterozoic (Gehrels, 1990) and early Paleozoic continental crust sets it apart from neighboring terranes (Berg *et al.*, 1972; Jones *et al.*, 1972). Unlike other terranes, rock of every Phanerozoic period occurs in the Alexander terrane, providing a long geologic record for interpretation (Gehrels and Saleeby, 1987).

In the center of southeast Alaska, Keku Strait lies between Kuiu and Kupreanof islands (**Figure 2**). Tidal activity exposes bedrock along most shorelines, and shorelines are abundant on the many smaller islands in the strait. Outcrop along shorelines is readily accessible by boat, while newer roads permit access to the less exposed inland outcrop on both Kuiu and Kupreanof islands. The area includes rocks ranging in age from Late Silurian through Tertiary and encompasses the most complete stratigraphic

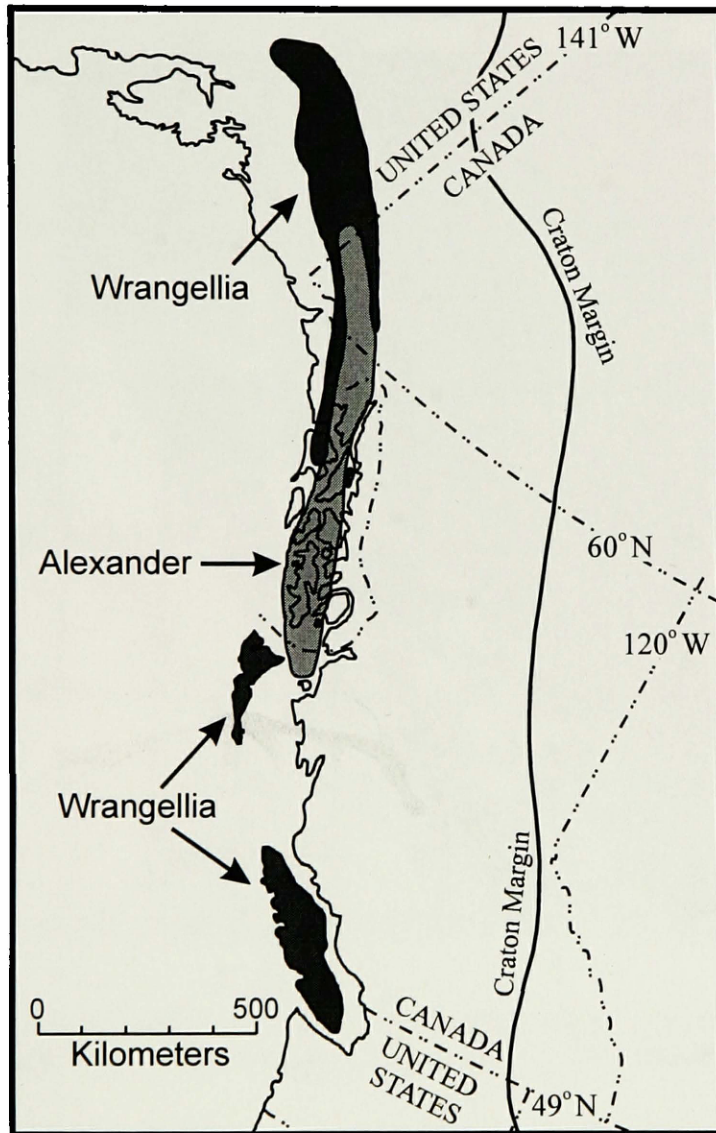


Figure 1. Generalized map of western North America showing position of Alexander and Wrangellia terranes. (modified from Jones *et al.*, 1972 and Jones *et al.*, 1977)

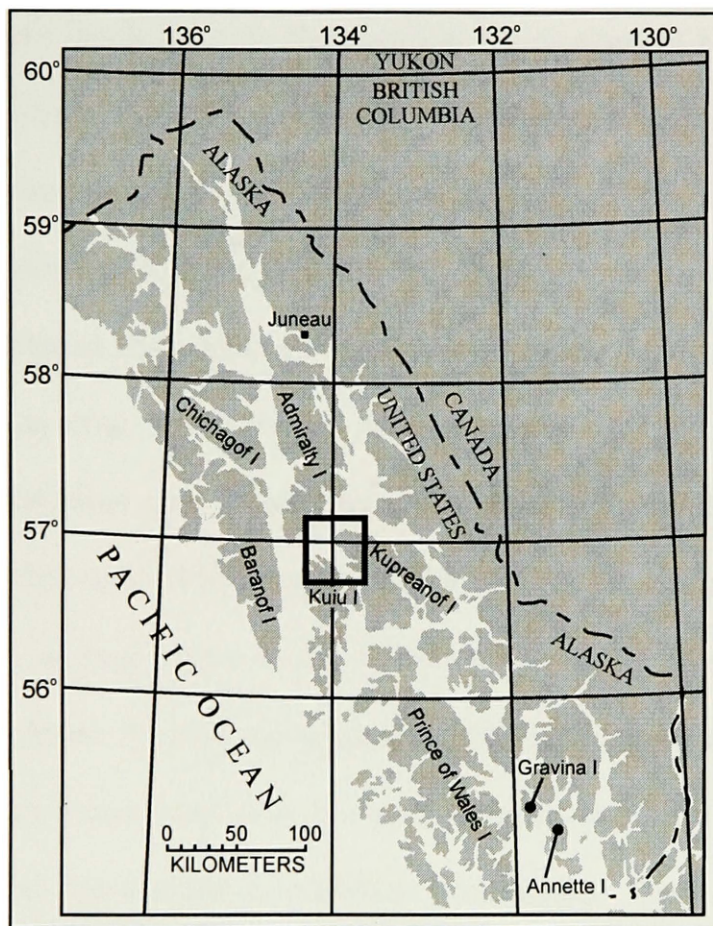


Figure 2. Map of southeast Alaska with major and referenced islands. Keku Strait map area is outlined. (after Muffler, 1967 and Berg, 1973)

section in southeast Alaska. **Figure 3** shows the distributions of Silurian through Triassic units (Muffler, 1967).

Wright and Wright (1908) were the first to comment on fossils and stratigraphy in the Keku Strait area. Atwood (1912) followed up their report and noted some of the Permian and Triassic fossils from the Hamilton Bay region south of Kake. Martin (1916) also made a few notes on the Triassic fossils and stratigraphy of Kupreanof Island. Smith (1927) followed this with a formal description of some of the Keku Strait fossils. Buddington and Chapin (1929) included the first detailed description of the Keku Strait area in their compilation of the geology of southeast Alaska. Many years later, Muffler (1967) published an even more detailed description and map focusing solely on the geology in the Keku Strait area. Furthermore, this paper also provided the first Triassic biostratigraphy of the region (Silberling *in* Muffler, 1967). These studies primarily used shoreline geology, as road access to the interior of the larger islands was extremely limited and the creeks are typically too vegetated to provide exposed strata.

Rock of Late Triassic age crops out throughout the north end of the Keku Strait, recording deposition over a variety of different environments. These deposits are part of a larger northwest-trending belt in southeast Alaska (Gehrels and Berg, 1984) which overlies both the Admiralty and Craig subterrane of the Alexander terrane (Berg *et al.*, 1978; Van Nieuwenhuyse, 1984; Gehrels *et al.*, 1987; Gehrels and Berg, 1994). These units unconformably overlie Paleozoic rock and are in turn overlain by Jurassic, Cretaceous, or younger rock (Muffler, 1967; Berg *et al.*, 1972; Rubin and Saleeby, 1991). In the Late Triassic, volcanic rock, volcanoclastic and lithoclastic sedimentary rock, and limestone record proximal and distal marine environments, and possibly terrestrial

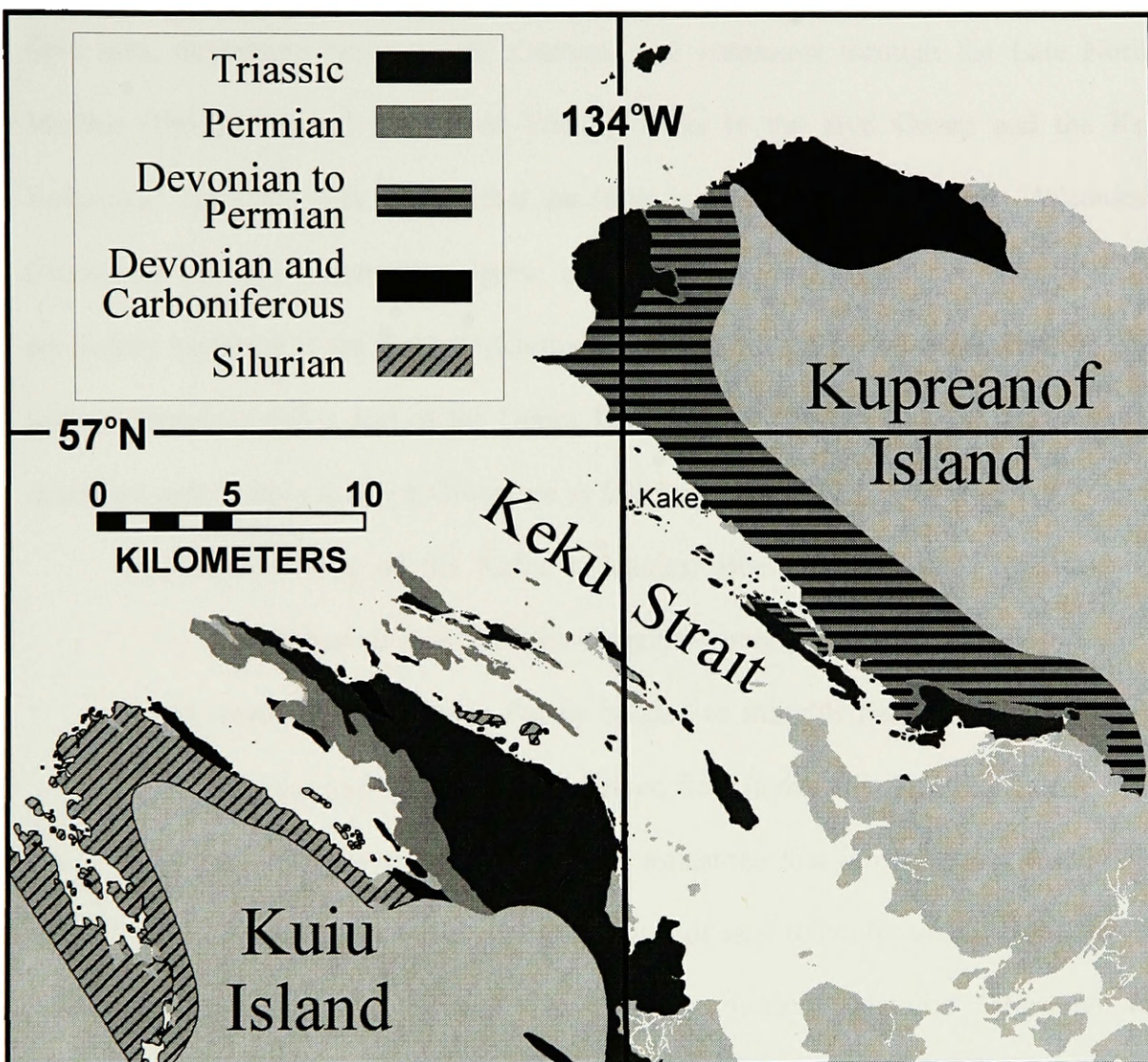


Figure 3. Map of Keku Strait area with generalized distributions of Silurian through Triassic rock. (modified from Muffler, 1967)

environments as well. The lithologies, sedimentary structures, and preserved fossil biota are consistent with deposition in an island arc succession (Soja, 1996). Abundant fossils, especially in limestone, provide a strong basis for biostratigraphic correlation. In the field area, deposition began in the Carnian, and continued through the Late Norian. Muffler (1967) assigned the Upper Triassic rocks to the Hyd Group and the Keku Volcanics. New age data suggest that the felsic igneous rock of the Keku Volcanics is Cretaceous in age (Mortenson, pers. comm. 2004). However, sedimentary beds previously assigned to the Keku Volcanics occur in succession with other Triassic units, and are therefore still a part of the Upper Triassic Hyd Group. Briefly, the previously described units within the Hyd Group are as follows (**Figure 4**):

Sedimentary rock of the Keku Volcanics: Bedded lithoclastic sandstone and conglomerate derived from underlying units; neptunian dikes

Burnt Island Conglomerate: Poorly bedded to massive basal conglomerate with angular and rounded clasts derived from underlying Paleozoic units

Cornwallis Limestone: Notably oolitic limestone that is commonly fossiliferous and has beds with variable amounts of sand to cobble sized clasts

Hamilton Island Limestone: Very thinly bedded aphanitic limestone with subordinate argillaceous laminae and sandy intervals

Hound Island Volcanics: Mainly basaltic pillow lava, basaltic pillow breccia, massive basalt, andesitic volcanic breccia, and hyaloclastic tuff with subordinate tuffaceous polymict conglomerate, limestone, and sandstone

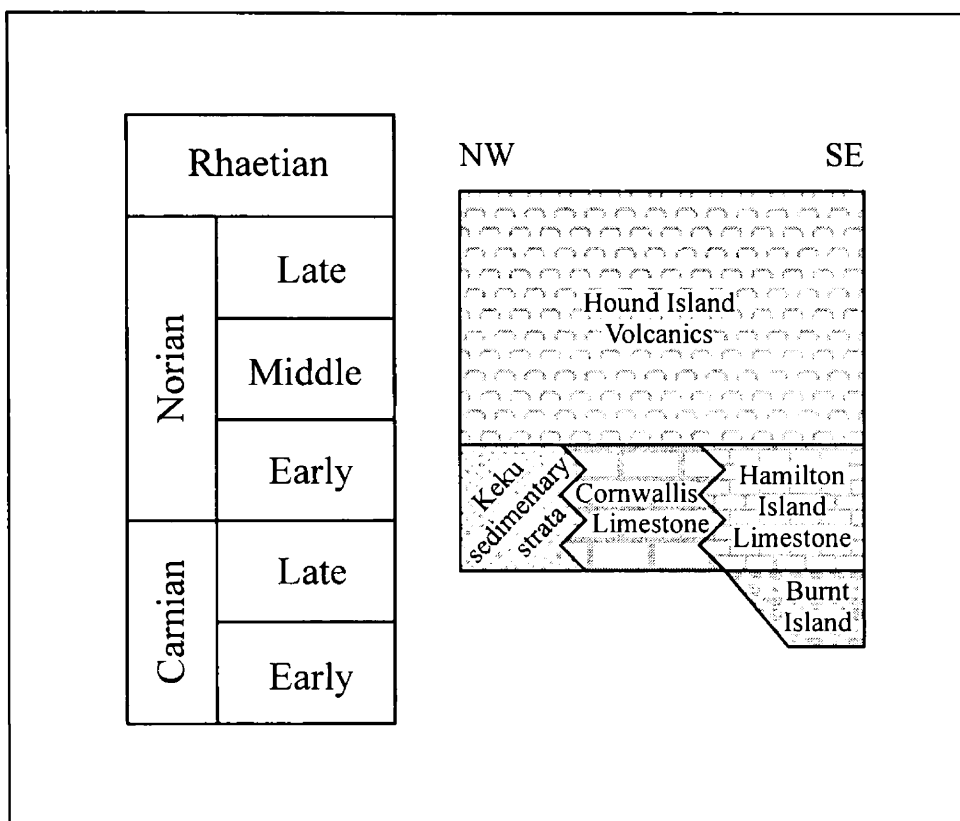


Figure 4. Simplified stratigraphic column for the Upper Triassic Hyd Group in the Keku Strait area.

Additional studies in the Keku Strait area have focused on individual portions of the geology, most commonly parts of the Triassic stratigraphy. Brew and Muffler (1965), and Muffler and others (1969) studied undevitrified volcanic glass in the Hound Island Volcanics. Several publications documented Triassic marine invertebrates from Keku Strait for taxonomic and paleogeographic studies (ammonoids and bivalves – Silberling and Tozer, 1968; corals – Montanaro-Gallitelli *et al.*, 1979; bivalves – Newton, 1983; brachiopods – Hoover, 1991; bivalves – Silberling *et al.*, 1997; McRoberts and Blodgett, 2000; gastropods – Blodgett and Frýda, 2001; gastropods – Frýda and Blodgett, 2001). Hillhouse and Grommé (1980), and Haeussler and others (1992) examined paleomagnetic data in the Hound Island Volcanics. Karl and others (1999) mapped the area to the east of Keku Strait, including many adjacent Triassic outcrops. Finally, abundant mineral deposits in the Keku Strait area related to the Keku Volcanics have been studied by a number of authors (Berg, 1981; Taylor *et al.*, 1995; McDonald *et al.*, 1998; Bittenbender *et al.*, 2000; Still *et al.*, 2002).

Muffler (1967), and Orchard and others (2001) emphasized the importance of age data in the terranes. Without a temporal scale, understanding structural and tectonic histories is extremely difficult. In terranes, this problem is compounded by incoherent regional stratigraphy, abrupt facies changes, and structural telescoping of dissimilar stratigraphic profiles (Orchard *et al.*, 2001). The major goal of this study is to refine the Triassic biostratigraphic data of the region, primarily by using conodonts. This work was designed to improve stratigraphic correlation within the area, refine Triassic biostratigraphy in the Alexander terrane, and build a stronger foundation for future biostratigraphic and lithostratigraphic research of Triassic age rocks in the terranes.

Furthermore, this study is associated with ongoing research on Late Triassic invertebrate fossils and their evolution, survival from mass extinction, and biogeographic potential in tectonostratigraphic terranes. An improved biostratigraphic framework will assist paleontologic determinations with Late Triassic invertebrates.

Over a total of six weeks during the summers of 2001, 2002, and 2003, we visited Triassic rocks throughout the Keku Strait area (**Figures 5 and 6, and Appendix A**). Past studies (Buddington and Chapin, 1929; Muffler, 1967) guided the selection of sites for paleontological sampling, though we also located new sites (**Appendix A**). Conodont samples were collected from measured sections or more frequently as individual site samples. Lab techniques for conodont recovery included acetic acid dissolution and heavy liquid separation (**Appendix C**). Macrofossils were collected whenever encountered. Many silicified macrofossils were recovered by etching blocks in acetic or hydrochloric acid. Biostratigraphically significant macrofossils, including those published in past studies (Muffler, 1967), are included in this paper to enhance or supplement the conodont biostratigraphy. While the focus of the work was collection of paleontological samples, we made an effort to examine each geologic unit throughout the study area, and collected samples from every major lithology encountered.

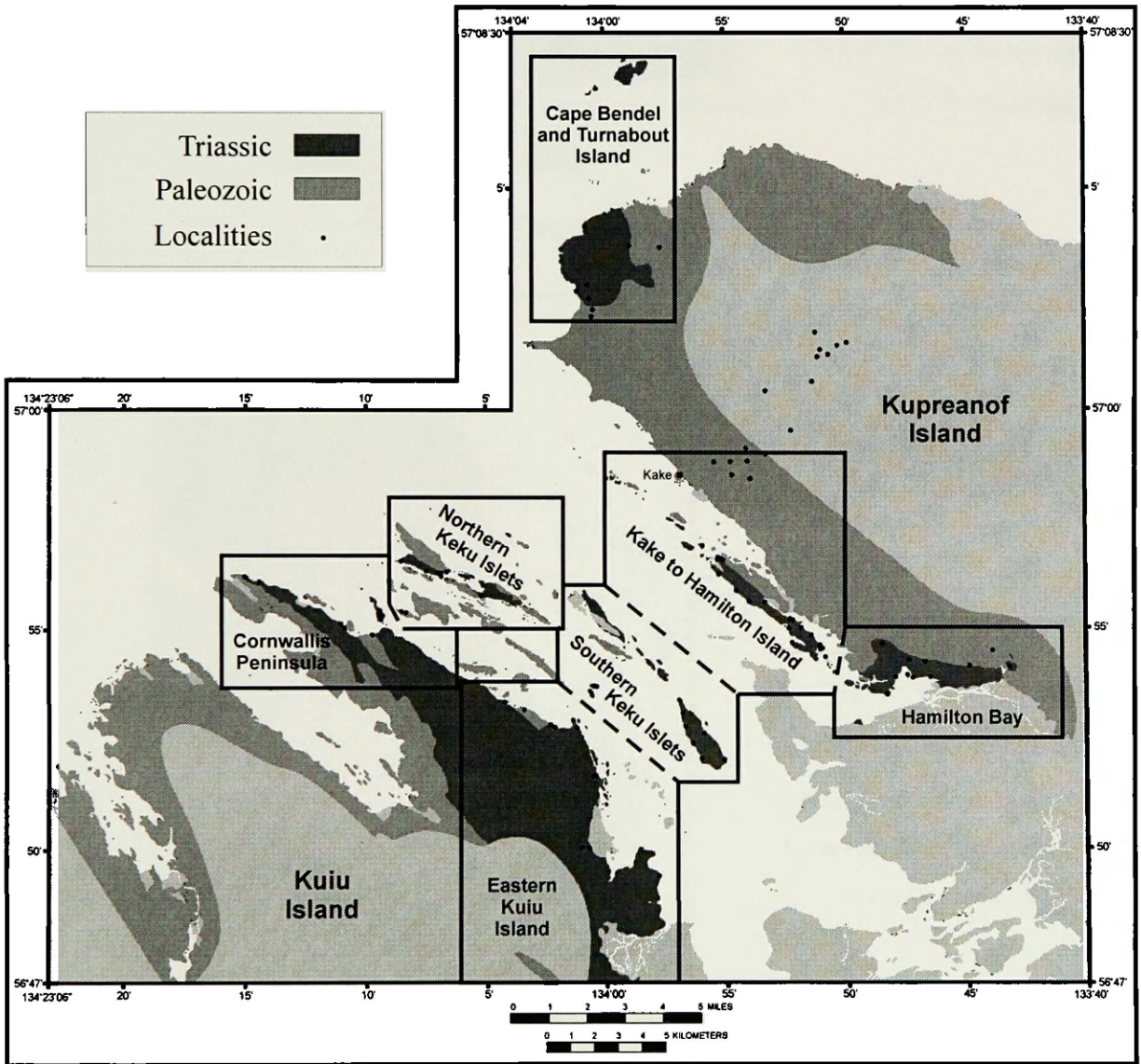


Figure 5. Map of Keku Strait with generalized distributions of Paleozoic and Triassic rock, localities visited, and areas of reference for Triassic rocks. (modified from Muffler, 1967)

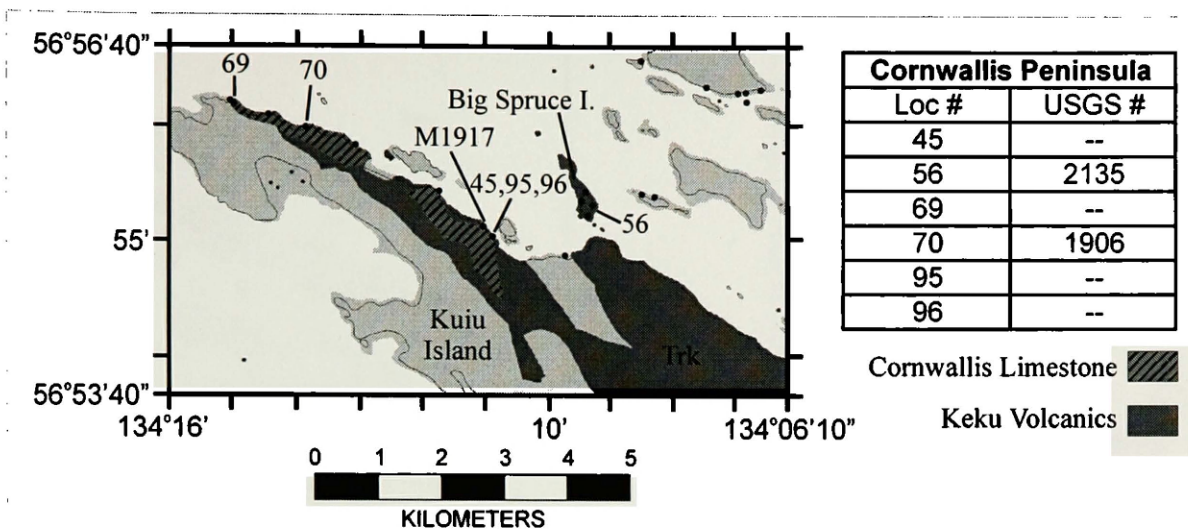


Figure 6a. Cornwallis Peninsula

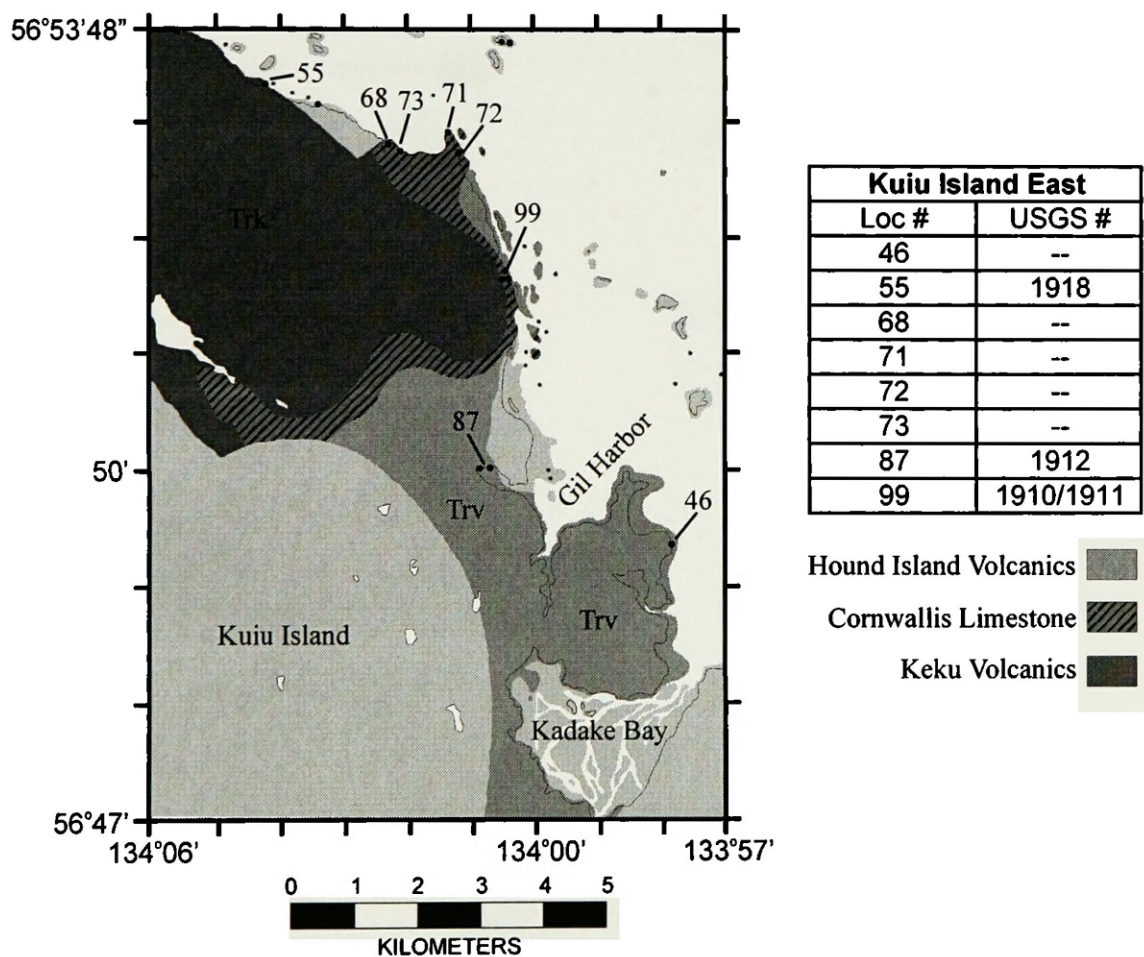
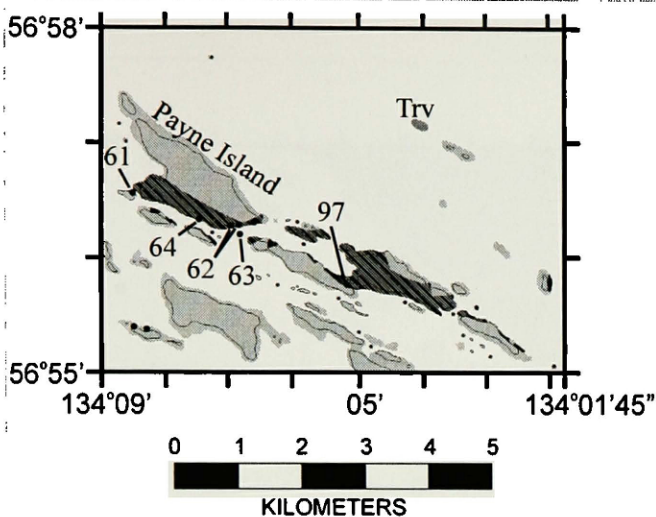


Figure 6b. Eastern Kuiu Island

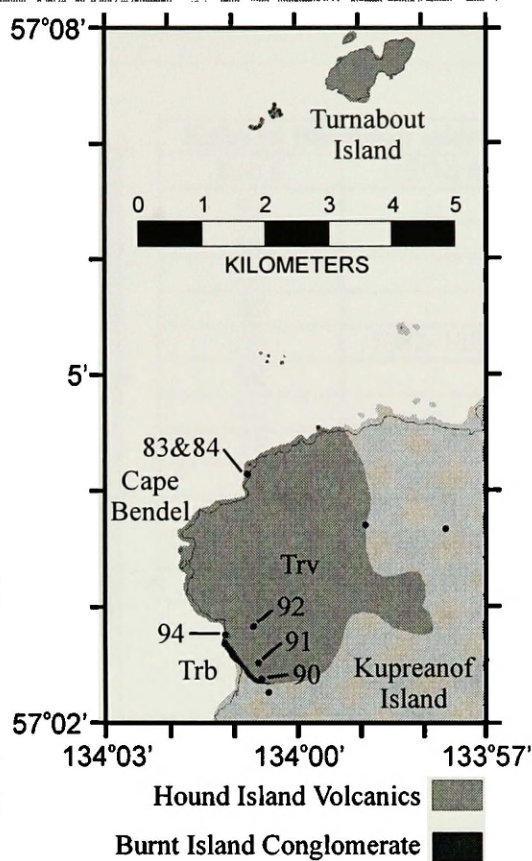
Figure 6. Larger scale maps of areas represented in Figure 5. Dots represent visited Triassic localities, and Loc numbers are University of Montana Museum of Paleontology locality numbers. Corresponding USGS numbers are given when appropriate. Trb is the Burnt Island Conglomerate, Trk is the Keku Volcanics, Trc is the Cornwallis Limestone, Trh is the Hamilton Island Limestone, and Trv is the Hound Island Volcanics. Outcrop extent is unchanged from Muffler, 1967.



- Hound Island Volcanics
- Hamilton Island Limestone
- Burnt Island Conglomerate

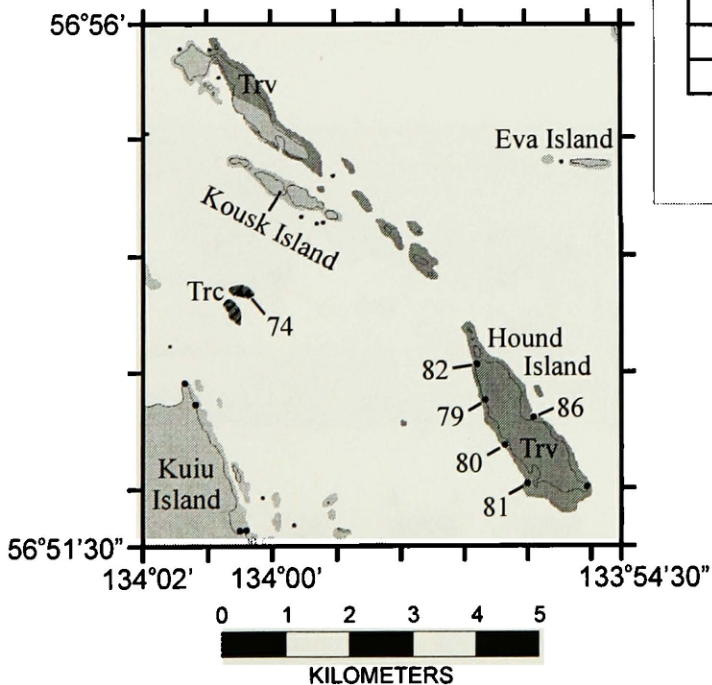
Northern Keku Islets	
Loc #	USGS #
61	1924
62	1904
63	--
64	1903
97	--

Figure 6c. Northern Keku Islets



Cape Bendel and Turnabout Island	
Loc #	USGS #
83	1913
84	--
90	--
91	--
92	--
94	--

Figure 6e. Cape Bendel and Turnabout Island



Southern Keku Islets	
Loc #	USGS #
74	2136
79	1899
80	1923
81	1921
82	--
86	1900/1901

- Hound Island Volcanics
- Cornwallis Limestone

Figure 6d. Southern Keku Islets

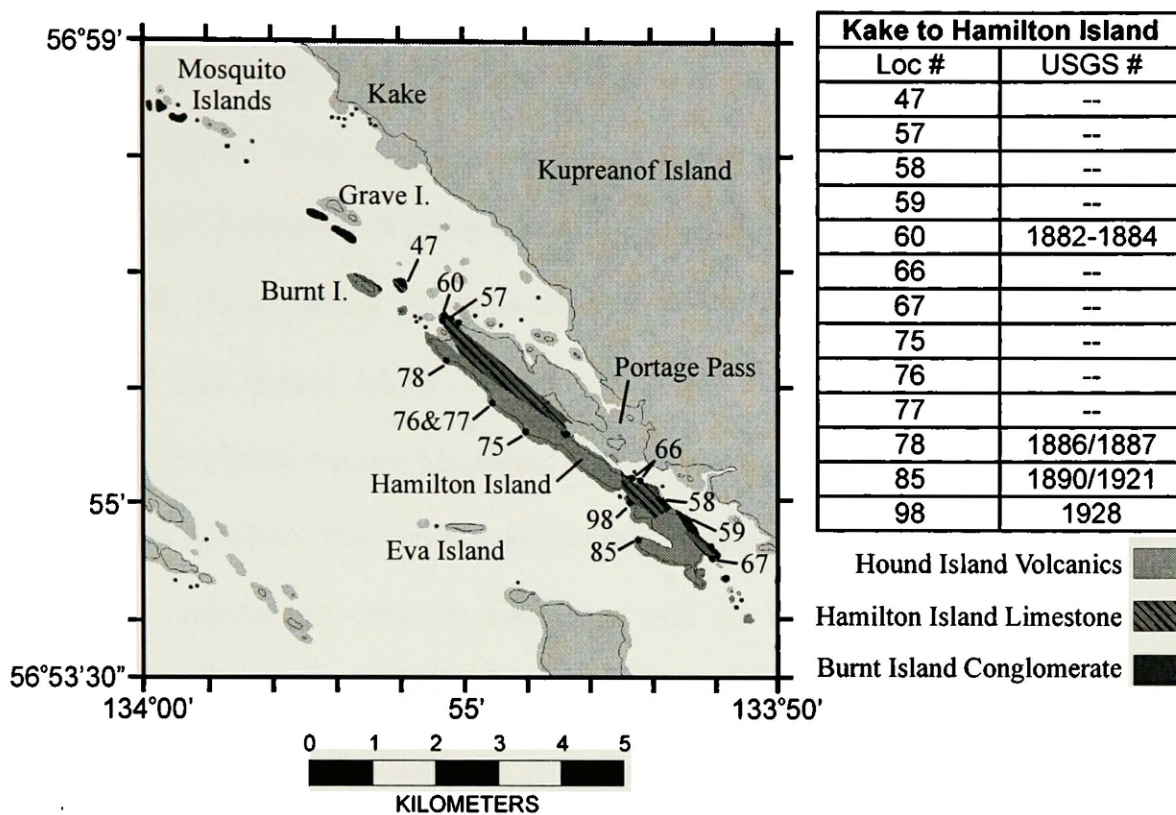


Figure 6f. Kake to Hamilton Island

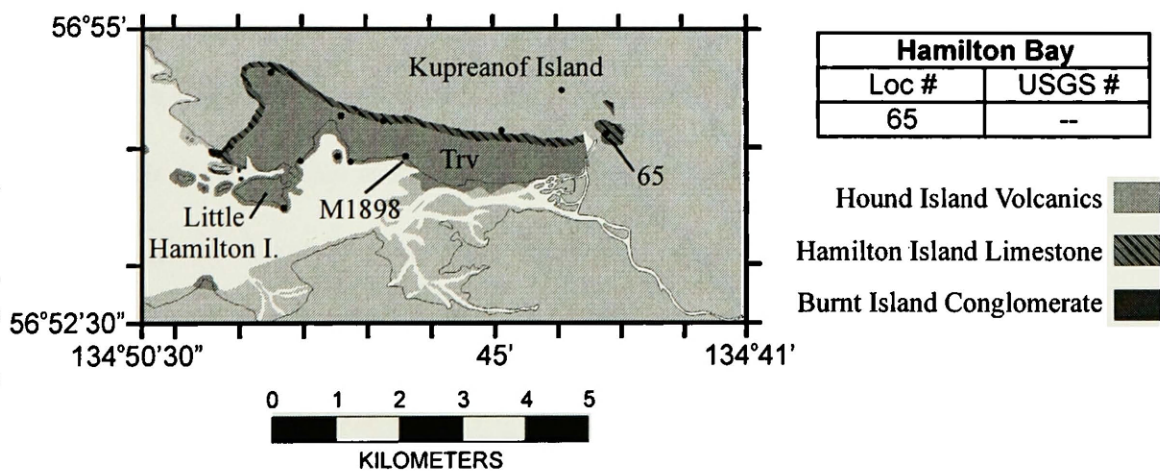


Figure 6g. Hamilton Bay

Lithostratigraphy and paleontology

Loney (1964) defined the Hyd Formation to the north of the Keku Strait area on Admiralty Island. With the better exposures in the Keku Strait area, Muffler (1967) raised the Hyd Formation to group status and subdivided it into four formations. These include the Burnt Island Conglomerate, Cornwallis Limestone, Hamilton Island Limestone, and Hound Island Volcanics. These formations loosely correlate with Loney's (1964) basal breccia, limestone, argillite, and volcanic members. Muffler (1967) also defined the Keku Volcanics, a unit mainly comprised of felsic volcanics which was inferred to underlie and partially interfinger with the Hyd Group. However, recently acquired age data from U-Pb zircon ratios measured from several samples of the Keku Volcanics indicate a Cretaceous age (Mortenson, pers. comm. 2004). Thus, the felsic igneous rock of the Keku Volcanics may have a Cretaceous intrusional origin. Sedimentary deposits formerly included in the Keku Volcanics occur in succession with the Cornwallis Limestone. Accordingly, in the descriptions below we remove specific sedimentary units from the Keku Volcanics and associate them with either the newly described Keku sedimentary strata or the Cornwallis Limestone in the Hyd Group.

The focus of this study was on sedimentary, particularly carbonate, units. Basic descriptions of Triassic units are included below to familiarize the reader. The descriptions presented follow Muffler (1967) and supplement the original definitions with new information and interpretations. Eroded Paleozoic rocks provided the detrital source for many Triassic units. The Paleozoic Cannery and Pybus formations are recognizable as clasts and basic descriptions of these units are included below to provide familiarity.

Fossils discovered during the course of this work are curated in the University of Montana Museum of Paleontology, and **Table 1** summarizes the major groups of Triassic fossils discovered in the Keku Strait area. Biostratigraphically significant fossils, including conodonts, ammonoids, and halobiid and monotiid bivalves, are discussed thoroughly in the section on biostratigraphy.

PALEOZOIC UNITS

Loney (1964) named the Cannery Formation for Permian exposures on southeastern Admiralty Island. This formation crops out throughout northeastern Kupreanof Island (**Figure 5**), and currently comprises units of Devonian to Carboniferous (Buddington and Chapin, 1929; Jones *et al.*, 1981), possibly Permian (Dutro *in* Muffler, 1967), age. In the Keku Strait area, the main lithology is thin-bedded, tuffaceous volcanic siltstone to sandstone with locally occurring chert, limestone, and pillow flows (Muffler, 1967). The main lithology characteristically weathers blue-green or reddish-brown in color and is intensely fractured (Muffler, 1967).

Loney (1964) defined the Pybus Dolomite for Permian exposures on southeastern Admiralty Island. Muffler (1967) renamed it the Pybus Formation and included the Permian outcrops of distinctively white limestone, dolomite, and chert in the Keku Strait area and on Admiralty Island. Silicified crinoids, bryozoans, and brachiopods are common. In the Keku Strait area, the Pybus Formation crops out near Hamilton Bay, inland of Cape Bendel, throughout the Keku Islets, and along the west side of Cornwallis Peninsula (**Figure 5**).

Locality Name	Loc #	Fossil groups	Fm	age
Neptunian Dike and M1918	55	algae?, aulacocerids, ammonoids, gastropods	C	Late Carnian or Early Norian
Big Spruce Island	56	ammonoids, brachiopods, corals, crinoids, echinoids, gastropods, oysters, sponges, spongiomorphs, <i>Stromatomorpha</i>	C	Late Carnian? to Early Norian
Hamilton Island Northeast	60	ammonoids, aulacocerids, halobiid bivalves, nautiloids, wood	HL	Late Carnian
Payne Island North, M1924	61	ammonoids, halobiid bivalves	HL	Late Carnian
Small Island south of Payne Island SW	63	ammonoids, halobiid bivalves	HL	--
Payne Island Southwest, M1903	64	halobiid bivalves	HL	Late Carnian or Early Norian
Top Cathedral Falls	65	halobiid bivalves	HL	Late Carnian or Early Norian
Portage Pass	66	ammonoids, halobiid bivalves, nautiloids, wood	HL	Late Carnian to Early Norian
Hamilton Island Southeast	67	ammonoids, halobiid bivalves	HL	Late Carnian
Cornwallis Peninsula East	69	brachiopods, corals, crinoids, <i>Stromatomorpha</i> , wood	C	Early Norian
Cornwallis Peninsula East, M1906	70	branching algae, "shelly" bivalves, brachiopods, corals, crinoids, gastropods, oysters, sponges, <i>Stromatomorpha</i> , wood	C	Late Carnian or Early Norian to Early Norian
Kuiu Island East-A	72	ammonoids, brachiopods, "shelly" bivalves, corals, crinoids, wood	C	Late Carnian or Early Norian
K(?) and K(not)	73	leaf and plant matter, wood	C	Late Carnian or Early Norian
Southwest of Kousk Island	74	branching algae, "shelly" bivalves, bone?, brachiopods, corals, crinoids, echinoids, gastropods, oysters, sponges, spongiomorphs, <i>Stromatomorpha</i>	C	Early Norian
Hamilton Island West - Site 5	77	brachiopods	HV	--
Hamilton Island West - Site 6	78	halobiid bivalves	HV	--
Hound Island West, M1899	79	aulacocerids, halobiid bivalves, trace fossils	HV	Early Norian
Hound Island West, M1923	80	halobiid bivalves	HV	Early Norian
Hound Island West, M1921	81	halobiid bivalves, trace fossils	HV	Early Norian
Hound Island North	82	trace fossils	HV	Early Norian
Cape Bendel Day 2	83	ammonoids, halobiid bivalves, brachiopods, crinoids	un	Late Carnian
Cape Bendel Day 2-A	84	halobiid bivalves	HL	Late Carnian
Hamilton Island Southwest	85	halobiid bivalves	HV	Early Norian
Hound Island East	86	ammonoids, halobiid bivalves, ichthyosaur bone	HV	Middle Norian
Gil Harbor	87	ammonoids, aulacocerids, halobiid and monotiid bivalves, "shelly" bivalves, brachiopods, corals, crinoids, echinoids, gastropods, <i>Heterastridium</i> , oysters, sponges, trace fossils, wood	HV	Late Norian
Squawking Crow	97	ammonoids, halobiid bivalves, brachiopods	HL	Late Carnian to Early Norian
Flounder Cove	99	ammonoids, halobiid bivalves, "shelly" bivalves, bone, brachiopods, corals, crinoids, echinoids, gastropods, nautiloids, oysters, sponges, spongiomorphs, <i>Stromatomorpha</i> , trace fossils, wood	C	Early Norian

Table 1. Triassic macrofossil groups recovered from the Keku Strait area. Loc # is the University of Montana Museum of Paleontology Locality and Fm is Formation including the following: C = Cornwallis Limestone, HL = Hamilton Island Limestone, HV = Hound Island Volcanics, un = unnamed shallow water limestone.

TRIASSIC UNITS

Burnt Island Conglomerate

Occurrence: The type locality is the small islands (reefs) below mean high tide between Burnt Island and Grave Island south of Kake (**Figure 6f**) (Muffler, 1967). The Burnt Island Conglomerate also occurs west of Kupreanof Island from Kake down into Hamilton Bay, in the Cape Bendel region, and on a few of the northern Keku Islets (**Figures 6c, 6e, 6f, and 6g**). Around Cape Bendel, Muffler (1967) noted the Burnt Island Conglomerate on the southern end of the Triassic outcrop, though this formation also occurs on the northeast end (Buddington and Chapin, 1929), and further inland between the Paleozoic outcrop and the Hound Island Volcanics (**Figure 6e**).

Description: This unit is a poorly bedded to massive, grain-supported conglomerate (**Figure 7**). It is dominated by rounded and angular clasts of the underlying unit, which mainly are eroded Paleozoic units (Muffler, 1967). Buddington and Chapin (1929) likened this unit to both conglomerate and breccia based on the variable rounding of clasts. At the type locality, most grains are pebbles (Muffler, 1967), but sand to boulder sized clasts also occur. More resistant rock types, such as chert and limestone clasts from the Pybus Formation, typically form larger pieces than less resistant lithologies of the Cannery Formation. The largest clasts observed were on the island east of Burnt Island and in the Cape Bendel region (**Figure 8**). Atwood (1912) observed boulders up to about a meter in diameter from the south end of Hamilton Island in what is probably this unit. These larger clasts are commonly somewhat rounded. Overall, the



Figure 7. Cut slab of pebble conglomerate in the Burnt Island Conglomerate from the island east of Burnt Island (Figure 6f, site 47). Scale is in centimeters.

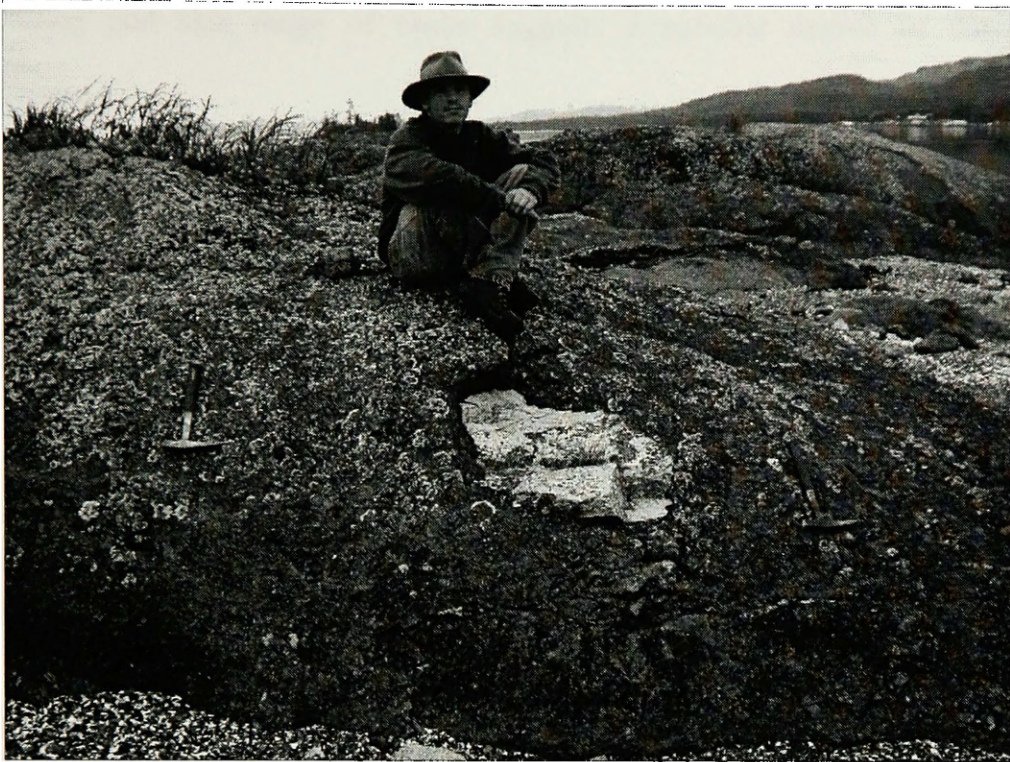


Figure 8a. Large Pybus Formation clast in the Burnt Island Conglomerate on the small island east of Burnt Island (Figure 6f, site 47). Person and hammers (33 cm) for scale.



Figure 8b. Burnt Island Conglomerate (top) with large Pybus Formation clast (bottom), from the Cape Bendel region (Figure 6e, south of site 94). Hammer (33 cm) for scale.

rounding and size range of clasts suggests a variable degree of recycling before deposition.

The Burnt Island Conglomerate overlies Paleozoic rock by an erosional unconformity. Either the lowest limestone bed of the Hamilton Island Limestone or volcanic rock of the Hound Island Volcanics overlies this formation.

Paleontology: Triassic fossils are extremely rare in this unit. An Early Carnian ammonoid and halobiid bivalve were reported in clasts (Silberling *in* Muffler, 1967) (**Figure 6f, site 67**). This constrains the age of the unit to Early and Late Carnian, as Upper Carnian rocks of the Hamilton Island Limestone overlie the unit on Hamilton Island. Clasts eroded from the Pybus Formation also contain Permian age crinoids, bryozoans, and brachiopods.

Interpretation: This basal conglomerate represents rapid infill above the pre-Late Triassic unconformity in the region. Triassic basal conglomerates in the Cornwallis Limestone and the Keku sedimentary strata probably correlate laterally, as they also overlie the regional unconformity. However, they are generally thin and of a different character. Thus, they are described with their respective units.

Keku sedimentary strata

Occurrence: Muffler (1967) defined the Keku Volcanics by the felsic igneous rock on Cornwallis Peninsula. Hence, Triassic sedimentary units that are associated with the Cretaceous volcanics on Cornwallis Peninsula do not have a type locality or name. Extensive lithoclastic conglomerate and sandstone crop out on the island informally

referred to as Big Spruce Island (**Figure 6a**). Lithoclastic beds also occur inland on Cornwallis Peninsula (Blodgett and Caruthers, pers. comm. 2003) and in scattered locations on the eastern shore of Cornwallis Peninsula (**Figures 6a and 6b**). The lateral extent of these beds is uncertain. A single site on Cornwallis Peninsula (**Figure 6b, site 55**) has neptunian dikes that were included in the Keku Volcanics by Muffler (1967).

Description: Lithoclastic sandstone and granule to cobble conglomerate of the Keku sedimentary strata are mainly composed of clasts eroded from underlying units. The clasts are mostly chert and limestone, and limestone cobbles occur near the base of the unit (Muffler, 1967). Exposures are not common on the shores of Keku Strait, but a thick exposure of these strata on Big Spruce Island (**Figure 6a, site 56, and Figure 9**) contains limestone and chert fragments eroded from Paleozoic units (**Figure 10**). These exposures consist of bedded sandstone and pebble conglomerate with intermittent cobbles containing abundant sedimentary scours (**Figure 11**). A large, angular boulder of crinoidal Carboniferous limestone lies within these units (**Figure 12**).

Neptunian dikes occur below the limestone bed at USGS Mesozoic locality M1918 (**Figure 6b, site 55, and Figure 13**). These dikes are sedimentary fillings in cracks formed in underlying rock, and contain abundant fossils in a siliceous mud matrix.

The base of the unit appears to be a widespread chert and limestone clast conglomerate overlying the erosional unconformity (Muffler, 1967). In places the unit interfingers with or is conformably overlain by the Cornwallis Limestone. Although it has not been observed, it is likely that volcanic rock of the widely distributed Hound Island Volcanics also overlies these beds in places. This would account for some of the mafic volcanic rock reported by Muffler (1967) in the interior of Cornwallis Peninsula.

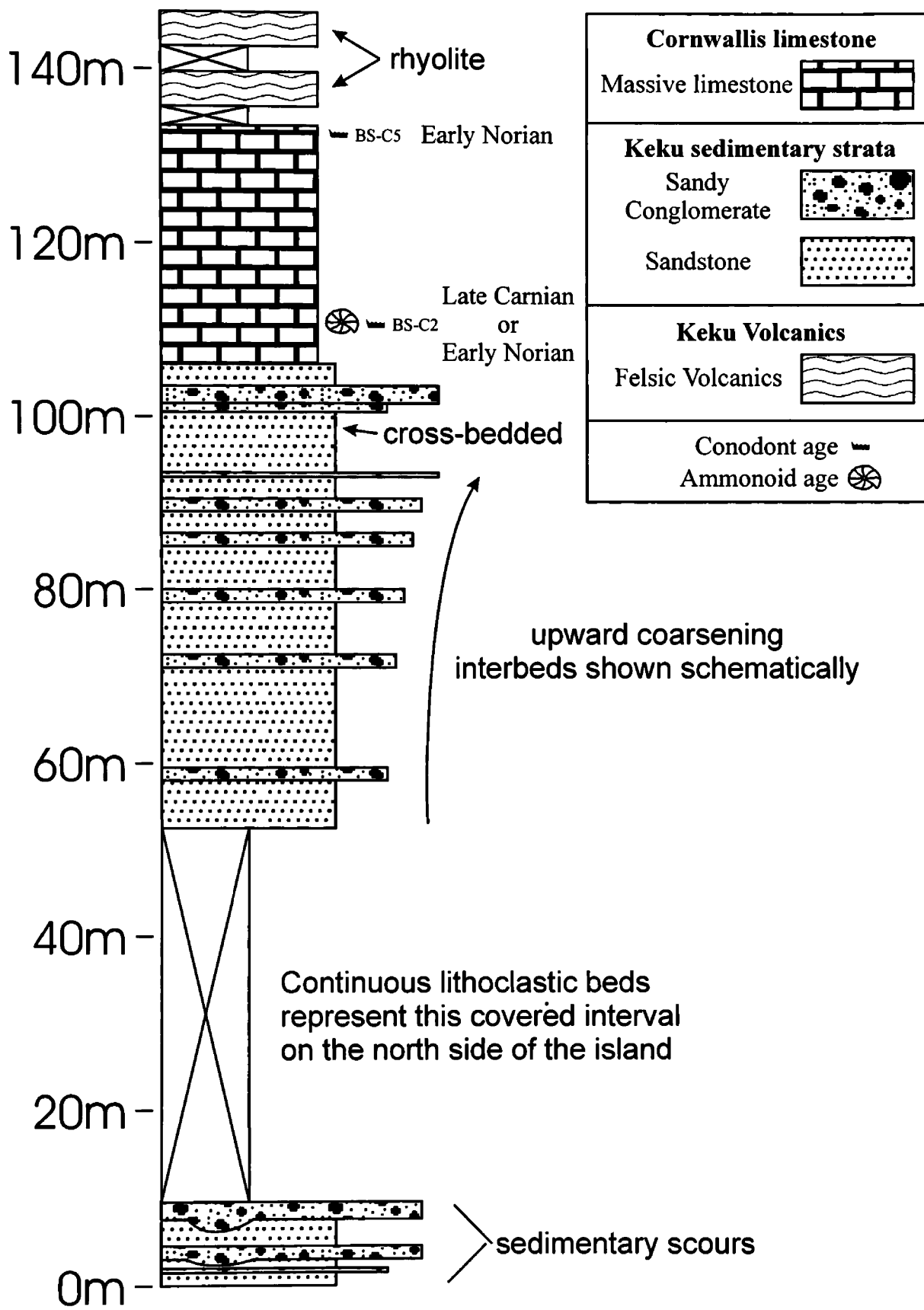


Figure 9. Representative stratigraphic section across the south side of Big Spruce Island with fossil determined ages. USGS Mesozoic locality M2135 occurs in the limestone.

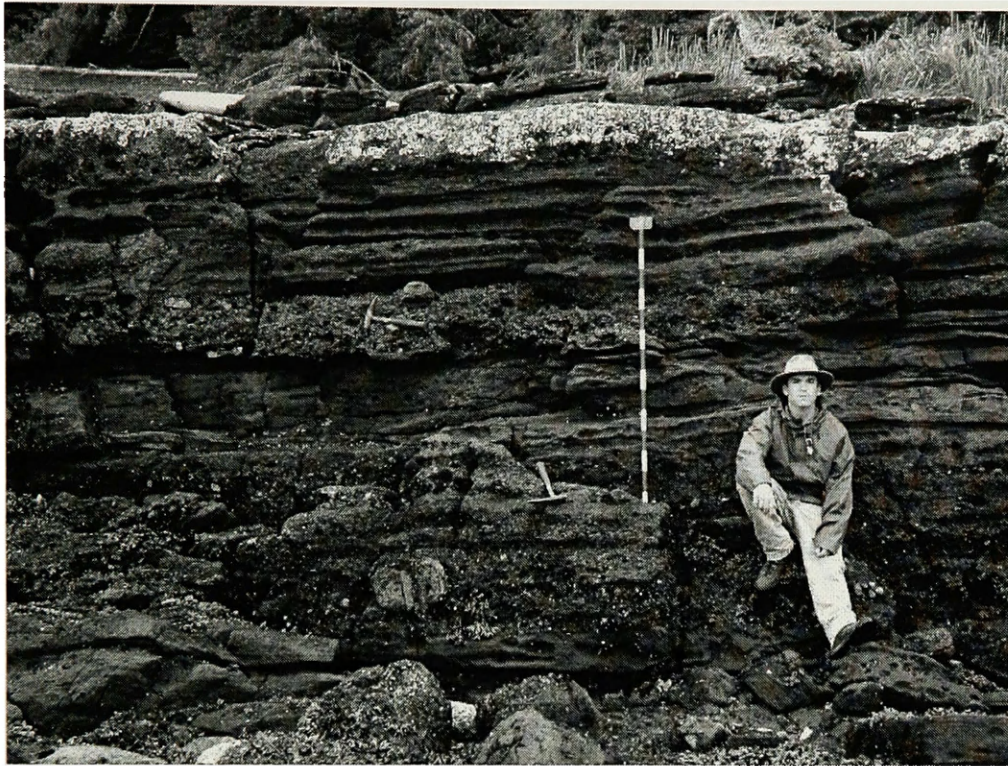


Figure 10. Lithoclastic sandstone and conglomerate succession of Keku sedimentary strata on Big Spruce Island (Figure 6a, site 56). Meter stick (10 cm subdivisions), and hammers (33 cm) for scale.



Figure 11. Sedimentary scour and fill structures in the lithoclastic succession of Keku sedimentary strata on Big Spruce Island (Figure 6a, site 56). Hammer (33 cm) for scale.

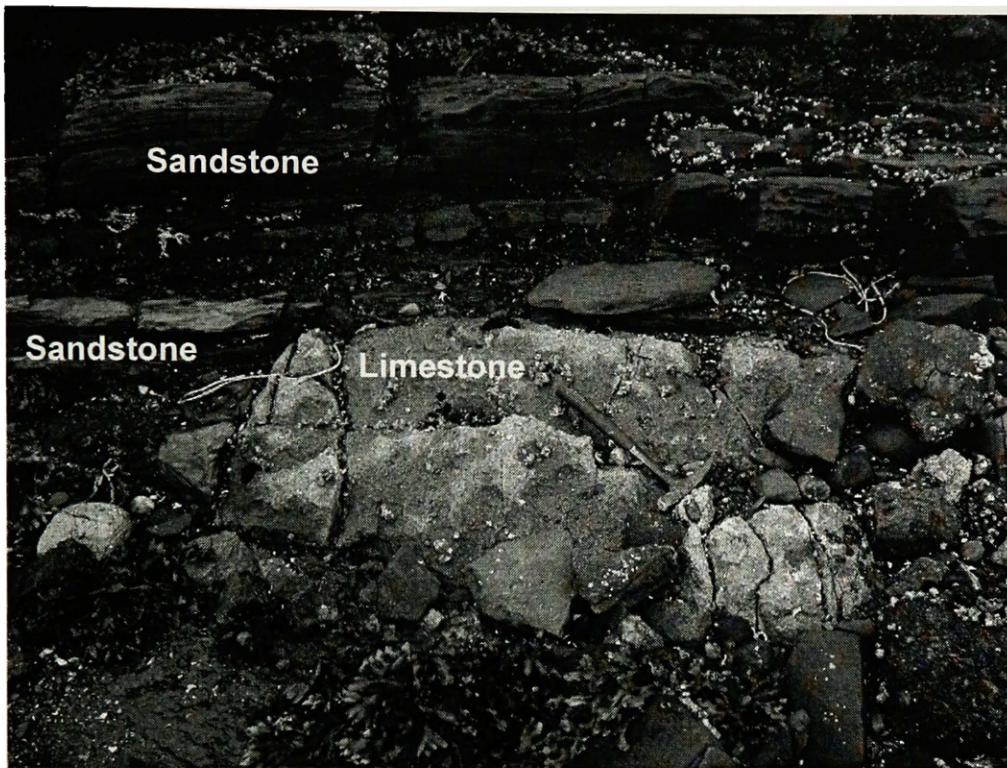


Figure 12. Large Carboniferous limestone clast in sandstone beds of the Keku sedimentary strata on Big Spruce Island (Figure 6a, site 56). Hammer (33 cm) for scale.

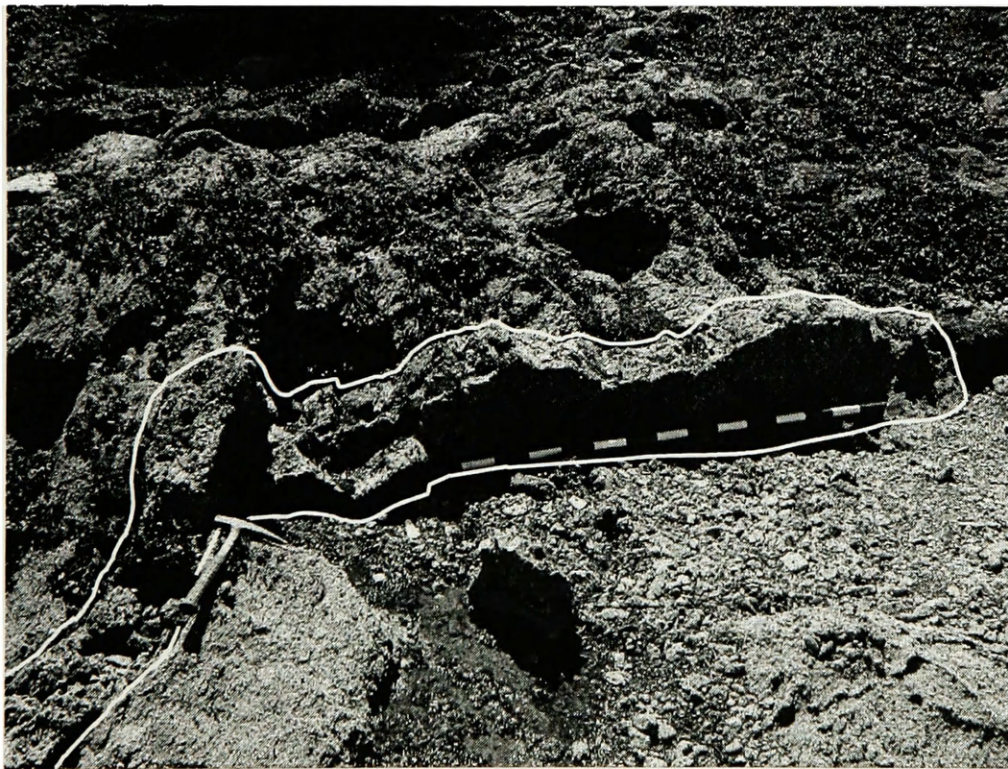


Figure 13. Neptunian dikes (outlined) of the Keku sedimentary strata which underlie Cornwallis Limestone of USGS Mesozoic locality M1918 on eastern Kuiu Island (Figure 6b, site 55). Meter stick (10 cm subdivisions) and hammer (33 cm) for scale.

Paleontology: The only deposits from the Keku sedimentary strata currently known to contain Triassic fossils are the neptunian dikes from eastern Cornwallis Peninsula (**Figure 6b, site 55**). These beds contain abundant gastropods, straight-shelled cephalopods (aulacocerids), and ammonoids (**Figure 14**). Removal of these fossils is difficult due to silicification and mineralization, though use of concentrated hydrochloric acid can yield molds. Though Triassic fossils are not known in the lithoclastic beds from the Keku sedimentary strata, lateral tongues of the Cornwallis Limestone provide additional biostratigraphic control. Limestone overlying the neptunian dikes from USGS Mesozoic locality M1918 (**Figure 6b, site 55**) was reported as Early Carnian based on the ammonoid fauna (Silberling *in* Muffler, 1967), though Silberling (pers. comm. 2002) informed us that improvements in ammonoid identification and biostratigraphic data actually place those fossils close to the Carnian-Norian boundary. Conodonts from that limestone confirm this age. Cornwallis Limestone overlying the lithoclastic beds on Big Spruce Island (**Figure 6a**) contains Early Norian conodonts. Overall, these place the Keku sedimentary strata in the Late Carnian and Early Norian, though they could extend down into the Early Carnian. On Big Spruce Island, lithoclasts of Carboniferous limestone contain abundant crinoids and bryozoans, and Permian brachiopod bioclasts (**Figure 15**) are reworked into a pebble conglomerate.

Interpretation: Overall, the Keku sedimentary strata represent near-shore and/or terrestrial environments. The neptunian dikes contain minimally transported fossils packed together in grain to grain contact, and surrounded and partially in-filled by siliceous mud matrix. These packstone beds probably represent a higher energy environment without significant sediment input, such as in the tidal zone. The abundant

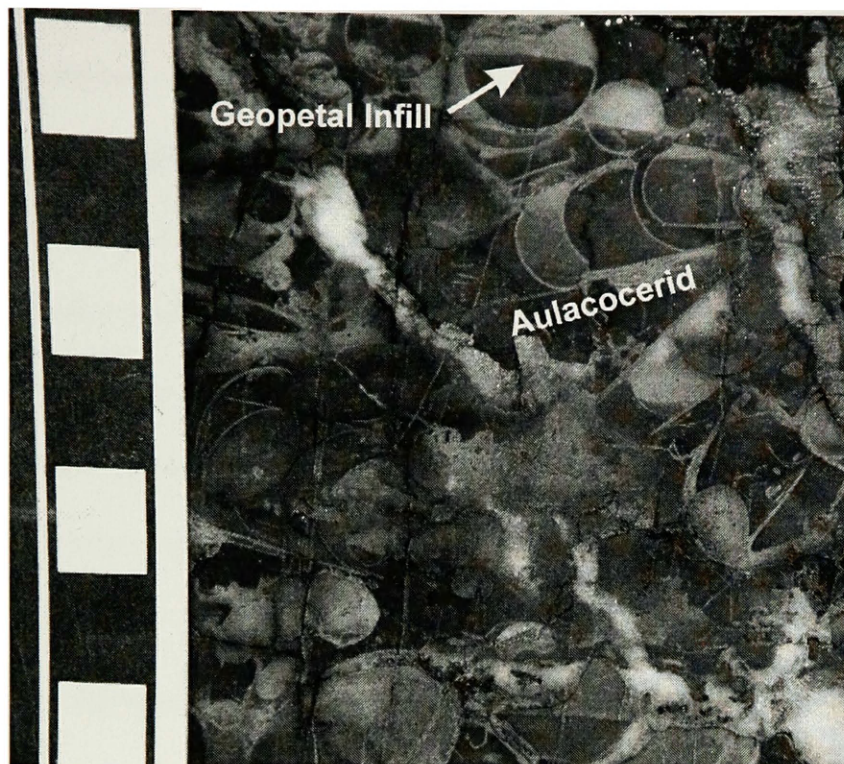


Figure 14. Cut slab of a neptunian dike with fossils (UMIP 303376), including many aulacocerids (Figure 6b, site 55). Note the light-colored, geopetal, crystalline infill in the fossils. Scale is in centimeters.

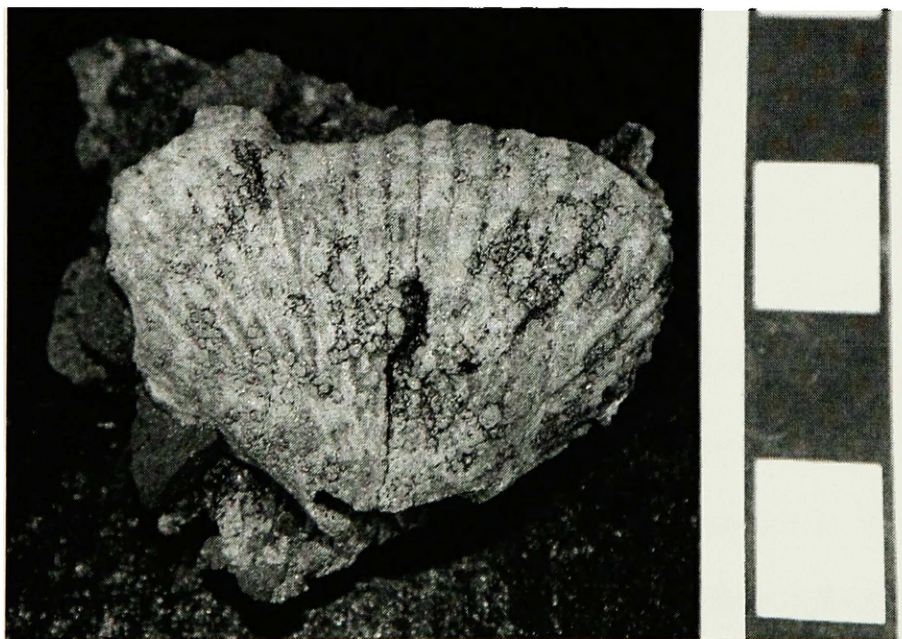


Figure 15. Reworked Permian brachiopod (UMIP 302543) from the Keku sedimentary strata on Big Spruce Island (Figure 6a, west of site 56). Scale is in centimeters.

fluvial sedimentary structures in the lithoclastic beds indicate terrestrial and/or marine fluvial deposition. The basal conglomerate is thin and displays more bedding than the Burnt Island Conglomerate. Muffler (1967) originally included interbeds of oolitic limestone in the Keku Volcanics based on the interpretation that the Keku Volcanics stratigraphically underlies the Cornwallis Limestone. Removal of the Keku Volcanics from the Hyd Group and interpretation of the Keku sedimentary strata as lateral facies of the Cornwallis Limestone (**Figure 4**) mean that it is prudent to include the limestone outcrops entirely within the Cornwallis Limestone.

Cornwallis Limestone

Occurrence: The type locality of the Cornwallis Limestone is the 2-3 km stretch of outcrop on the northeasternmost shore of Cornwallis Peninsula on Kuiu Island (Muffler, 1967). Overall, the unit occurs on the Cornwallis Peninsula and on some of the adjacent Keku Islets (**Figures 6a, 6b, and 6d**).

Description: The Cornwallis Limestone is a medium- to very thick- bedded, characteristically oolitic limestone (Muffler, 1967). It includes both massive, fossiliferous limestone (**Figure 16**) and bedded, less fossiliferous, lithoclastic limestone (**Figure 17**). Wispy interbeds of darker, aphanitic limestone occur locally (Muffler, 1967). Variations in fossil type and abundance are apparent in the rocks and may represent either lateral variability or facies changes. The lithoclastic limestone generally has smaller, better-defined bedding, and contains a variety of clasts from eroded Paleozoic units. Ooids are also common in these lithoclastic units (**Figure 18**), so it is



Figure 16. Massive fossiliferous limestone of the Cornwallis Limestone with large, toppled colony of *Spongiomorpha* (outlined) from Big Spruce Island (Figure 6a, site 56). Meter stick (10 cm subdivisions) for scale.

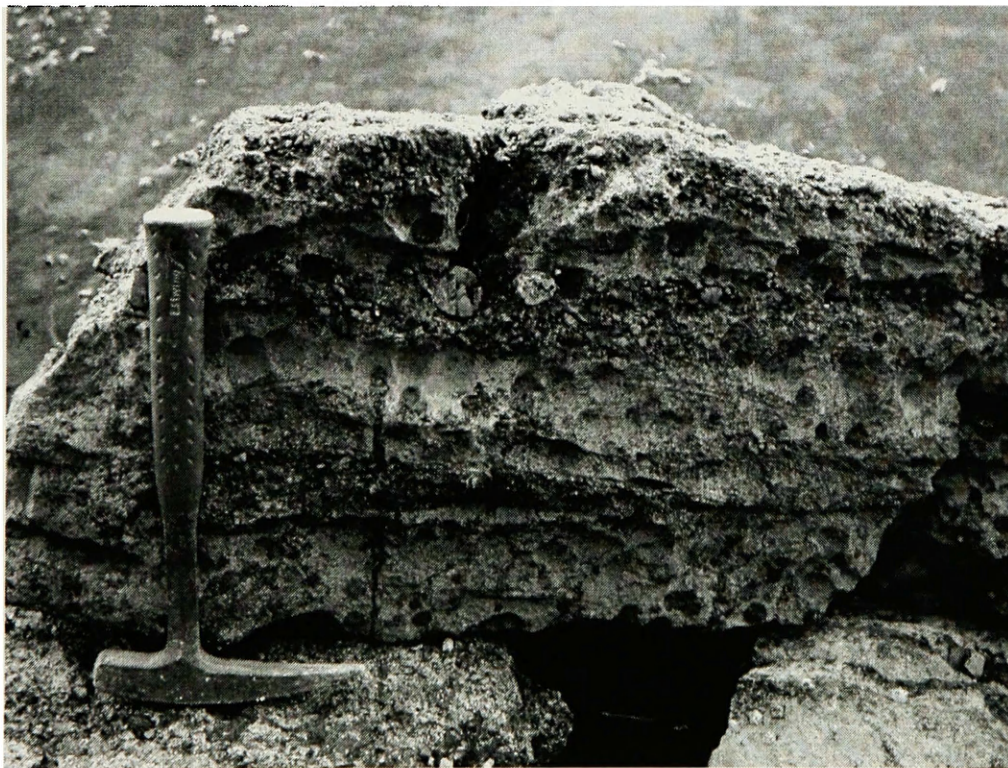


Figure 17. Lithoclastic limestone with pebbly and sandy layers from the Cornwallis Limestone on the eastern side of Kuiu Island (Figure 6b, site 68). Hammer (33 cm) for scale.

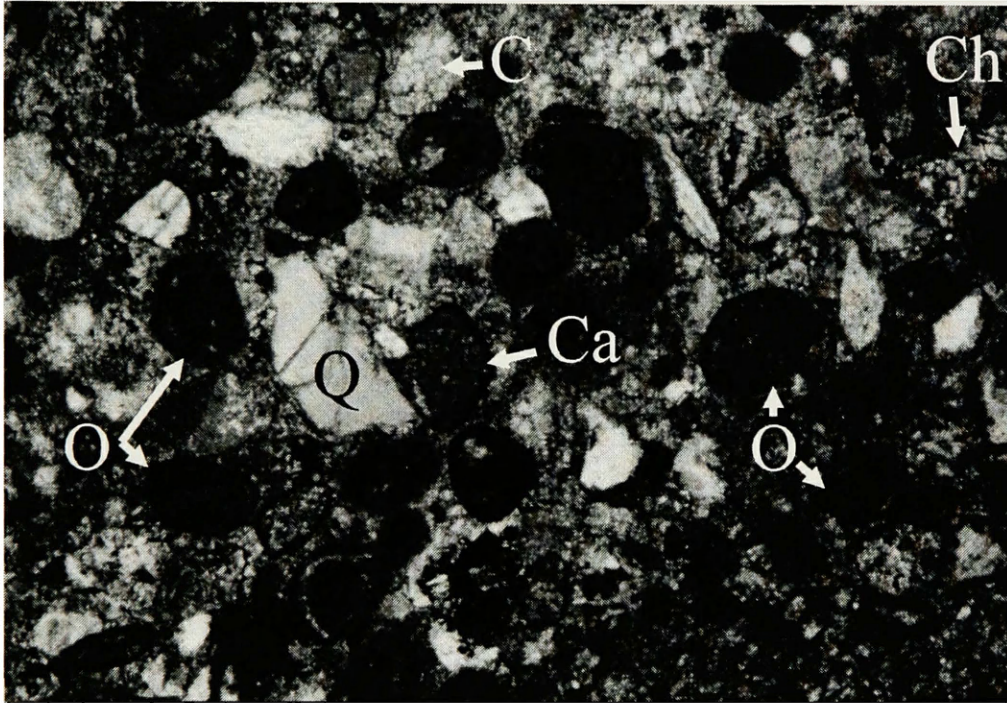


Figure 18. Photograph of a thin section of Cornwallis Limestone from eastern Kuiu Island (Figure 6b, site 72) in cross-polarized light. This sandy carbonate contains ooids (O), and quartz (Q), chert (Ch), detrital calcite (C) and carbonate (Ca) grains. Picture width is 7.94 mm.

easy to recognize them as Cornwallis Limestone. Pybus Formation clasts are the most common, though Devonian limestone, Carboniferous limestone, and unidentified chert clasts have been distinguished. The lithoclastic beds display sorting and occur as sandy, pebbly, and cobbly limestone beds. These lithoclastic units are more common near the base of the unit (Muffler, 1967), though in some places they dominate the section. In the area of the prominent point west of Hound Island on eastern Kuiu Island (**Figure 6b, sites 68 and 71-73**), the limestone is particularly lithoclastic. Shallow-water fossils are rare to absent here, and much of the rock is calcareous oolitic sandstone (**Figure 18**). Clastic grains comprise a variety of mineral and rock types, including quartz, feldspar, biotite, zircon, limestone fragments, volcanic rock fragments, and metamorphic rock fragments. A loose block of sandy to pebbly limestone displays large-scale cross-beds (**Figure 19**). These cross-beds underlie horizontal layers containing a round boulder of Pybus Formation limestone (**Figure 19**). To the south of this area, at the Flounder Cove locality (**Figure 6b, site 99**), the limestone beds are finer-grained, and are adjacent to rhyolite of the Keku Volcanics. Upsection, these beds are unconformably overlain by coarser grained limestone (**Figures 20 and 21**) before being capped by basalt of the Hound Island Volcanics. The finer-grained beds do not contain as many shallow-water fossils, but extremely fossiliferous, coarser-grained beds are present. These concentrated fossil beds are up to several decimeters thick, scour into the underlying carbonate mud, have randomly oriented fossils, and have upward fining layers of carbonate grains and bioclasts. These fossil beds probably represent turbiditic deposits with material reworked from shallower facies. An oncoidal bed of undetermined thickness (**Figure 22**) characterizes the base of the section at the Flounder Cove locality.



Figure 19. Sandy to pebbly lithoclastic limestone with cross-beds overlain by horizontal bedding. The horizontal beds contain a rounded boulder of Pybus Limestone. Float block of Cornwallis Limestone from eastern Kuiu Island (Figure 6b, site 72). Meter stick (10 cm subdivisions) for scale.

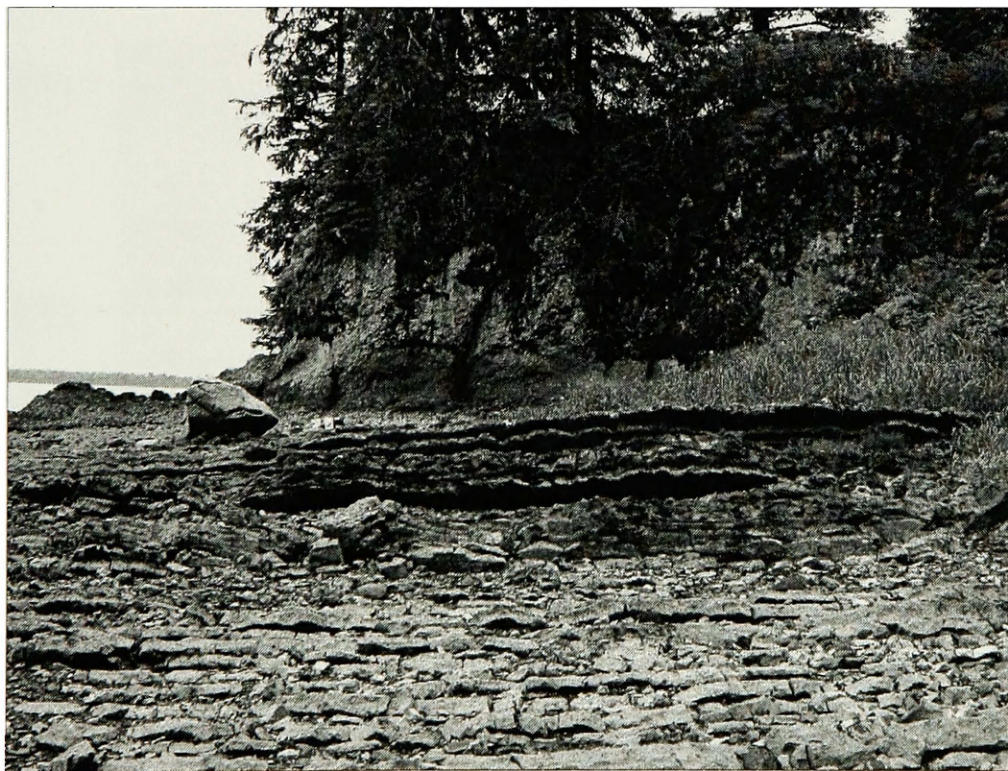


Figure 20. Flounder Cove succession of Cornwallis Limestone with coarser limestone in cliff unconformably overlying finer-grained, bedded limestone (Figure 6b, site 99). Large boulder in center-left of picture is about 1 m high.

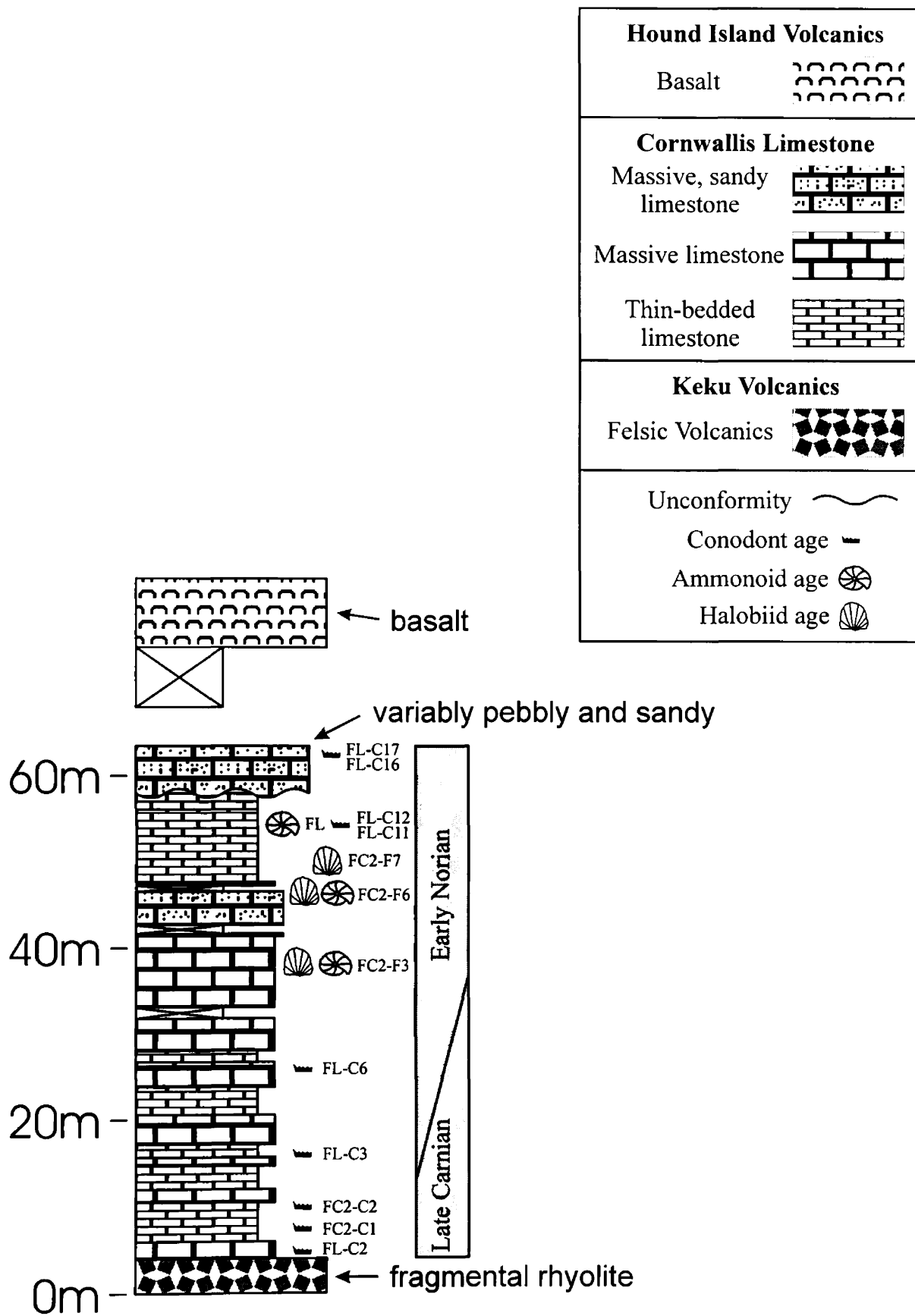


Figure 21. Representative stratigraphic section at the Flounder Cove locality with fossil determined ages. This section includes USGS Mesozoic Localities M1910 and M1911.

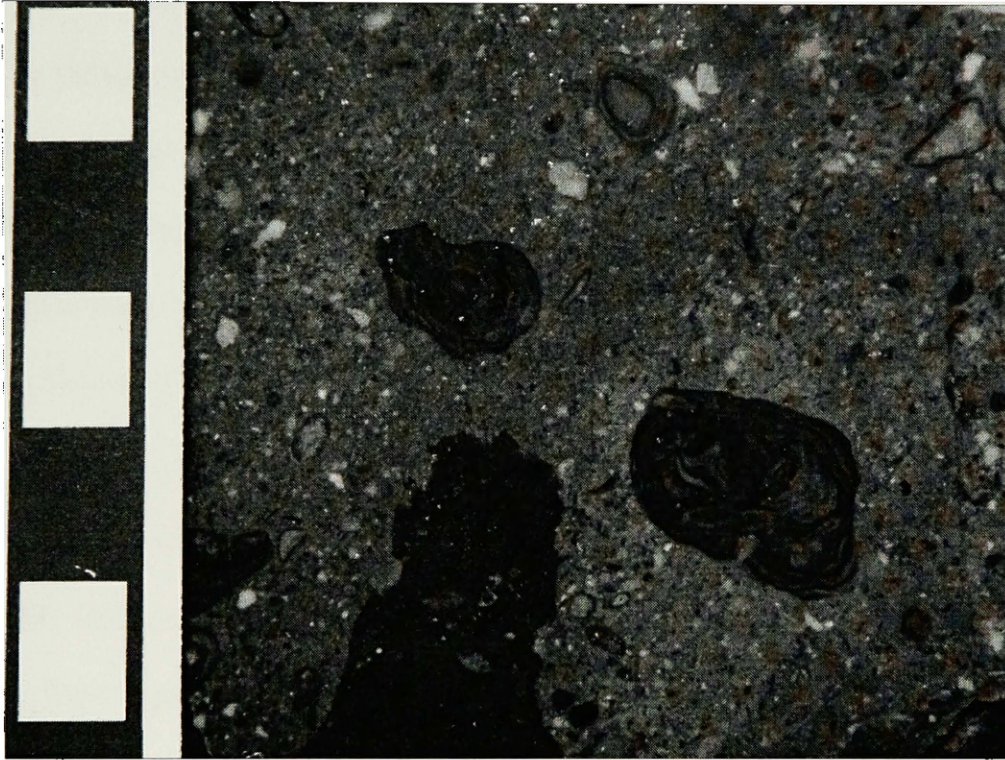
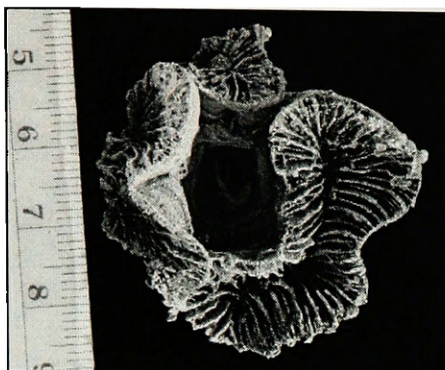


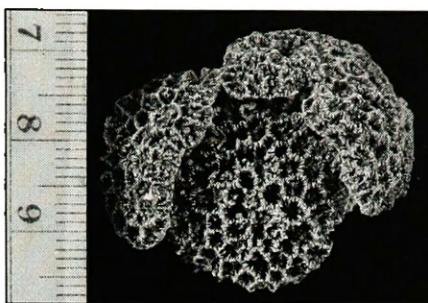
Figure 22. Cut slab of oncolidal limestone with chert lithoclasts (UMIP 303377) from Cornwallis Limestone at the base of the Flounder Cove succession (Figure 6b, site 99). Scale is in centimeters.

The Cornwallis Limestone directly overlies either the Paleozoic units via an erosional unconformity, or the Keku sedimentary strata. The Cornwallis Limestone also intertongues into the Keku sedimentary strata. Volcanic beds of the Hound Island Volcanics overlie the Cornwallis Limestone.

Paleontology: The Cornwallis Limestone is typified by many shallow-water fossils, including corals, sponges, spongiomorphs, gastropods, large oysters, brachiopods, *Stromatomorpha*, echinoid fragments, nautiloids, branching algae, and algal laminations (**Figure 23**). Many of these fossils, including the corals, spongiomorphs, and gastropods, are under study by George Stanley and Andrew Caruthers of the University of Montana and by Robert Blodgett of Anchorage, Alaska. *Stromatomorpha californica* is a large laminar fossil common to the terranes of western North America. In the past, Smith (1927) classified it as a hydrozoan, but it is probably a stromatoporoid. The unit also contains ammonoids, aulacocerids, and other bivalves. Boring and soft-sediment trace fossils were found at the Flounder Cove locality. In the area on eastern Kuiu Island area with sandier lithoclastic carbonates, carbonized plant remains are actually common (**Figure 6b, sites 71-73**). Most of the plant fossils display no diagnostic features, but some are well-preserved enough to see detail of leaves and branches (**Figure 24**). Well-preserved plant fossils do not occur in the purer carbonates, however carbonized wood fragments are common there (**Figure 24**). Conodonts, a scleractinian coral, and a brachiopod confirm a Late Triassic age for these plant fossils. Acid-etched carbonate blocks from the Flounder Cove locality (**Figure 6b, site 99**) yielded small bones of uncertain taxonomic affinity (**Figure 25**). A long rib-like bone (**Figure 25**) was also found in calcareous sandstone on the eastern side of Kuiu Island (**Figure 6b, site 72**).



Margarastraeid coral, MI 0099
UMIP 400043



Ceriod coral, MI 0099
Crassetella sp.
UMIP 228216



Branching Algae,
MI 0074
UMIP 302961



Sphinctozoid Sponge, MI 0056
UMIP 302765



Echinoid, MI 0056
UMIP 228300



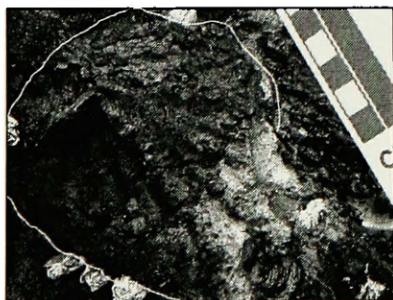
Spongiomorph, MI 0056
Spongiomorpha ramosa
UMIP 302764



Stromatoporoid?, MI 0056
Stromatomorpha californica
UMIP 302763



Gastropod, MI 0099
Spinidelphinulopsis whaleni
UMIP 228247
Blodgett and Frýda, 2001



Oyster, MI 0056
Field Picture



Brachiopods, MI 0099
Spondylospira sp.
UMIP 303089



Nautiloid, MI 0099
UMIP 228281

Figure 23. Representative macrofossils from the Cornwallis Limestone. Scales are in centimeters except for *Spinidelphinulopsis whaleni* where the scale is in millimeters.

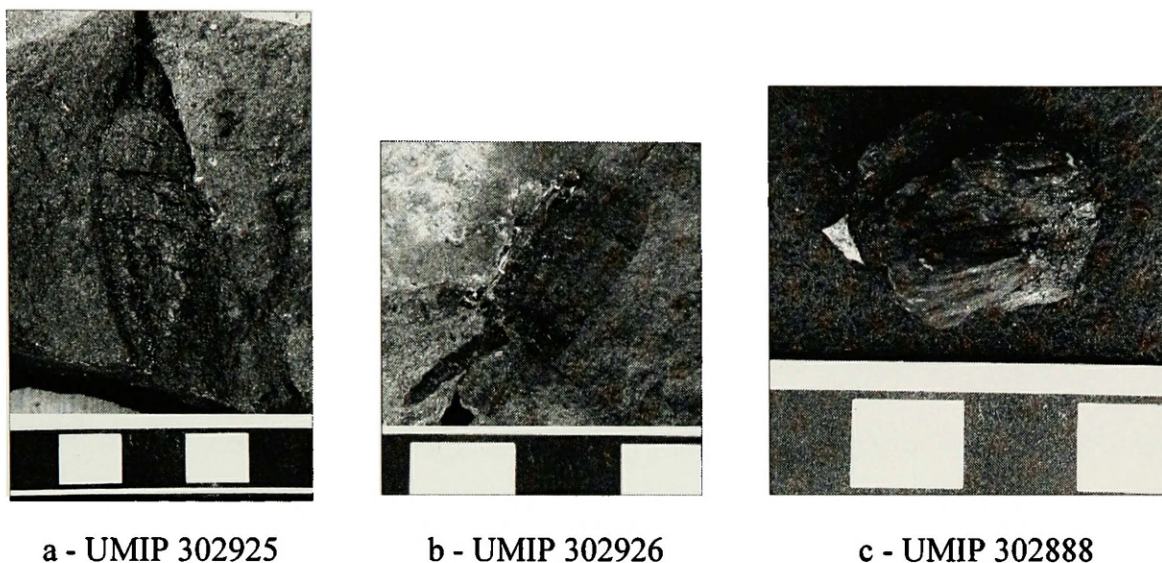


Figure 24. Plant specimens from the Cornwallis Limestone. (a) and (b) are leaves from eastern Kuiu Island (Figure 6b, site 73), and (c) is a carbonized piece of wood from eastern Cornwallis Peninsula (Figure 6a, site 70). Scales are in centimeters.

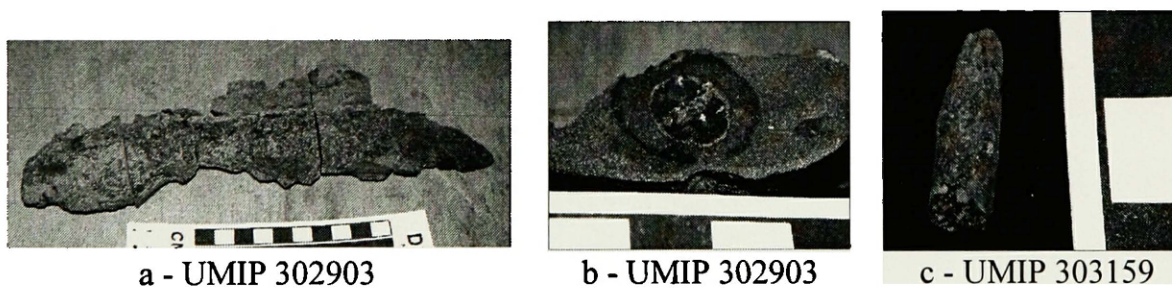


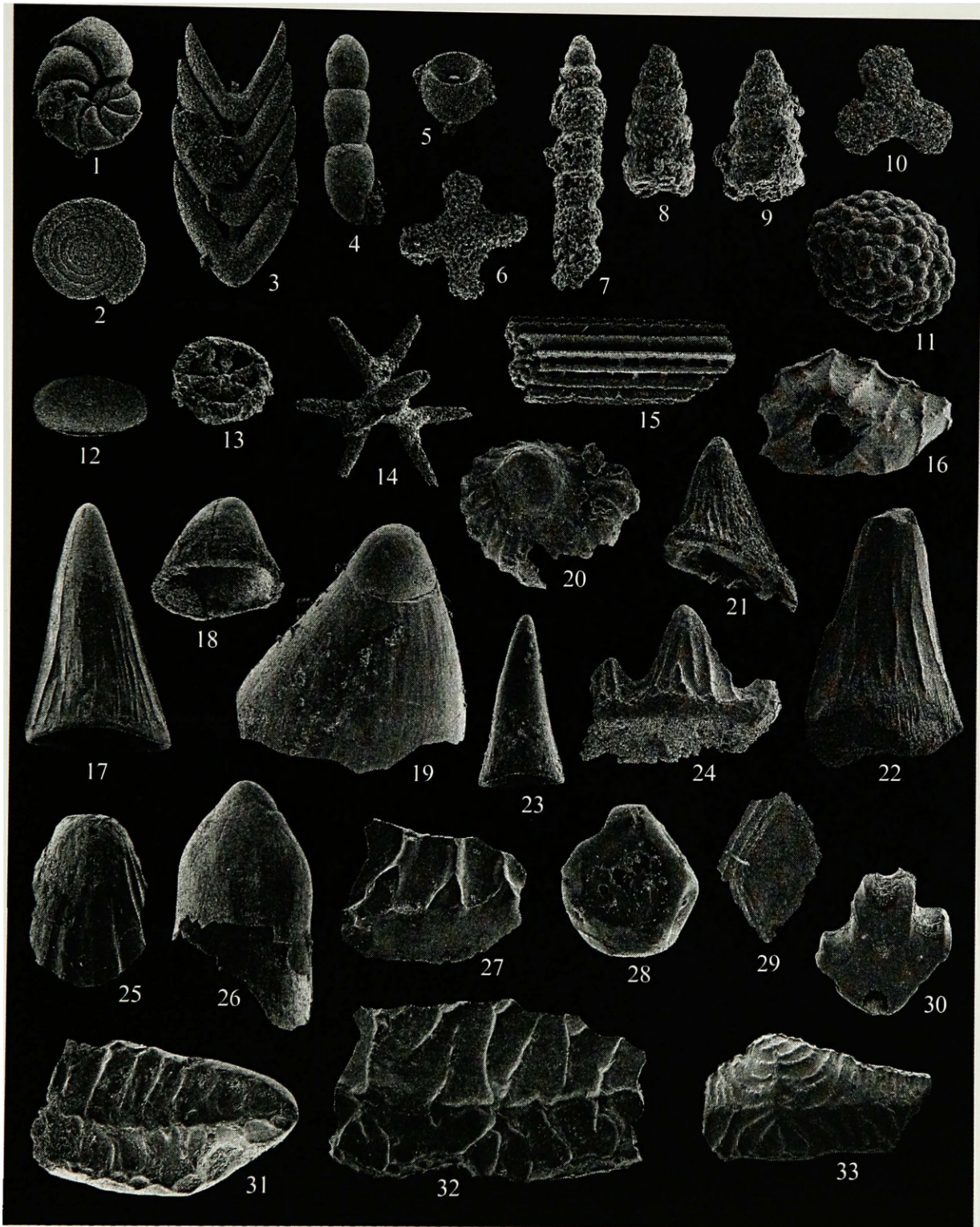
Figure 25. Vertebrate specimens from the Cornwallis Limestone. (a) is a bone from eastern Kuiu Island (Figure 6b, site 72), (b) is a cross section of (a), and (c) is a small bone from the Flounder Cove locality (Figure 6b, site 99). Scales are in centimeters.

Halobiid bivalves occur throughout the Flounder Cove locality and are useful for age determinations. Chris McRoberts of the State University of New York (SUNY) at Cortland is studying these bivalves. Microfossil residues from the Cornwallis Limestone include conodonts, bony fish teeth, bony fish scales, fish bones, shark teeth, shark dermal denticles, bivalves, gastropods, ammonoids, ostracodes, foraminifers, holothurian sclerites, sponge spicules, and echinoid spines (**Figure 26**). Conodonts reveal most of the Cornwallis Limestone to be of earliest Norian to late Early Norian age. Outcrops at the base of the Flounder Cove locality are of latest Carnian age, passing into Early Norian upsection (**Figure 21**).

Interpretation: The abundant shallow-water fossils (Silberling *in* Muffler, 1967), mildly reworked plant fossils, ooids, and oncoids strongly indicate a shallow marine environment for the Cornwallis Limestone. Lithoclastic and volcanoclastic clasts reveal sediment input from terrestrial erosion. Sedimentary structures such as various cross-beds and erosional surfaces in these lithoclastic units indicate higher current velocity and probable proximity to shore. Higher clastic input may have excluded many marine organisms in some deposits. Interbeds of finer-grained limestone may represent facies transitions into lagoonal or deeper water environments. The Flounder Cove locality may exemplify this as a lagoonal or inner slope deposit. A combination of boring and soft-sediment trace fossils from the Flounder Cove locality indicates intermittent development of hard-grounds in the carbonate. An erosional unconformity within the Flounder Cove section resulted in coarser-grained, mildly lithoclastic, massive limestone overlying the muddier beds. Overall, this unit represents shallow marine environments with good

Figure 26. Representative microfossils from the Cornwallis Limestone. Magnification is at x65 unless otherwise indicated.

- 1-5: foraminifers. 1) UMIP 303230, Loc 0099; 2) UMIP 303192, Loc 0056;
3) UMIP 303231, Loc 0099; 4) UMIP 303247, Loc 0099; 5) UMIP 303239,
Loc 0099
- 6-10: radiolarians. 6) UMIP 303228, Loc 0099, 7) x130, UMIP 303244, Loc 0099;
8) x130, UMIP 303229; Loc 0099; 9) x130, UMIP 303252, Loc 0099;
10) UMIP 303234, Loc 0099
- 11: frambooid, UMIP 303208, Loc 0070
- 12: ostracode at x43, UMIP 303242, Loc 0099
- 13: holothurian sclerite, UMIP 303232, Loc 0099
- 14: sponge spicule, UMIP 303187, Loc 0056
- 15: echinoid spine, UMIP 303237, Loc 0099
- 16-26: various teeth. 16) UMIP 303217, Loc 0074; 17) UMIP 303219, Loc 0074;
18) UMIP 303204, Loc 0069; 19) UMIP 303215, Loc 0070; 20) UMIP 303213,
Loc 0070; 21) UMIP 303198, Loc 0056; 22) x26, UMIP 303207, Loc 0070;
23) UMIP 303202, Loc 0069; 24) x43, UMIP 303222, Loc 0070;
25) UMIP 303203, Loc 0069; 26) UMIP 303201, Loc 0069
- 27-33: fish scales and dermal denticles. 27) UMIP 303205, Loc 0069;
28) UMIP 303194, Loc 0056; 29) x26, UMIP 303211, Loc 0070;
30) UMIP 303199, Loc 0069; 31) UMIP 303200, Loc 0069; 32) UMIP 303218,
Loc 0074; 33) x26, UMIP 303206, Loc 0070



carbonate production. It is distal to the Keku sedimentary strata, and coeval with the deeper water Hamilton Island Limestone.

Unnamed shallow-water limestone

Lithoclastic limestone similar to that of the Cornwallis Limestone occurs in two places on the east side of Keku Strait. In the Cape Bendel region (**Figure 6e, site 83**), lithoclastic limestone underlies units (**Figure 27**) identified with conodonts as Upper Carnian. This limestone contains chert pebbles of the Pybus Formation as well as other unidentified clasts. Microfossil residues from Cape Bendel include bony fish teeth, bony fish scales, and shark dermal denticles. The limestone deposits in this area (**Figure 6e, sites 83 and 84**) are entirely fault-bound, so their association with the Hound Island Volcanics is suspect. We remove these beds from the Hound Island Volcanics due to the absence of volcanoclastic material and their fault-bound nature. In Portage Pass (**Figure 6f, site 59**), lithoclastic limestone with Cannery Formation and Pybus Formation clasts contains a suspected Late Triassic oyster (**Figure 28a**). This limestone was previously mapped as Burnt Island Conglomerate (Muffler, 1967), and the lithoclastic limestone is still very close lithologically to the Burnt Island Conglomerate (**Figure 28b**). In both cases, these outcrops occur on the opposite side of the strait from the Cornwallis Limestone. Furthermore, the relationship between Triassic units on either side of the strait is unclear, as the amount of post-Triassic tectonic compression is unknown. The detached relationship of these unnamed limestone units to the defined Cornwallis Limestone prompts tentative classification of these outcrops as a separate unit. These



Figure 27a. Beds of lithoclastic, cross-bedded, unnamed shallow water limestone from Cape Bendel (Figure 6e, site 83). Hammer (33 cm) for scale.



Figure 27b. Beds of lithoclastic, unnamed shallow water limestone with boulders from Cape Bendel (Figure 6e, site 83). Hammer (33 cm) for scale.



Figure 28a. Oyster (UMIP 302920) from lithoclastic unnamed shallow water limestone from Portage Pass (Figure 6f, site 59). Scale is in centimeters.

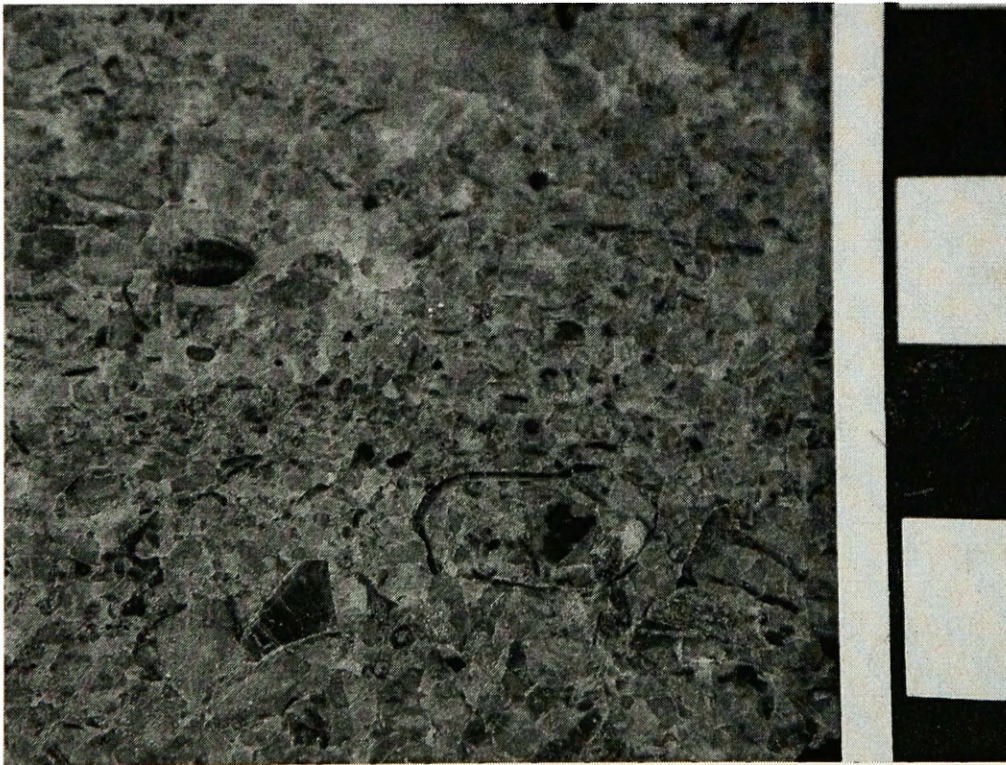


Figure 28b. Cut slab of lithoclastic unnamed shallow water limestone (UMIP 302920) with oyster (Figure 28a) from Portage Pass (Figure 6f, site 59). Scale is in centimeters.

rocks represent shallow marine deposition separate from the rocks on Cornwallis Peninsula, but may be assigned to the Cornwallis Limestone after further study.

Hamilton Island Limestone

Occurrence: The type locality of the Hamilton Island Limestone is the northern tip of Hamilton Island (Muffler, 1967). Elsewhere, it crops out west of Kupreanof Island in Hamilton Bay and on Hamilton Island, in the Keku Islets, and in the Cape Bendel region (**Figures 6c, 6d, 6e, 6f, and 6g**). Only two isolated outcrops represent the Hamilton Island Limestone in the Cape Bendel region (**Figure 6e, sites 84 and 91**).

Description: Very thin bedded, fine-grained limestone with black argillaceous laminae is typical of the Hamilton Island Limestone (Muffler, 1967). Debris flows and thin to medium beds of calcareous sandstone occur locally. The debris flows are beds with matrix-supported and poorly sorted sand to cobble sized clasts; the larger clasts show no preferred orientation. These debris flows contain clasts of Triassic limestone, clasts of the Cannery and Pybus formations, and reworked shallow-water Triassic fossils. A succession of strata at the northern end of Hamilton Island is a series of turbidite deposits based on fining-upwards beds and local low-angle cross-bedding (**Figure 6f, site 60, and Figure 29**). Soft sediment deformation interpreted as slump folding (**Figure 30**) and deposition of the majority of the succession in a single conodont zone (**Figure 29 and Appendix B**) suggest rapid deposition. The debris flows with Paleozoic clasts and Triassic limestone clasts that occur in the lower part of the succession are superficially similar to the Burnt Island Conglomerate (**Figure 6f, site 57, Figure 29, and Figure 31**).

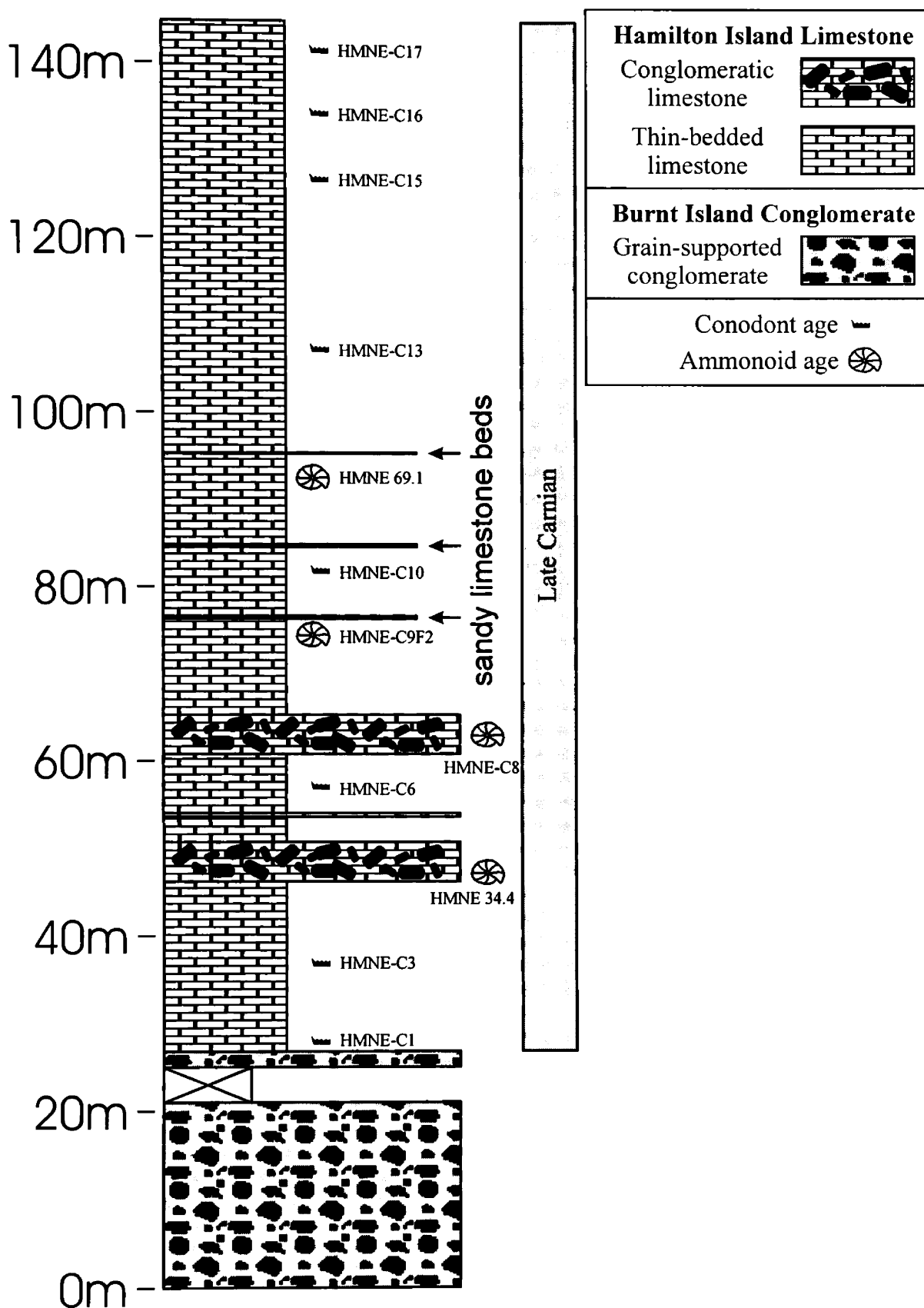


Figure 29. Representative stratigraphic section at the northeast shore of Hamilton Island with fossil determined ages. This section includes USGS Mesozoic localities M1882-84.



Figure 30. Slump fold from the Hamilton Island Limestone on northeast Hamilton Island (Figure 6f, site 60). The white plastic “S” is about 10 cm tall.

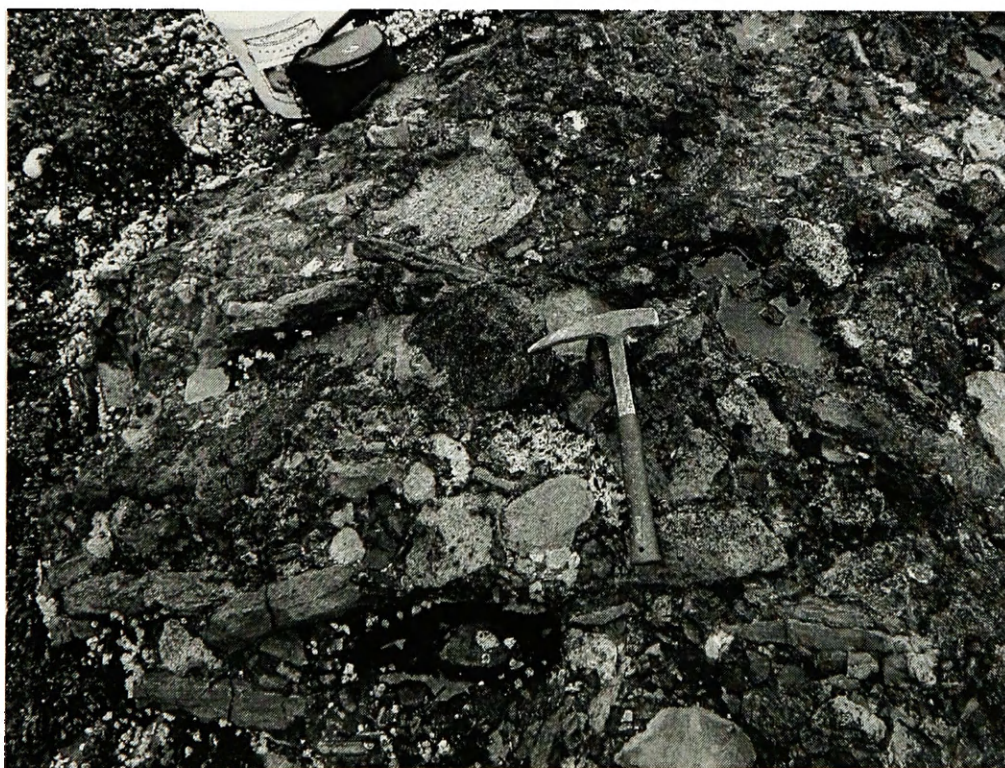


Figure 31. Debris flow conglomerate with Permian and Triassic clasts from the Hamilton Island Limestone on northeast Hamilton Island (Figure 6f, site 60). Hammer (33 cm) for scale.

Upsection, these conglomeratic beds contain fewer Paleozoic clasts and more Triassic clasts. Many of the Triassic clasts appear to be locally reworked from the Hamilton Island Limestone. These conglomeratic deposits get finer-grained upsection and calcareous sandstone represents them upsection.

The lower contact of this unit is the first limestone bed above the Burnt Island Conglomerate. Although it was not observed, the lower contact may onlap the erosional unconformity truncating Paleozoic units. For example, on the northeast side of the central part of Hamilton Island, and the northeast side of Hamilton Bay, the Hamilton Island Limestone appears to rest disconformably on the Pybus Formation (Muffler, 1967). However, exposure of the contact is not adequate to preclude a thin unit of Burnt Island Conglomerate (Muffler, 1967). Basalt and volcanoclastics of the Hound Island Volcanics conformably and sometimes transitionally overlie the Hamilton Island Limestone (Muffler, 1967). We speculate that the Hamilton Island Limestone is a deeper water facies of the Cornwallis Limestone, but lateral transitions confirming such a relationship are absent in the field area.

Paleontology: The bivalve *Halobia* characteristically dominates beds of the Hamilton Island Limestone (**Figure 32**). Bivalves from this unit are under study by Chris McRoberts of SUNY at Cortland. Based on ammonoid, halobiid, and conodont faunas, this unit is predominantly Late Carnian, though the uppermost beds are of Early Norian age. Fossiliferous clasts in the debris flow conglomerates within the northern Hamilton Island succession are of Late Carnian age. These indicate the erosion of Late Carnian limestone in the Late Carnian. In the Hamilton Island Limestone on the southern shore of Hamilton Island, shallow-water corals rarely occur in debris flow deposits, indicating a



Figure 32. Bedding surface covered in *Halobia* (UMIP 303065) from the Hamilton Island Limestone at the Squawking Crow locality (Figure 6c, site 97). Scale is in centimeters.

proximal source for the debris flows. Also, carbonized wood fragments occur locally in the Hamilton Island Limestone, and a silicified piece of wood was found on the northern end of Hamilton Island (**Figure 33**), further indicating reworking from proximal environments. A locality in Portage Pass preserved well-silicified *Halobia* (**Figure 34**); silicification of this thin bivalve is rare. Microfossil residues in the Hamilton Island Limestone include conodonts, bony fish teeth, shark dermal denticles, foraminifers, radiolarians, sponge spicules, a pyritized scolecodont tooth, and various tubular fossils (**Figure 35**). Finally, clasts of the Pybus Formation in the debris flow conglomerates on northern Hamilton Island have Permian crinoids, bryozoans, and brachiopods.

Interpretation: The dominance of *Halobia*, the presence of ammonoids, and the lack of other macrofossils are suggestive of a deep-water environment (Silberling *in* Muffler, 1967). The turbiditic nature and uniform age of the beds overlying the Burnt Island Conglomerate suggest that rapid infill of the basin continued after deposition of the Burnt Island Conglomerate and probably slowed into the Norian. Upper Carnian rock fitting this description crops out in the Cape Bendel region and was formerly included in the Hound Island Volcanics (**Figure 6e, site 84**). Similar, undated beds occur inland of Cape Bendel near outcrops of Burnt Island Conglomerate (**Figure 6e, site 91**). The absence of volcanoclastic material in these beds, and their fault-bound nature suggests they are separate from the Hound Island Volcanics and equivalent to the Hamilton Island Limestone.



Figure 33. Silicified wood fragment (UMIP 303378) from the Hamilton Island Limestone on northeast Hamilton Island (Figure 6f, site 60). Scale is in centimeters.

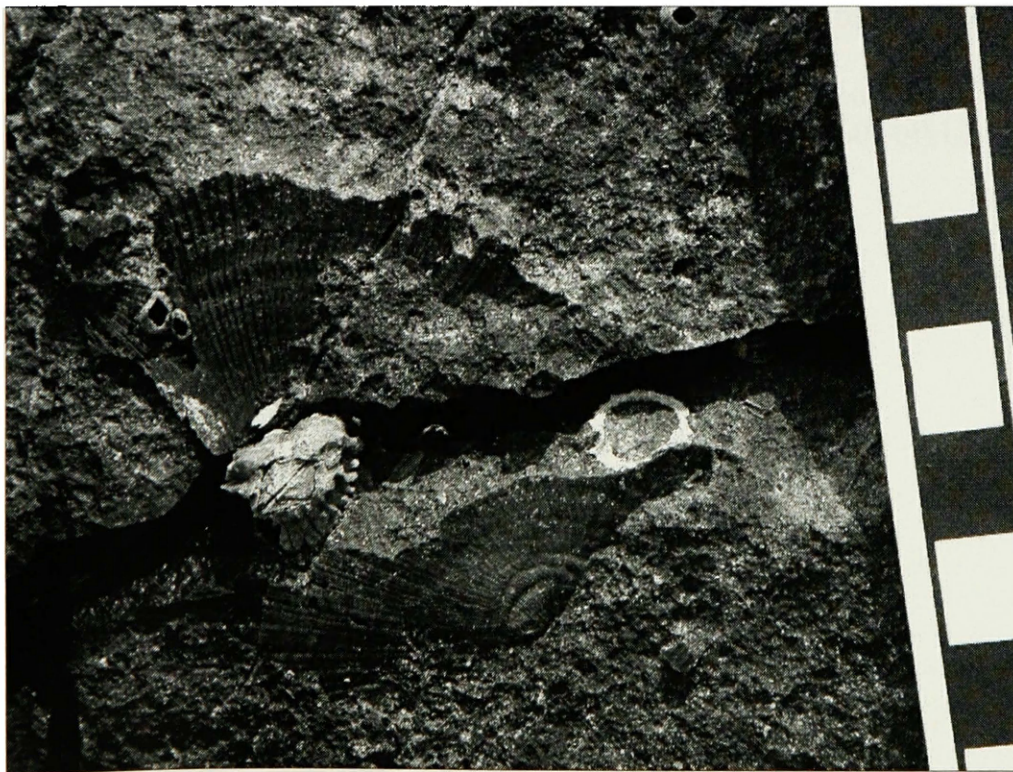
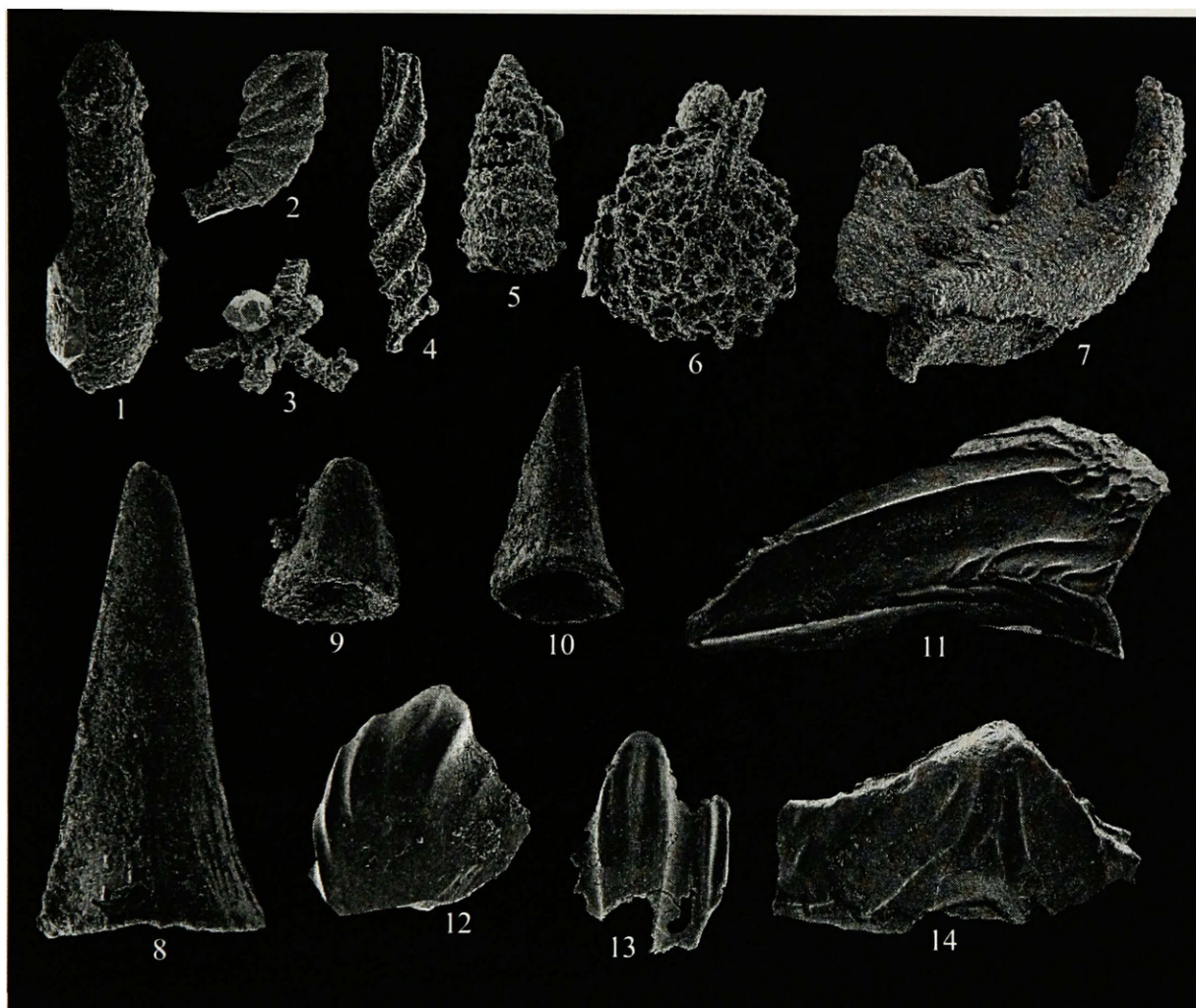


Figure 34. Silicified *Halobia ornatissima* (uncollected) from the Hamilton Island Limestone in Portage Pass (Figure 6f, site 66). Scale is in centimeters.

Figure 35. Representative microfossils from the Hamilton Island Limestone. Magnification is at x65 unless otherwise indicated.

- 1-2: foraminifers. 1) UMIP 303265, Loc 0060; 2) UMIP 303276, Loc 0060
- 3: sponge spicule, UMIP 303272, Loc 0060
- 4-6: radiolarians at x130. 4) UMIP 303268, Loc 0060, 5) UMIP 303269, Loc 0060;
6) UMIP 303273; Loc 0060
- 7: scolecodont, UMIP 303279, Loc 0060
- 8-10: various teeth. 8) UMIP 303261, Loc 0067; 9) UMIP 303263, Loc 0067;
10) UMIP 303260, Loc 0067
- 11-14: fish scales and dermal denticles. 11) UMIP 303262, Loc 0067;
12) UMIP 303280, Loc 0060; 13) UMIP 303281, Loc 0060; 14) UMIP 303274,
Loc 0060



Hound Island Volcanics

Occurrence: The type locality of the Hound Island Volcanics is the shores of Hound Island (Muffler, 1967). The unit also occurs on Kuiu Island, the Keku Islets, around Hamilton Bay, on Hamilton Island, in the Cape Bendel region, and on Turnabout Island (**Figures 6b, 6c, 6d, 6e, 6f, and 6g**).

Description: The Hound Island Volcanics consists mainly of basaltic pillow lava, basaltic pillow breccia, massive basalt, andesitic volcanic breccia, and hyaloclastic tuff with subordinate tuffaceous polymict conglomerate, limestone, and volcanoclastic sandstone (Muffler, 1967). Nomenclature for many of the volcanic deposits described by Muffler (1967) followed Carlisle (1963). Undevitrified, basaltic volcanic glass occurs locally in hyaloclastic tuff due to rapid cooling underwater (Brew and Muffler, 1965; Muffler *et al.*, 1969). The andesitic breccia and polymict conglomerate frequently form thick beds that are prominent in the field. The matrix of the breccia is commonly calcareous (Muffler, 1967), and breccia fragments are mostly Triassic limestone and volcanic rock, but sometimes are derived from Paleozoic units. The breccia beds resemble huge debris flows, as they are matrix-supported and poorly sorted units with a wide range of grain sizes (**Figure 36**). The largest clasts show no preferred orientation. Pumice fragments occur rarely in the Hound Island Volcanics (Muffler, 1967) and Buddington and Chapin (1929) reported volcanic bombs in places. Additionally, pahoehoe was found in the Cape Bendel region (**Figure 37**). The limestone is fine-grained, and generally occurs as interbeds or sometimes as a sediment drape over basalt pillows (**Figure 38**). These interbeds are often lenticular (**Figure 39**) or occur as

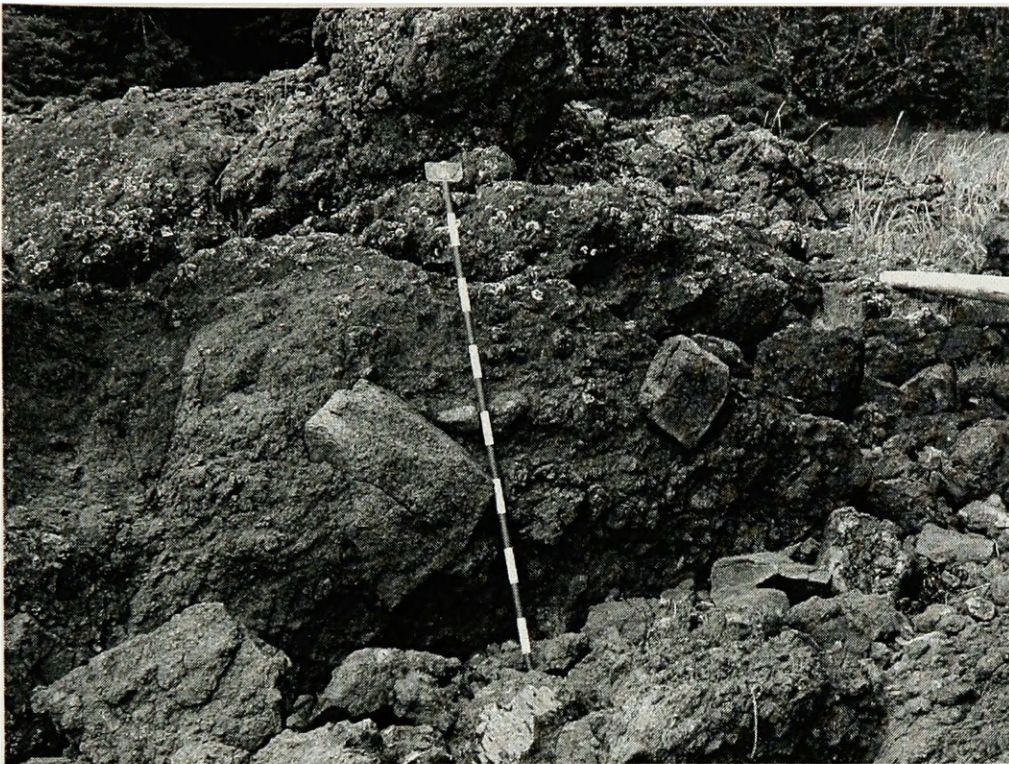


Figure 36. Debris flow breccia from the Hound Island Volcanics on western Hamilton Island (Figure 6f, north of site 77). Meter stick (10 cm subdivisions) for scale.

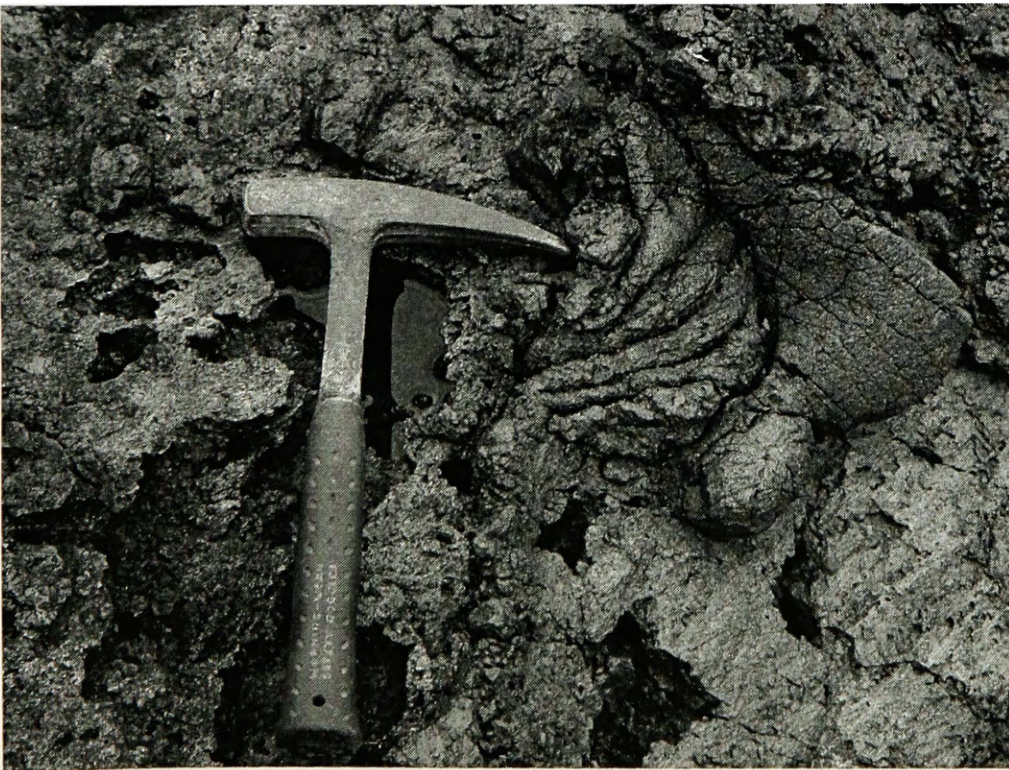


Figure 37. Pahoehoe from the Hound Island Volcanics in the Cape Bendel region. Hammer (33 cm) for scale.

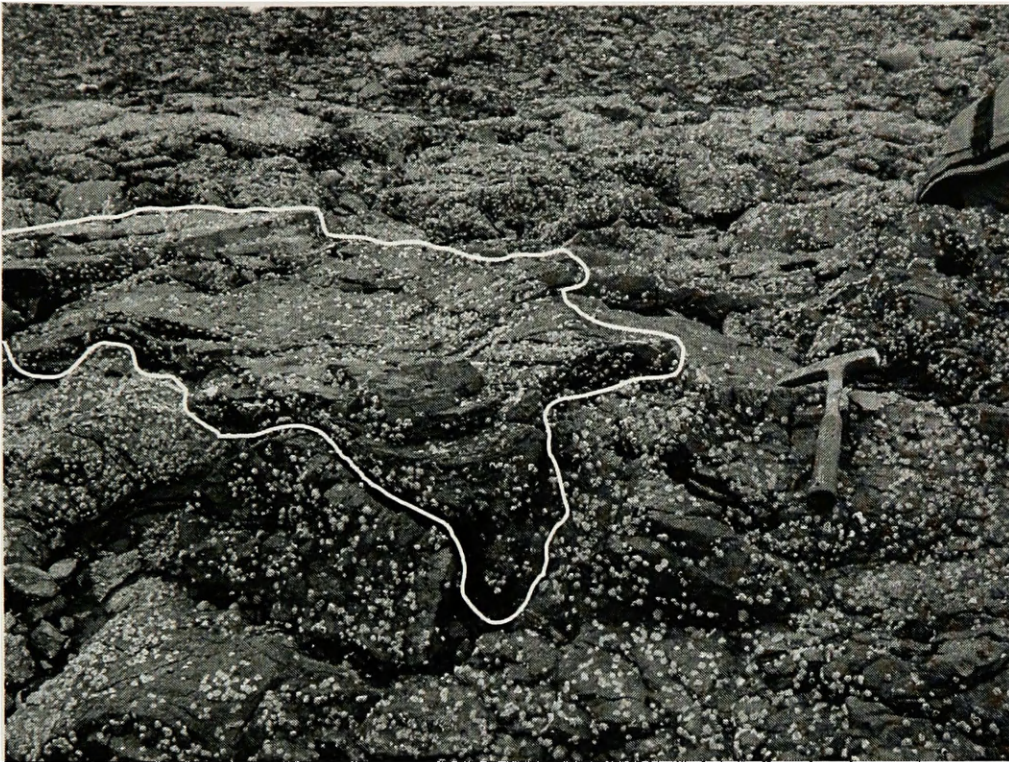


Figure 38. Limestone (outlined) draping basalt pillows from the Hound Island Volcanics. Outcrop is in Hamilton Bay, along the shoreline northeast of Little Hamilton Island (Figure 6g). Hammer (33 cm) for scale.

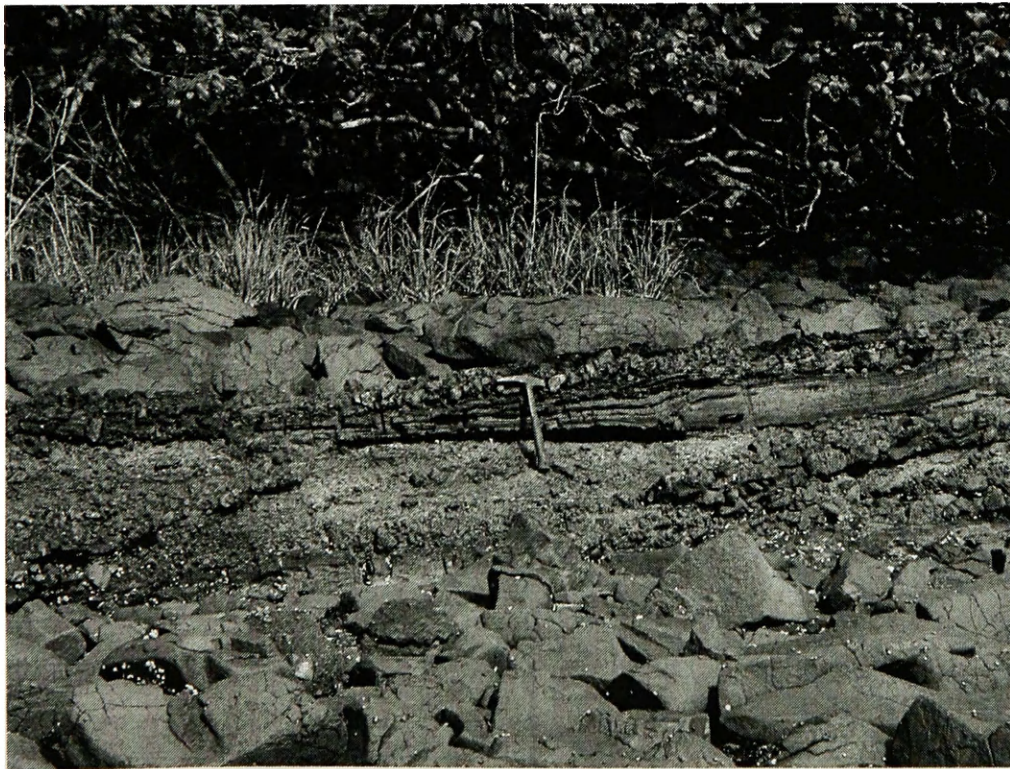


Figure 39. Pinching out of lensoid limestone bed (behind hammer) in Hound Island Volcanics from the western coast of Hound Island (Figure 6d, site 81). The succession includes, from bottom to top, basalt, volcaniclastics, limestone, volcaniclastics, and basalt. Hammer (33 cm) for scale.

stringers of limestone (Muffler, 1967). Its lithology and appearance is very similar to that of the Hamilton Island Limestone, but its association with volcanic rock of this unit leads to a higher concentration of fine-grained siliciclastics. A thicker succession of this limestone crops out on the eastern shore of Hound Island (**Figure 6d, site 86, and Figure 40**). Limestone beds lower in the succession overlie an andesitic debris flow (**Figure 40**). Within this succession are numerous lag deposits containing sulfides, volcanoclastic debris, and abundant bones. Another limestone succession, though structurally disjointed, crops out in the Gil Harbor mudflat (**Figure 6b, site 87**). The older beds in this area are typical fine-grained limestone beds, while the younger beds are thicker, fossiliferous packstone with abundant shallow-water fossils. Additional shallow-water limestone crops out along the coast south of Gil Harbor and in Kadake Bay (**Figure 6b**).

The base of the Hound Island Volcanics is marked by the first occurrence of major basaltic and andesitic volcanism or associated volcanoclastic deposits. The pre-Upper Jurassic unconformity overlies this unit.

Paleontology: With the wide variety of different facies in the Hound Island Volcanics, a wide variety of fossil types also occur. Buddington and Chapin (1929) reported carbonized plant fossils in sandstones of this unit on Turnabout Island, north of Cape Bendel. Trace fossils occur in some of the volcanoclastic sandstone (**Figure 41**). The presence of a starfish resting trace (**Figure 41a**) indicates a marine environment for these volcanoclastic beds. Some of the vertebrate material in the limestone succession on the eastern shore of Hound Island is ichthyosaur bone. Neogondolellid conodonts are particularly abundant in the eastern Hound Island succession as well. Throughout the area, halobiid bivalves dominate the fine-grained limestone beds, as in the Hamilton

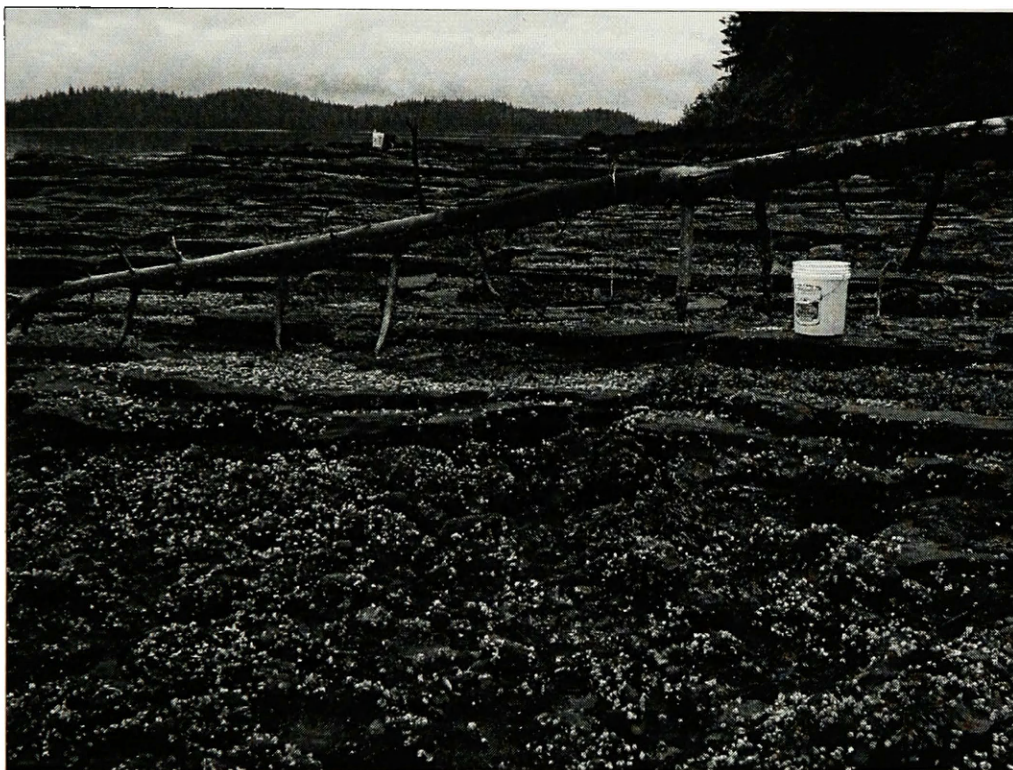


Figure 40. Succession of gently-dipping, fine-grained, *Halobia*-rich limestone overlying andesitic conglomerate (foreground). The outcrop is in the Hound Island Volcanics on the east coast of Hound Island (Figure 6d, site 86). Both buckets are about 40 cm tall.

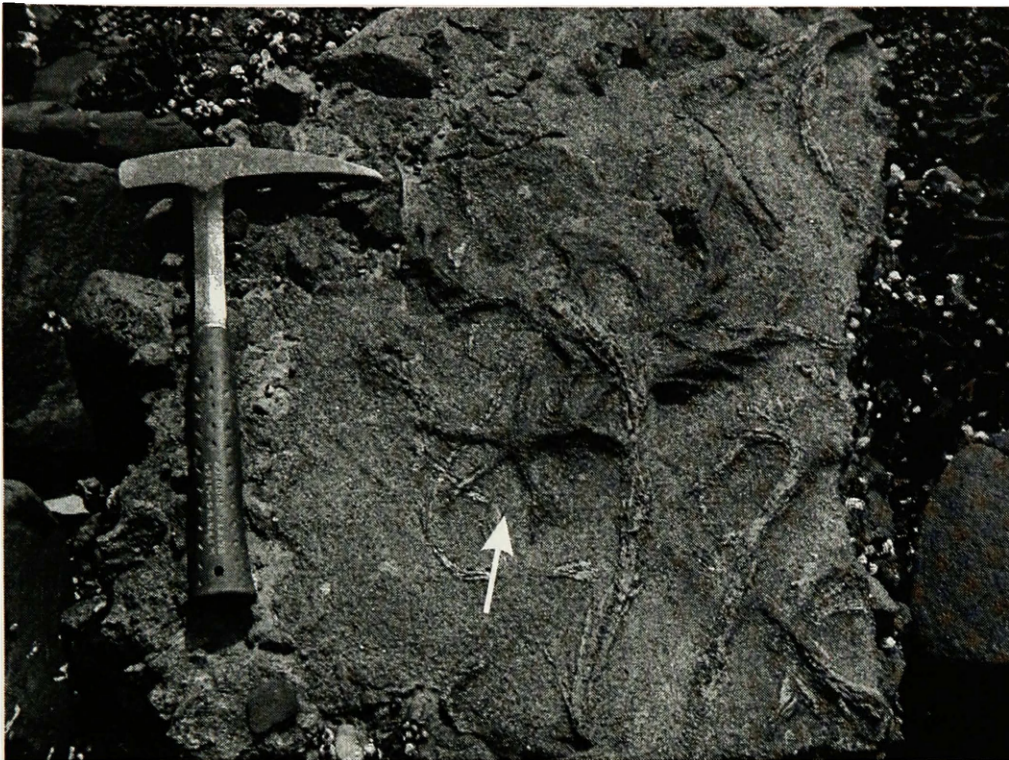


Figure 41a. Trace fossils in volcanic sandstone from the Hound Island Volcanics on western Hound Island (Figure 6d, site 81). White arrow points to starfish resting trace. Hammer (33 cm) for scale.

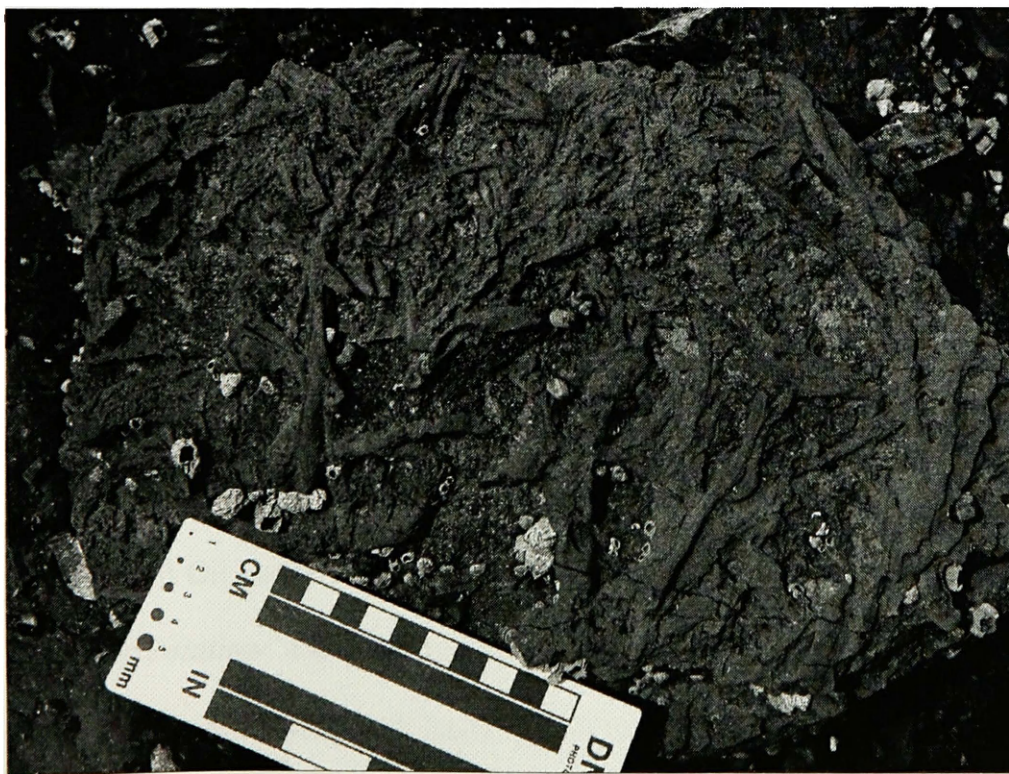


Figure 41b. Trace fossils in volcanic sandstone from the Hound Island Volcanics on western Hound Island (Figure 6d, site 79). Scale is in centimeters

Island Limestone. *Monotis* also occurs in a locality in southeastern Hamilton Bay (**Figure 6g, site M1898**), and in deposits at the Gil Harbor mudflat (Muffler, 1967) (**Figure 6b, site 87**). These younger deposits in Gil Harbor contain abundant silicified fossils including corals, many different bivalves, gastropods, ammonoids, aulacocerids, *Heterastridium*, echinoid spines, and trace fossil tubes (**Figure 42**), as well as carbonized wood fragments. Each bed from these deposits contains a distinct combination of fossil taxa, probably representing different biofacies. Gastropods from Gil Harbor (**Figure 6b, site 87**) include the genus *Chulitnacula*, which is endemic to the Chulitna, Farewell, and Alexander terranes (Frýda and Blodgett, 2001). One trace fossil consists of sinuous tubes that burrowed through softer sediment around the other fossils in three dimensions. The other trace fossil is a tubular boring oriented at various angles and directions through fossil material. A few shallow-water limestone samples from south of Gil Harbor have echinoid spines (**Figure 6b, site 46**). Shallow-water microfossil residues yielded conodonts, bony fish teeth, bony fish scales, fish bones, shark dermal denticles, bivalves, gastropods, ostracodes, foraminifers, and various tubular fossils (**Figure 43**). Deep-water microfossil residues yielded conodonts, bony fish teeth, bony fish scales, fish bone, bivalves, foraminifers, radiolarians, and various tubular fossils (**Figure 43**). Biostratigraphically significant fossils encompass ages from late Early Norian through Late Norian. The *Monotis* occurrences represent the only two Late Norian localities, and conodonts from Gil Harbor confirm a Late Norian age.

Interpretation: This unit represents basaltic and andesitic volcanism throughout the area. Fossils associated with basaltic rock indicate volcanism began in the late Early Norian. This coincides with the youngest age obtained in carbonate units of the



Figure 42. Silicified fossil bed with mostly shallow-water bivalves from the Hound Island Volcanics in the Gil Harbor mudflat (Figure 6b, site 87). Scale is in centimeters.

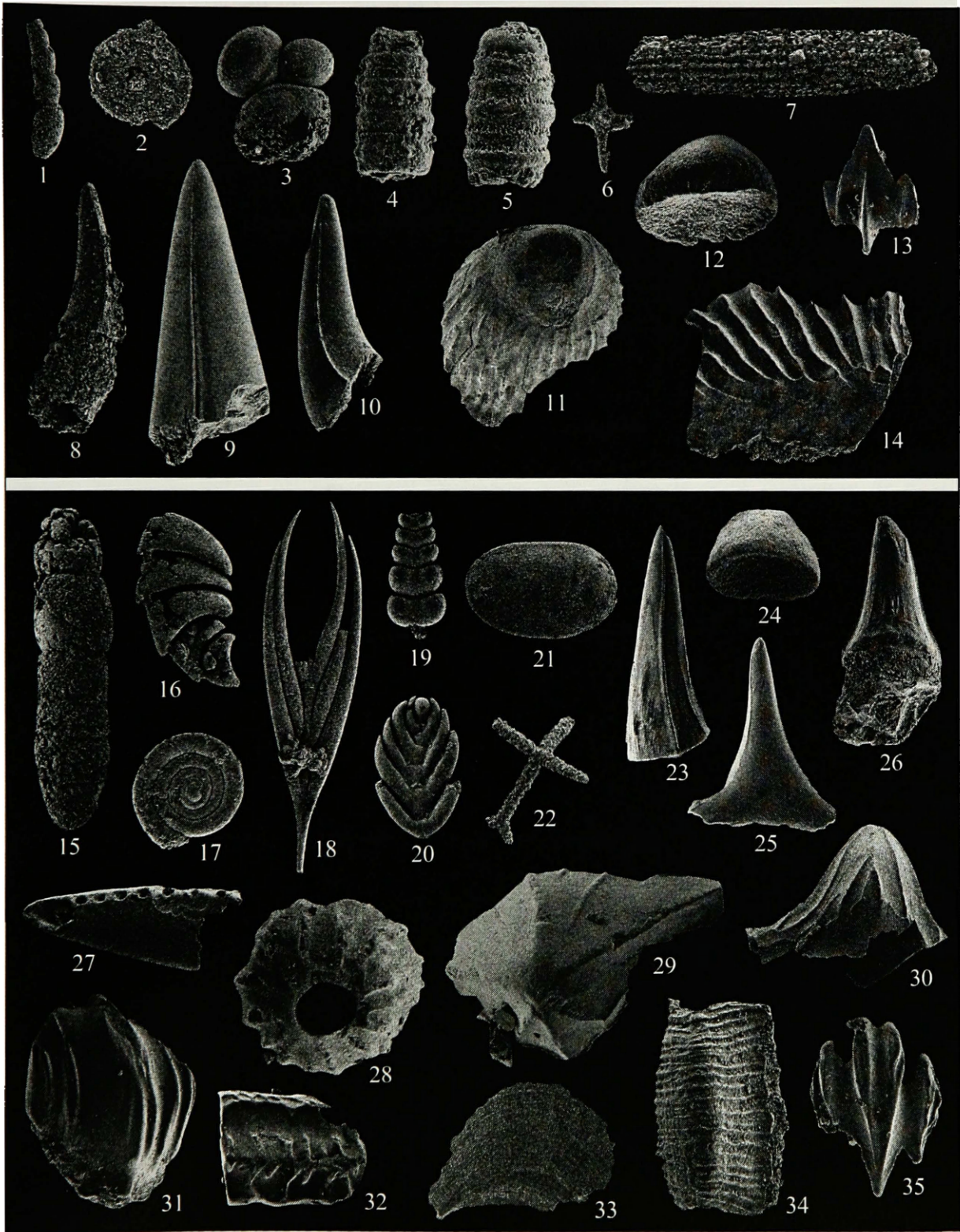
Figure 43. Representative microfossils from the Hound Island Volcanics. Magnification is at x65 unless otherwise indicated.

Shallow water carbonate facies:

- 1-3: foraminifers. 1) UMIP 303287, Loc 0086; 2) UMIP 303294, Loc 0086;
 3) UMIP 303290, Loc 0082
 4-5: radiolarians at x130. 4) UMIP 303291, Loc 0082, 5) UMIP 303292, Loc 0082
 6: sponge spicule, UMIP 303299, Loc 0081
 7: echinoid spine at x43, UMIP 303298, Loc 0086
 8-12: various teeth. 8) UMIP 303286, Loc 0086; 9) x43, UMIP 303297, Loc 0086;
 10) x43, UMIP 303288, Loc 0082; 11) x43, UMIP 303295, Loc 0086;
 12) UMIP 303285, Loc 0086
 13-14: fish dermal denticle and scale. 13) UMIP 303284, Loc 0086; 14) x43,
 UMIP 303296, Loc 0086

Deep water carbonate facies:

- 15-20: foraminifers. 15) UMIP 303305, Loc 0087; 16) UMIP 303304, Loc 0087;
 17) UMIP 303308, Loc 0087; 18) UMIP 303307, Loc 0087; 19) UMIP 303321,
 Loc 0087; 20) UMIP 303309, Loc 0087
 21: ostracode at x43, UMIP 303320, Loc 0087
 22: sponge spicule, UMIP 303311, Loc 0087
 23-26; 28-30: various teeth. 23) x26, UMIP 303317, Loc 0087; 24) UMIP 303312,
 Loc 0087; 25) x43, UMIP 303324, Loc 0087; 26) UMIP 303302, Loc 0046;
 28) UMIP 303318, Loc 0087; 29) UMIP 303316, Loc 0087; 30) x43,
 UMIP 303315, Loc 0087
 27: jawbone? at x26, UMIP 303322, Loc 0087
 31-35: fish scales and dermal denticles. 31) x26, UMIP 303323, Loc 0087; 32) x43,
 UMIP 303313, Loc 0087; 33) x26, UMIP 303303, Loc 0046; 34) UMIP 303300,
 Loc 0046; 35) UMIP 303314, Loc 0087



Cornwallis Limestone. Carbonates from the Cornwallis Limestone are not associated with basaltic volcanism but contain late Early Norian fossils. Volcanism continued into at least the Middle Norian and possibly into the Late Norian. Pumice fragments, pahoehoe, volcanic bombs, and erosional debris flows along with pillow lavas suggest volcanism in both subaerial and subaqueous environments. The scarcity of Late Norian fossils may suggest post-Triassic erosion.

Carbonate units in the Hound Island Volcanics preserve both shallow and deep-water depositional environments. Packstone beds from Gil Harbor contain abundant silicified shallow-water fossils. These fossils are reworked, but not enough occurred before burial to break up the many large and fragile fossils with complete or nearly complete preservation. Additionally, the presence of many different biofacies indicates relatively little transport. Trace fossils show no vertical variation within each bed, indicating relatively uniform conditions. Overall, these features and the lack of adjacent beds with finer-grained sediments or turbiditic or storm-related sedimentary structures indicate deposition in a shallow-water environment above normal wave base. On eastern Hound Island, the abundance of neogondolellid conodonts and the fine-grained, well-bedded rocks suggest a deeper water environment (Mercantel, 1973; Behnken, 1975; Babcock, 1976; Carey, 1984; Carr *et al.*, 1984; Carter and Orchard, 2000).

Biostratigraphy

Ammonoids, specific bivalves, and conodonts are the most important index fossils in the Upper Triassic, and combining data from these taxonomic groups provides powerful biostratigraphic resolution (**Figure 44**). Using complete exposures in northeast British Columbia, Tozer (1967; 1984; 1994) pieced together a complete ammonoid zonation for the Upper Triassic of western Canada. The “flat clams” *Halobia* and *Monotis* occur worldwide and are important in Triassic biostratigraphy (McRoberts, 1997; Silberling *et al.*, 1997). *Halobia* ranged from the Carnian into the Middle Norian where it coexisted with *Monotis* briefly before being succeeded by *Monotis* (McRoberts, 1997; Silberling *et al.*, 1997). *Monotis* continued into the Upper Norian, but not to the end of the Triassic (Silberling *et al.*, 1997). The spherical hydrozoan *Heterastridium conglobatum* also occurs in the Keku Strait and adds to age determinations. It is abundant in deposits of Cordilleranus Zone age (**Figure 44**) in the North American Cordillera (Silberling and Tozer, 1968; Tozer, 1994). *Heterastridium* may range down into the Columbianus Zone (**Figure 44**) of the Middle Norian (Tatzreiter, 1975; Krystyn and Wiedmann, 1986; Stanley *et al.*, 1994) and possibly into the Rhaetian (Gonzalez *et al.*, 1996). Krystyn (pers. comm. 2003) and Stanley (e.g. Stanley *et al.*, 1994) postulate that within *Heterastridium* populations, individuals display an increase in their maximum diameter through time, possibly permitting determination of age.

While ammonoids, *Halobia*, *Monotis*, and to some extent *Heterastridium*, are valuable and provide good biostratigraphic data, macrofossils can be difficult to locate because tectonostratigraphic terranes often have limited outcrop extent due to restricted

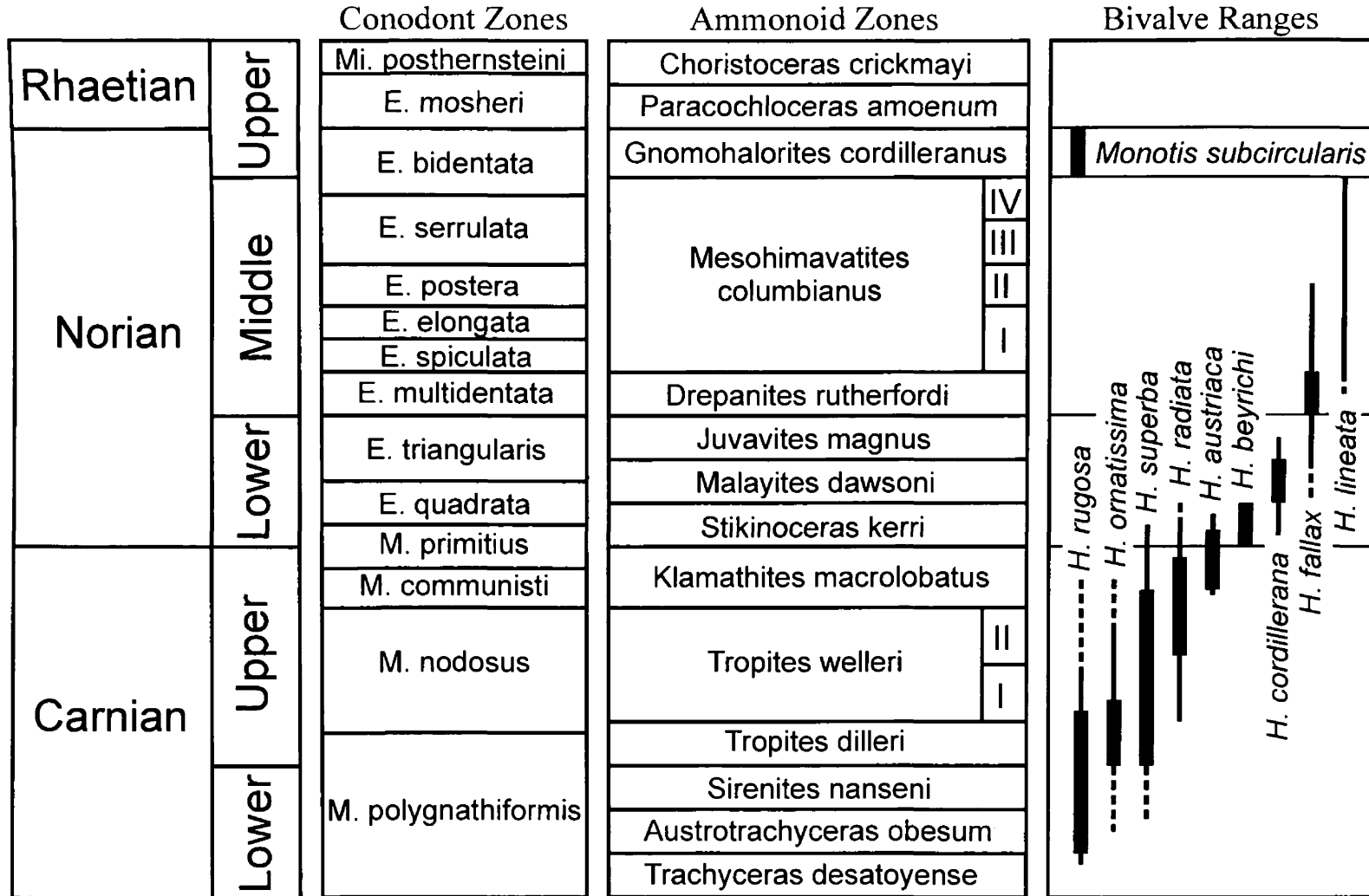


Figure 44. Late Triassic biochronology displaying conodont zones, ammonoid zones, and selected bivalve ranges. *Heterastridium conglobatum* occurs in the Cordilleranus ammonoid zone with *Monotis subcircularis*. Generic abbreviations are: M.= *Metapolygnathus*, E.= *Epigondolella*, Mi.= *Misikella*, H.= *Halobia*. (ammonoid zones after Tozer, 1967; 1984; 1994; Orchard and Tozer, 1997) (approximate bivalve ranges after McRoberts, 1993; 1997; Silberling *et al.*, 1997; McRoberts, pers. comm. 2003) (conodont zones after Orchard, 1991b; Orchard and Tozer, 1997)

original lateral extent and structural complications. Conodonts occur in a greater variety of facies, are less susceptible to destructive diagenetic processes, and commonly occur in the smallest outcrop or individual clast. Detailed biostratigraphic work with conodonts is still lacking in most terrane localities. A complete conodont biostratigraphy for the Upper Triassic is still being developed (Kozur, 1980; Krystyn, 1980; Orchard, 1991a; 1991b; Buryi, 1997; Orchard and Tozer, 1997). The zonations presented by Orchard are based on a “highly resolved and intercalibrated conodont-ammonoid zonation” (Carter and Orchard, 2000) from extensive work done in northeast British Columbia (Orchard, 1991b; Orchard and Tozer, 1997; Carter and Orchard, 2000). This zonation is applicable to Triassic rocks in a number of Cordilleran terranes, including the Queen Charlotte Islands of Wrangellia (Orchard, 1991a; Carter and Orchard, 2000). It is also applicable to the biostratigraphic succession in the Keku Strait area.

Conodonts were the focus of this study. In addition, L. Krystyn and N.J. Silberling examined and/or identified associated ammonoids and C.A. McRoberts identified halobiid bivalves. Following Orchard (1991b) and Tozer (1994), standard ammonoid zones begin with an upper case letter and are not in italics, while conodont zones are presented in italics as their formal species names. In the sections below, we discuss only biostratigraphically significant fossils, which are listed in **Appendix B**.

Reworked Paleozoic fossils occur locally in the Late Triassic deposits of the Keku Strait area. Carboniferous and Permian macrofossils in reworked clasts are common in the Burnt Island Conglomerate, lithoclastic beds of the Keku sedimentary strata, and the Cornwallis Limestone, while Devonian clasts also occur in the Cornwallis Limestone.

Conodonts of Devonian and Early Permian age were identified in Late Triassic rock (**Plate 1 and Appendix B**).

Tozer (1967) picked the base of the Kerri Zone as the Carnian-Norian boundary (**Figure 44**), but the precise position of this boundary remains undefined. Previously, the conodont *Neogondolella navicula* was used as an indicator of the Carnian-Norian boundary. This taxon has since been shown to be facies controlled, and occurrences of the genus in the Late Carnian appear similar to the Early Norian form (Carter and Orchard, 2000; Orchard, pers. comm. 2003). Furthermore, *Metapolygnathus primitius* originates in the Macrolobatus Zone and overlaps into the Kerri Zone, so no current conodont origination coincides with the base of the Kerri Zone (Orchard, 1983; 1991a; 1991b; Orchard and Tozer, 1997). Radiolarian distributions also do not coincide well with the base of the Kerri Zone (Carter and Orchard, 2000). We use the traditional definition in this paper for convenience (**Figure 44**), but it is important to note that workers are striving to define the Carnian-Norian precisely.

Middle Triassic

Only one fossil indicating a Triassic age earlier than Late Triassic has been reported in the Alexander terrane. The uppermost Anisian (Middle Triassic) conodont *Neogondolella acuta* was found on Big Saltery Island, just east of the Keku Strait area, southeast of Kupreanof Island (Wardlaw *in* Karl *et al.*, 1999). However, because this fossil was in a limestone debris flow, its occurrence may indicate deposition and

subsequent erosion of pre-Late Triassic age rock, accounting for the lack of Middle Triassic rock in the field area.

Early Carnian

Fossils indicating an Early Carnian age also are rare. Silberling *in* Muffler (1967) reported the bivalve *Halobia* sp. cf. *H. rugosa* and the ammonoid *Coroceras* sp. cf. *C. suessi* from the Burnt Island Conglomerate on southeastern Hamilton Island (**Figure 6f, site 67**). Silberling *in* Berg (1981) identified *Halobia rugosa* (**Figure 44**) in fossiliferous metasedimentary strata about 25 km southwest of Petersburg, east of the map area. Wardlaw (1982) described primitive forms of the Early Carnian conodont *Metapolygnathus polygnathiformis* (**Figure 44**) from metamorphosed carbonate east of the map area at USGS Mesozoic locality 32771. The presence of Early Carnian fossils in the Burnt Island Conglomerate, and Early Carnian fossils in units nearby, suggests that Early Carnian limestone was being eroded after deposition. This could account for the lack of preservation of Early Carnian and older units in the field area.

Late Carnian

Biostratigraphically significant fossils of Late Carnian age occur in the Burnt Island Conglomerate, throughout the Hamilton Island Limestone, in the Cornwallis Limestone, and in the unnamed shallow-water limestone. Late Carnian conodonts recovered include *Metapolygnathus polygnathiformis*, *M. carpathicus*, *M. nodosus*, *M.*

reversus, *M. zoeae*, and *M. primitius* (**Plates 2 and 3 and Appendix B**). Other than *M. primitius*, all of these occur in the *nodosus* Zone *sensu* Orchard (1991b) (**Figure 44**). *Metapolygnathus nodosus* ranges into the Early Norian, but when abundant, and not co-occurring with Norian fossils, it is interpreted as Late Carnian in age. *Metapolygnathus primitius* ranges into the Early Norian further than *M. nodosus*, and is interpreted as either Late Carnian or Early Norian in age. Populations of *M. primitius* are covered in the next section. Furthermore, in the genus *Metapolygnathus*, the basal pit begins shifting towards the anterior end of the conodont in the Late Carnian (Orchard, 1991b). This progression can indicate an approximate biostratigraphic position within the Late Carnian, particularly in the latest Carnian. *Metapolygnathus primitius* has a medially located pit, and specimens which look like *M. primitius*, but have a posterior pit, are referred to *M. sp. cf. M. primitius*. This conodont ranges into the Early Norian, and is treated the same as *M. nodosus* biostratigraphically. Silberling *in* Muffler (1967) reported a number of Late Carnian ammonoids and halobiid bivalves; both fossil groups were recovered in this study.

Cornwallis Limestone samples from the base of the section at the Flounder Cove locality (**Figures 6b, site 99, and Figure 21**) yielded *Metapolygnathus nodosus*, *M. sp. cf. M. nodosus*, *M. sp. aff. M. zoeae*, and *M. sp. cf. M. primitius*. In conjunction with *Halobia ornatissima* (McRoberts, pers. comm. 2003), these samples are Late Carnian in age (**Figure 44**). The overlying beds contain Early Norian fossils and are discussed below.

On the northeast shore of Hamilton Island (**Figure 6f, site 60, and Figure 29**), in a thick section of Hamilton Island Limestone, the conodonts *Metapolygnathus nodosus*,

M. polygnathiformis, *M. carpathicus*, and *M. sp. aff. M. zoeae*, halobiid bivalves (McRoberts, pers. comm. 2003), and tropitid ammonoids, including *Discotropites?* sp., *Shastitas* sp., and *Hannoceras* sp. (Krystyn, pers. comm. 2003), all contribute to a Late Carnian age. Anterior migration of the basal pit in some of the specimens of *M. nodosus* indicates the upper portion of the *nodosus* Zone (Orchard, 1991b), while the ammonoids indicate the Dilleri and Welleri ammonoid zones (Krystyn, pers. comm. 2003). All of the Dilleri Zone ammonoids occur in a debris flow conglomerate (**Figure 30**), but younger conodonts of the upper portion of the *nodosus* Zone (Welleri Zone) occur in the host rocks, suggesting intraformational reworking.

In the Hamilton Island Limestone on the southeast shore of Hamilton Island (**Figure 6f, site 67**), a variant of *Metapolygnathus nodosus*, called here *M. sp. aff. M. nodosus*, is believed to be from the youngest part of the *nodosus* Zone (Orchard, pers. comm. 2003). It co-occurs with *M. sp. aff. M. zoeae*, the ammonoid *Discotropites?* sp. (Krystyn, pers. comm. 2003) and *Halobia* sp. cf. *H. superba* (McRoberts, pers. comm. 2003), all of which indicate a Late Carnian age (**Figure 44**).

In the Cape Bendel region (**Figure 6e**), two different lithologies are faulted into proximity. The first lithology (**Figure 6e, site 84**), of the Hamilton Island Limestone, contains *Metapolygnathus* sp. cf. *M. nododus*, *M. reversus?*, *M. sp. cf. M. reversus*, and *M. polygnathiformis*. These conodonts are less developed than later specimens of *Metapolygnathus* and are indicative of the lower portion of the *nodosus* Zone (**Figure 44**). The other lithology (**Figure 6e, site 83**) belongs to the currently unnamed shallow-water limestone, and contained *M. polygnathiformis* and *M. sp. aff. M. nodosus*. As at

the southeast shore of Hamilton Island, this variation of *M. nodosus* is believed to be from the youngest portion of the *nodosus* Zone (Orchard, pers. comm. 2003).

Several other sites in the Hamilton Island Limestone also produced Late Carnian fossils, though these sites did not have well-exposed sections like those on Hamilton Island. In the Hamilton Island Limestone on southwestern Payne Island (**Figure 6c, site 62**), the conodonts *Metapolygnathus nodosus*, *M. polygnathiformis*, and *M. sp. cf. M. reversus* indicate the middle portion of the *nodosus* Zone (**Figure 44**). A sample from the Hamilton Island Limestone at the Squawking Crow locality (**Figure 6c, site 97**) yielded *M. nodosus* and *M. polygnathiformis*. Along with a few tropitid ammonoids, and *Halobia ornatissima?* (McRoberts, pers. comm. 2003), these conodonts indicate the upper portion of the *nodosus* Zone (**Figure 44**). In the Hamilton Island Limestone on a small island west of Payne Island (**Figure 6c, site 61**), the bivalves *H. sp. cf. H. superba* and *H. sp. cf. H. ornatissima* (McRoberts, pers. comm. 2003) and a tropitid ammonoid indicate a Late Carnian age. Finally, an isolated sample from the Hamilton Island Limestone in Portage Pass (**Figure 6f, site 66**) produced *M. polygnathiformis* and *M. carpathicus*, indicating the *nodosus* Zone. This same area had silicified *H. ornatissima* (**Figure 6f, site 66, and Figure 34**), which is also Late Carnian (**Figure 44**).

Late Carnian or Early Norian

In the absence of a conodont origination at Tozer's (1967) Carnian-Norian boundary, conodonts alone indicate either latest Carnian or earliest Norian age. In conjunction with short-ranging ammonoids and halobiid bivalves, samples may be

specifically assigned to either the Late Carnian or Early Norian. Not every site or sample can be determined so precisely, however, so this section documents those samples determined to be either Late Carnian or Early Norian. Samples with *Metapolygnathus primitius*, or *M. primitius* and other metapolygnathids (**Plate 3 and Appendix B**), conform to the *primitius* Zone of Late Carnian or Early Norian age (**Figure 44**). The bivalves *Halobia radiata*, *H. austriaca*, and *H. superba* (McRoberts, pers. comm. 2003) also overlap the boundary (**Figure 44**). The Cornwallis Limestone and the Hamilton Island Limestone have produced fossils of this age.

A sample from Cornwallis Limestone on a small island southwest of Kousk Island (**Figure 6d, site 74**) and two samples from Cornwallis Limestone adjacent to the Keku Volcanics on Cornwallis Peninsula (**Figure 6a, sites 95 and 96**) yielded *Metapolygnathus primitius*. A sample from Cornwallis Limestone overlying the neptunian dikes on the eastern side of Kuiu Island (**Figure 6b, site 55**) yielded *M. sp. cf. M. primitius*. Ammonoids from this bed indicate proximity to the Carnian-Norian boundary (Silberling, pers. comm. 2002), placing these beds in the *primitius* Zone (**Figure 44**). Several samples from Cornwallis Limestone on Cornwallis Peninsula (**Figure 6a, site 70**) contain *M. primitius*, *M. sp. cf. M. primitius*, *M. sp. aff. M. primitius*, and *Neogondolella* sp. These are all of Late Carnian or Early Norian age in the *nodosus* and/or *primitius* conodont zones (**Figure 44**). The lower portion of the Cornwallis Limestone on Big Spruce Island (**Figure 6a, site 56, and Figure 9**) yielded an indeterminate metapolygnathid or epigondolellid of Upper Carnian or Lower Norian age respectively.

Fewer samples in the Hamilton Island Limestone show Carnian-Norian boundary affinities. Hamilton Island Limestone from the top of Cathedral Falls (**Figure 6g, site 65**) had *Halobia radiata* (McRoberts, pers. comm. 2003) and the same unit on southwest Payne Island (**Figure 6c, site 64**) had *H. radiata* and *H. sp. cf. H. austriaca* (McRoberts, pers. comm. 2003). Both of these are of Late Carnian or Early Norian age (**Figure 44**).

Early Norian

Early Norian fossils occur in the Cornwallis Limestone, the Hamilton Island Limestone, and in the Hound Island Volcanics. The conodonts *Metapolygnathus primitius*, *Epigondolella quadrata*, *E. sp. aff. E. quadrata*, *E. sp. aff. E. spatulata*, *E. triangularis uniformis*, *E. triangularis triangularis*, and *Misikella longidentata* all occur in the Cornwallis Limestone. However, only *E. quadrata*, *E. sp. aff. E. spatulata*, *E. triangularis uniformis*, and *E. triangularis triangularis* occur in the Hound Island Volcanics during this time interval (**Plates 3-5 and Appendix B**). *Epigondolella triangularis* progressively develops more ornate forms during the Early Norian (Orchard, 1991b), allowing further refinement of age within the *triangularis* Zone (**Figure 44**). Additionally, a sample can be interpreted as Early Norian when *M. primitius* and *E. quadrata* are abundant and co-occur with *E. triangularis*. Less developed forms of *E. triangularis* are typical of the Cornwallis Limestone, while the more ornate forms are common in the Hound Island Volcanics. Halobiid bivalves are also useful in determining an Early Norian age (McRoberts, 1997), and are the only definitive Early Norian fossils recovered from the Hamilton Island Limestone. *Epigondolella triangularis* ranges into

the Middle Norian (**Figure 44**) in the field area as supported by the co-occurrence of *E. triangularis* with Middle Norian faunas as discussed in the next section. Faunas that solely contain *E. triangularis* are assumed to be Early Norian.

Many samples in the Cornwallis Limestone indicate an Early Norian age. On one of the small islands southwest of Kousk Island (**Figure 6d, site 74**), *Metapolygnathus primitius* and *Epigondolella* sp. cf. *E. quadrata* occur in the Cornwallis Limestone. This indicates an age of Early Norian in the *primitius* or *quadrata* zones (**Figure 44**). Samples from the Cornwallis Limestone on northern Cornwallis Peninsula (**Figure 6a, site 70**) contain *M.* sp. cf. *M. primitius*, and *E.* sp. cf. *E. quadrata*. This indicates an Early Norian age in the *quadrata* conodont zone (**Figure 44**). Another sample from Cornwallis Peninsula with no corresponding USGS locality yielded *M. primitius*, *E. quadrata*, *E.* sp. aff. *E. quadrata*, and *E. triangularis uniformis* (**Figure 6a, site 69**). These are of the lower part of the *triangularis* Zone (**Figure 44**). The upper portion of the Cornwallis Limestone on Big Spruce Island (**Figure 6a, site 56, and Figure 9**) contains *E.* sp. cf. *E. quadrata* of Early Norian age.

Most of the Cornwallis Limestone at the Flounder Cove succession (**Figure 6b, site 99, and Figure 21**) is of Early Norian age. Samples in the fine-grained limestones above the lower few meters contain *Metapolygnathus primitius*, *M.* sp. aff. *M. primitius*, the bivalves *Halobia beyrichi* and *H. cordillerana* (McRoberts, pers. comm. 2003) and the ammonoids *Stikinoceras kerri* and *Greisbachites?* sp. (Krystyn, pers. comm. 2003). These are from the Kerri Zone and correspond with the Norian portion of the *primitius* Zone (**Figure 44**). In the coarse-grained limestone capping the section, the conodonts *Epigondolella quadrata*, *E.* sp. aff. *E. quadrata*, *E. triangularis uniformis*, *E. triangularis*

triangularis, and *Misikella longidentata* indicate the *triangularis* Zone in the Early Norian (**Figure 44**).

In the area of the prominent point west of Hound Island on eastern Kuiu Island, the ammonoid *Guembelites clavatus* of the Kerri Zone (**Figure 44**) was found in calcareous sandstone of the Cornwallis Limestone (**Figure 6b, site 72**). West of here (**Figure 6b, site 73**), an epigondolellid was found in calcareous sandstone with abundant plant fossils, and even further west (**Figure 6b, site 68**), *Epigondolella* sp. cf. *E. quadrata* and a metapolygnathid were found in lithoclastic sediments with reworked Devonian conodonts (**Plate 1**). These indicate an overall Early Norian age for this area.

In the Hamilton Island Limestone in Portage Pass (**Figure 6f, site 66**), the bivalves *Halobia beyrichi*, *H. cordillerana*, and *H. sp. cf. H. lineata* (McRoberts, pers. comm. 2003) together indicate an Early Norian age (**Figure 44**). Also in the Hamilton Island Limestone, *H. cordillerana* and *H. lineata* (McRoberts, pers. comm. 2003) occur at the Squawking Crow locality, indicating an Early to Middle Norian age (**Figure 6c, site 97**). These are the only definitive Early Norian ages in the Hamilton Island Limestone.

In the Hound Island Volcanics on the southwest side of Hamilton Island (**Figure 6f, site 85**) the bivalves *Halobia* sp. cf. *H. beyrichi* and *H. sp. cf. H. fallax* (McRoberts, pers. comm. 2003) indicate a probable Early Norian age (**Figure 44**). On the west side of Hound Island, USGS Mesozoic locality M1899 (**Figure 6d, site 79**) produced *Epigondolella quadrata*, *E. triangularis uniformis*, *E. triangularis triangularis*, and the bivalves *H. sp. cf. H. beyrichi* and *H. sp. cf. H. lineata* (McRoberts, pers. comm. 2003) while locality M1923 (**Figure 6d, site 80**) had *H. beyrichi*? (McRoberts, pers. comm.

2003). Locality M1921 on the west side of Hound Island (**Figure 6d, site 81**) produced specimens of *E. sp. cf. E. triangularis* and a sample on the western side of northern Hound Island (**Figure 6d, site 82**) yielded *E. triangularis?* of Early Norian age. All of these indicate a late Early Norian age for the western side of Hound Island (**Figure 44**).

Middle Norian

Biostratigraphically significant fossils of Middle Norian age occur only in the Hound Island Volcanics. They include the conodonts *Epigondolella spiculata*, *E. sp. aff. E. spatulata*, *E. sp. aff. E. matthewi*, *E. sp. cf. E. postera*, *E. sp. aff. E. transitia*, *Neogondolella sp. cf. N. steinbergensis* (**Plate 5 and Appendix B**), the bivalve *Halobia fallax*, and the Early Norian conodont *E. triangularis* which continues into the Middle Norian (**Figure 44**). Elsewhere, *E. spatulata* originates in the Early Norian (Orchard, 1991b), but *E. sp. aff. E. spatulata* only occurs with *E. spiculata* in the field area. The occurrence of *E. spiculata* with *E. triangularis* supports the presence of Middle Norian *E. triangularis*. *Neogondolella steinbergensis* ranges from Middle to Late Norian. In the North American Cordillera, the conodont *Epigondolella multidentata* (**Figure 44**) normally signifies the base of the Middle Norian (Orchard, 1991b). In Europe, other species are used to identify the base of the Middle Norian (e.g. Kozur *in* Channel *et al.*, 2003). Since neither *E. multidentata* nor the European species occur in the field area, the base of the Middle Norian may be absent or not preserved.

In the lower, finer-grained beds in the Gil Harbor mudflat (**Figure 6b, site 87**), samples yielded *Epigondolella triangularis triangularis*, *E. spiculata*, *E. sp. aff. E.*

spatulata, *E. sp. aff. E. transitia*, and *E. sp. aff. E. matthewi*. These are indicative of the *spiculata* Zone (**Figure 44**). Between Gil Harbor and Kadake Bay along the coast (**Figure 6b, site 46**), an individual sample yielded *E. triangularis triangularis* and *E. spiculata* of the Middle Norian *spiculata* Zone (**Figure 44**). Finally, samples from the east side of Hound Island (**Figure 6d, site 86**) had *E. sp. cf. E. postera*, *E. spiculata*, *Neogondolella sp. cf. N. steinbergensis*, other *Neogondolella sp.* and the bivalve *Halobia fallax* (McRoberts, pers. comm. 2003). These indicate the *postera* Zone higher in the Middle Norian (**Figure 44**). The bivalves *H. cordillerana* and *H. beyrichi* (McRoberts, pers. comm. 2003) also support a Middle Norian age.

Late Norian

Only two localities in the Hound Island Volcanics yielded Late Norian fossils, and this study only investigated the Gil Harbor site. In the Gil Harbor mudflat, conodonts recovered from the silicified fossil beds (**Figure 6b, site 87**) include *Epigondolella bidentata*, *E. tozeri*, *E. englandi*, and *E. sp. aff. E. mosheri* (**Plate 5 and Appendix B**). *Epigondolella tozeri* originates in the Middle Norian, while *E. bidentata* and *E. englandi* originate in the Late Norian. This association suggests the *bidentata* Zone in the Late Norian (**Figure 44**). *Monotis subcircularis* and the hydrozoan *Heterastridium conglobatum* occur in these beds and at USGS Mesozoic locality M1898 in Hamilton Bay (**Figure 6g**) (Muffler, 1967). *Monotis subcircularis* only occurs in the Late Norian Cordilleranus Zone (**Figure 44**), agreeing with the conodont data. Based on the abundant Late Norian fossils, the conodont *E. sp. aff. E. mosheri* is a Late Norian

predecessor of the Rhaetian *E. mosheri*. Large individuals of *Heterastridium* in the Gil Harbor mudflat (**Figure 6b, site 87**) have a size range of 2-3 centimeters. According to the theory that maximum diameters of *Heterastridium* can assist age determination (Stanley *et al.*, 1994), these sizes indicate an age of upper Middle Norian (Stanley, unpublished data). Conodonts and bivalves clearly place these beds as latest Late Norian in age, contradicting this theory.

Discussion

Pre-Late Triassic Uplift

Throughout the Alexander terrane, uplift and erosion during and/or prior to Upper Triassic deposition is recorded by the following: (1) a regional unconformity with incision of Paleozoic units, (2) a lack of Middle Permian to Middle Triassic rocks, and (3) the occurrence of rocks of a variety of ages beneath the unconformity (Gehrels *et al.*, 1987). The clasts of Devonian through Early Permian age (**Appendix B**) found in the Cornwallis Limestone and lithoclastic beds of the Keku sedimentary strata strongly support pre-Late Triassic uplift in the Keku Strait area. Furthermore, this uplift happened, at least partly, after deposition in the Early Permian and was large enough to expose much of the Paleozoic succession.

This uplift resulted in a complicated paleotopography during the Late Triassic. Paleozoic outcrops of Silurian, Devonian, Carboniferous, and Permian age occur in close proximity on the west side of Keku Strait (**Figure 3**). The overlying Triassic units are

less complicated structurally, and locally surround Paleozoic units. These “islands” of Paleozoic rock are likely sources for the abundant and locally large Paleozoic clasts deposited in Upper Triassic units. The large, angular block of Carboniferous limestone in Upper Triassic sandstone on Big Spruce Island (**Figure 12**) supports the existence of a steep, proximal source area. A similar situation is present on Kupreanof Island, as the Devonian to Permian Cannery Formation (**Figure 3**) is more intensely folded than the overlying Triassic units.

Muffler (1967) postulated that Permian thrusting could have juxtaposed dissimilar Permian facies prior to deposition of the Pybus Formation. In fact, Devonian and Mississippian clasts of the Cannery Formation on Kupreanof Island were reported in Permian units underlying the Pybus Formation on Kuiu Island (Berg *et al.*, 1978; Jones *et al.*, 1981). Karl and others (1999) noted that the Paleozoic rocks on eastern Kupreanof Island were of higher metamorphic grades than the Triassic rocks, supporting a pre-Mesozoic metamorphic event. On Kupreanof Island, numerous thrust faults from at least two generations of thrusting (Karl *et al.*, 1999) support a complex compressional history for the Alexander Terrane. Overall, this thrusting could account for much of the pre-Late Triassic uplift, though some uplift after deposition of the Pybus Formation is necessary to account for its inclusion in shallow marine or terrestrial Late Triassic units. Furthermore, the presence of Devonian clasts in Late Triassic sediments (**Figure 6b, site 68**) suggests a long history of erosion, supporting earlier uplift.

This uplift has been attributed to latest Permian or Triassic rifting in the past (Gehrels and Saleeby, 1987; Gehrels *et al.*, 1987). This interpretation depends partly on the presence of felsic to mafic bimodal volcanism and a lack of deformation associated

with uplift. However, the Burnt Island Conglomerate represents the earliest Triassic deposition in the field area and does not contain any late Permian or Triassic volcanic rocks, although it does contain older volcanoclastic rock. Additionally, new age data places the felsic igneous rock of the Keku Volcanics in the Cretaceous (Mortenson, pers. comm. 2004) instead of the Triassic, thereby withdrawing the Keku Volcanics from the Hyd Group. Furthermore, there is abundant evidence of pre-Late Triassic deformation as noted above. The removal of the Keku Volcanics from the Hyd Group, the lack of volcanic rock in the Burnt Island Conglomerate or Hamilton Island Limestone, and evidence for compressional tectonics in the Permian all seem to preclude rifting as the major source of pre-Late Triassic uplift.

Hyd Group Deposition

Though a Middle Triassic age was reported nearby (Wardlaw *in* Karl *et al.*, 1999), the earliest age of deposition indicated in the Hyd Group is Early Carnian. The Burnt Island Conglomerate of Early Carnian to Late Carnian age represents initial, rapid infill of the basin. This probably occurred at the end of a period of uplift and erosion (Gehrels *et al.*, 1987), in conjunction with subsidence and/or sea level rise.

Widespread carbonate deposition began in the Late Carnian as represented in the Hamilton Island Limestone and the Cornwallis Limestone. Turbiditic successions and debris flows in the Hamilton Island Limestone record continued and relatively rapid infill in deeper portions of the basin (**Figure 29**). Fossils from the Hamilton Island Limestone indicate deposition through most or all of the Upper Carnian. These thick, deeper water

Upper Carnian deposits without significant facies change suggest relative sea level rise throughout this interval.

Fewer Upper Carnian deposits are exposed in the Cornwallis Limestone. These deposits directly overlie either the pre-Late Triassic erosional unconformity or the more proximal facies of the Keku sedimentary strata. This also supports relative sea level rise during the Upper Carnian. Though thicker Carnian deposits of the Cornwallis Limestone were not located on the surface, they may be preserved east of Kuiu Island in the waters of Keku Strait or in the subsurface. The unnamed shallow-water limestone on the east side of the strait is Upper Carnian and may represent an Upper Carnian equivalent of the Cornwallis Limestone on the opposite side of the basin.

Placing the felsic igneous rock of the Keku Volcanics in the Cretaceous leaves the formerly associated, Keku sedimentary strata in the Hyd Group. The lithoclastic beds and neptunian dikes represent near shore deposition and they underlie or laterally grade into the Cornwallis Limestone. Lithoclastic limestone beds of the Cornwallis Limestone are transitional between the purely lithoclastic beds and the massive carbonate of the Cornwallis Limestone. Based on their stratigraphic relationship with the Cornwallis Limestone and the fossils adjacent to the neptunian dikes, these near shore deposits are mainly Late Carnian, but could be Early Carnian to Early Norian in age.

Widespread carbonate deposition continued into the Early Norian, where more extensive shallow-water carbonates developed, as represented by most of the Cornwallis Limestone. Few Early Norian deposits are documented in the Hamilton Island Limestone. The only areas with the upper contact of the Hamilton Island Limestone exposed are on Hamilton Island and in Hamilton Bay (**Figures 6f and 6g**).

Unfortunately, on northern Hamilton Island, this contact is intruded by Tertiary gabbro, on southern Hamilton Island this contact is intruded and deformed, and in Hamilton Bay this same contact is cut by several faults. This may account for the scarcity of Early Norian deposits in the Hamilton Island Limestone.

Though no transitional facies have been found in the field area, the shallow-water Cornwallis Limestone and the deeper water Hamilton Island Limestone are probably lateral facies of each other (Muffler, 1967). Shallow-water corals and plant material are present as reworked bioclasts in the Hamilton Island Limestone and the same Upper Carnian ages occur in both units. A west-dipping thrust fault occurs just west of Payne Island (**Figure 6c, site 61**) and brings the Permian Pybus Formation over top of the ductile Hamilton Island Limestone (**Figure 45**). This fault was previously mapped as a high-angle fault (Muffler, 1967). This thrust fault separates the Keku sedimentary strata and all of the Cornwallis Limestone from outcrops of Burnt Island Conglomerate and Hamilton Island Limestone, and could account for their current proximity.

Relatively continuous carbonate deposition through the Carnian-Norian boundary in the field area presents potential for refinement of data surrounding this boundary. Ammonoids, bivalves, conodonts, and radiolarians are preserved in fossil assemblages of the Hyd Group, providing abundant fossil age control. To date, preservation of this interval has been found only in the Cornwallis Limestone. If more Norian fossils can be recovered from the Hamilton Island Limestone, there is potential for examination of this boundary in both shallow- and deep-water sediments. Orchard (1991a; 1991b) suggested the *nodosus*, *communisiti*, and *primitius* conodont zones as other potential levels for formal definition of the Carnian-Norian boundary. The abundance of Upper Carnian

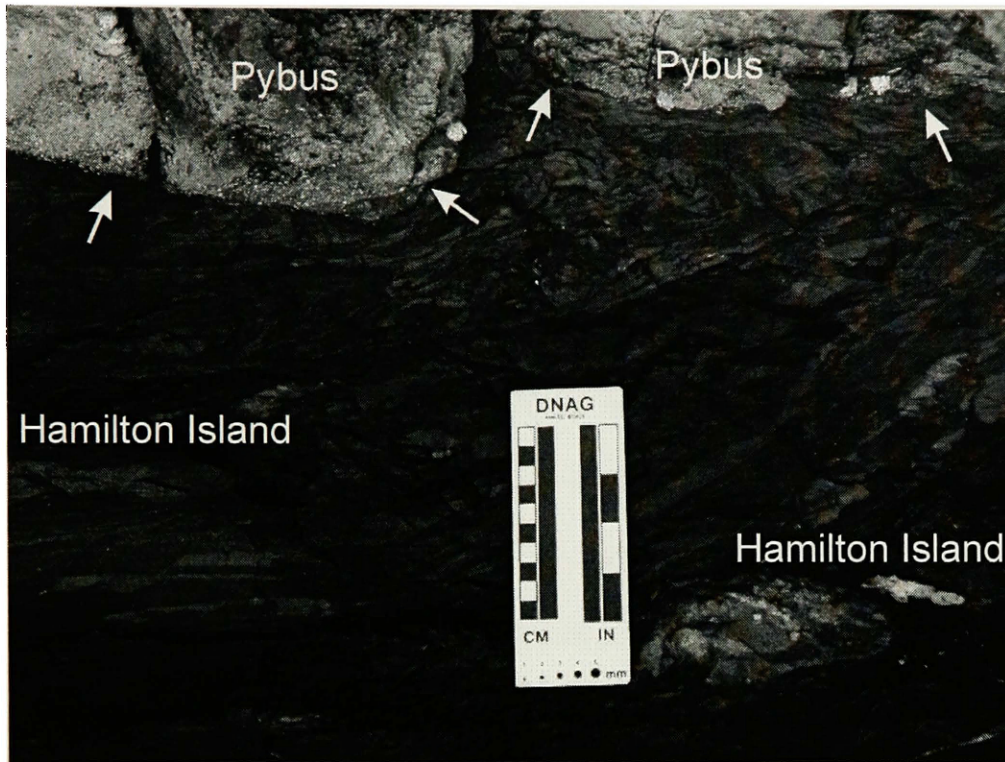


Figure 45a. Close-up of the thrust fault in the Keku Islets. Dark-colored, folded beds of the Hamilton Island Limestone underlie light-colored, massive Permian limestone of the Pybus Formation (Figure 6c, site 61). White arrows indicate the fault boundary. Scale is in centimeters.

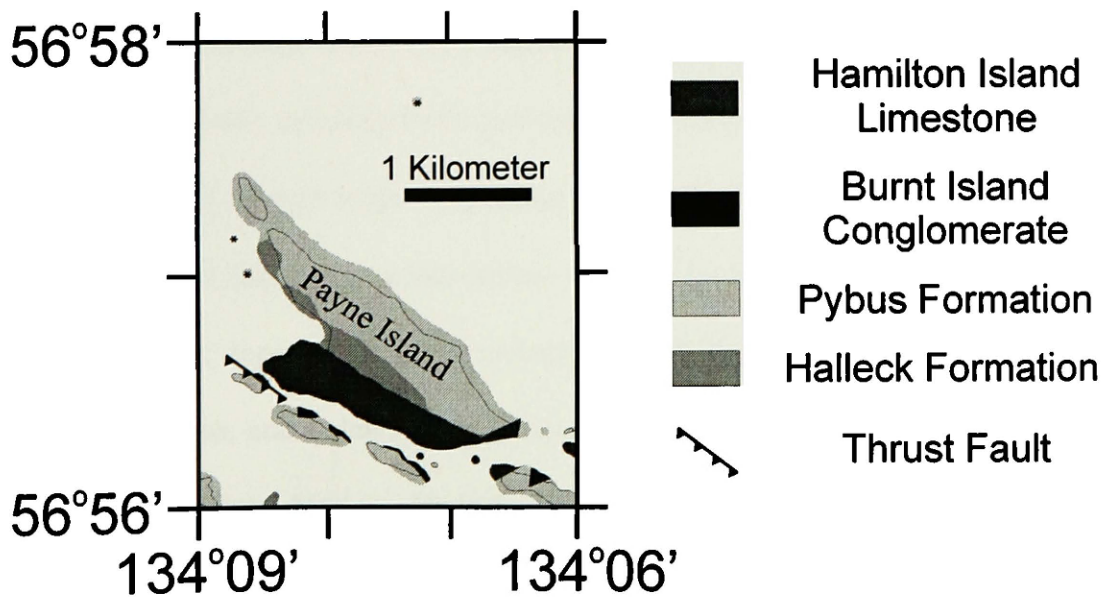


Figure 45b. Map of Payne Island and surrounding islets in the northern Keku Islets. Southwest-dipping thrust fault just southwest of Payne Island indicated on map.

limestone in the Hamilton Island Limestone provides potential for investigating these intervals. Though this study does not have enough data to securely place a boundary, the section at the Flounder Cove locality (**Figure 6b, site 99 and Figure 21**) exhibits the most potential.

The youngest conodont ages in the Cornwallis Limestone are indicative of the *triangularis* Zone. The oldest conodonts in the Hound Island Volcanics are more advanced morphologically and are indicative of the upper part of the *triangularis* Zone. Assuming the onset of extensive basaltic and andesitic volcanism was relatively synchronous throughout the area, this implies an age of onset within the *triangularis* Zone of late Early Norian age. This is supported by the lack of Triassic volcanic material in Carnian and earliest Norian deposits in the Burnt Island Conglomerate, Keku sedimentary strata, the Cornwallis Limestone, and the Hamilton Island Limestone.

Deeper water limestone of the Hound Island Volcanics overlies shallower water facies of the Cornwallis Limestone on Eastern Kuiu Island (**Figure 6b**) and the unnamed shallow-water limestone in the Cape Bendel region (**Figure 6e**). This suggests continued relative sea level rise, possibly from tectonic subsidence linked to the onset of volcanism. Deposition of the Hound Island Volcanics continued into the Middle and Late Norian, and the youngest deposits are limestones of Late Norian age. Due to the scarcity of youngest Triassic deposits, it is not currently possible to determine the level of volcanism in the Late Norian, and volcanism may have diminished or ceased in the Middle Norian. The scarcity of late Norian deposits is presumably due to the pre-Upper Jurassic unconformity.

Figures 46 and 47 depict chronostratigraphic cross-sections across the strait. The northern cross-section begins in Cornwallis Peninsula, passes through the northern Keku Islets, and ends in the Cape Bendel region (**Figures 5 and 46**). The southern cross-section begins on eastern Kuiu Island, passes through Hound Island, and ends in the Hamilton Island region (**Figures 5 and 47**). In both cross-sections, the break between the Cornwallis Limestone and the Hamilton Island Limestone occurs roughly the same distance across the strait. On the northern cross-section, this point matches the position of the post-Triassic thrust fault (**Figure 6c, site 61, and Figure 45**). Furthermore, it becomes clear on the cross-sections that the Cornwallis Limestone, Hamilton Island Limestone, and Hound Island Volcanics have similar age ranges throughout their respective geographic distributions.

Figure 48 portrays a block diagram representing depositional extent and facies correlations for the Burnt Island Conglomerate, Keku sedimentary strata, the Cornwallis Limestone, and the Hamilton Island Limestone in the Carnian to Early Norian. This diagram displays deposition of clastic rock in near-shore and terrestrial environments, shallow-water and deep-water limestone further out in the basin respectively, and the initial basin infill underlying them all in the center of the basin. The island on the left side of the diagram represents a topographic high of Paleozoic limestone in Triassic time. A question mark denotes the possible presence of clastic Triassic rock on the right side of the diagram. A break in the block diagram between the Cornwallis Limestone and the Hamilton Island Limestone represents the post-Triassic thrust fault shown in **Figure 45**.

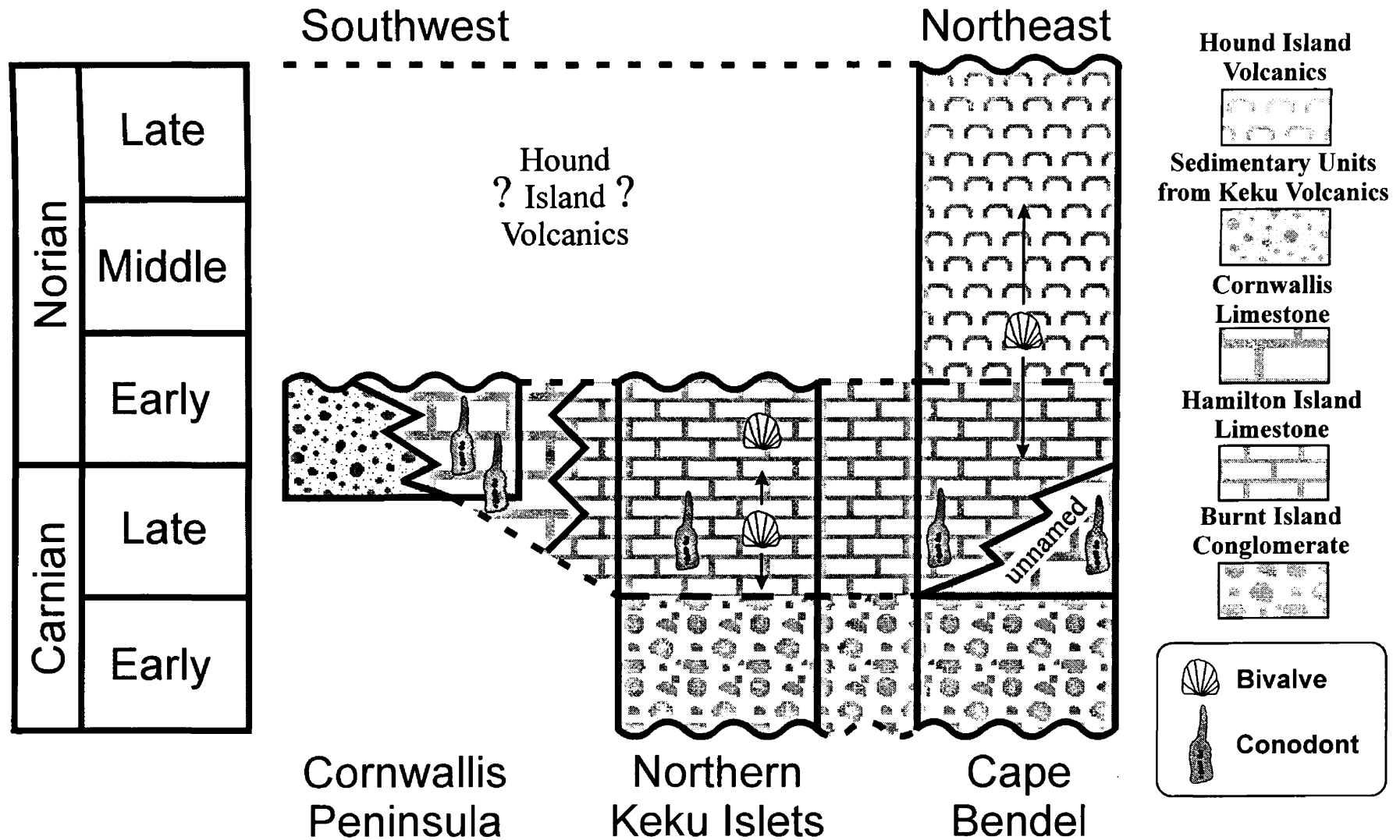


Figure 46. Generalized chronostratigraphic cross-section across the northern end of Keku Strait. Fossil symbols for ammonoids, bivalves, and conodonts indicate biostratigraphic age control with possible ranges indicated by arrows. Specific information on biostratigraphic fossils is in Appendix B.

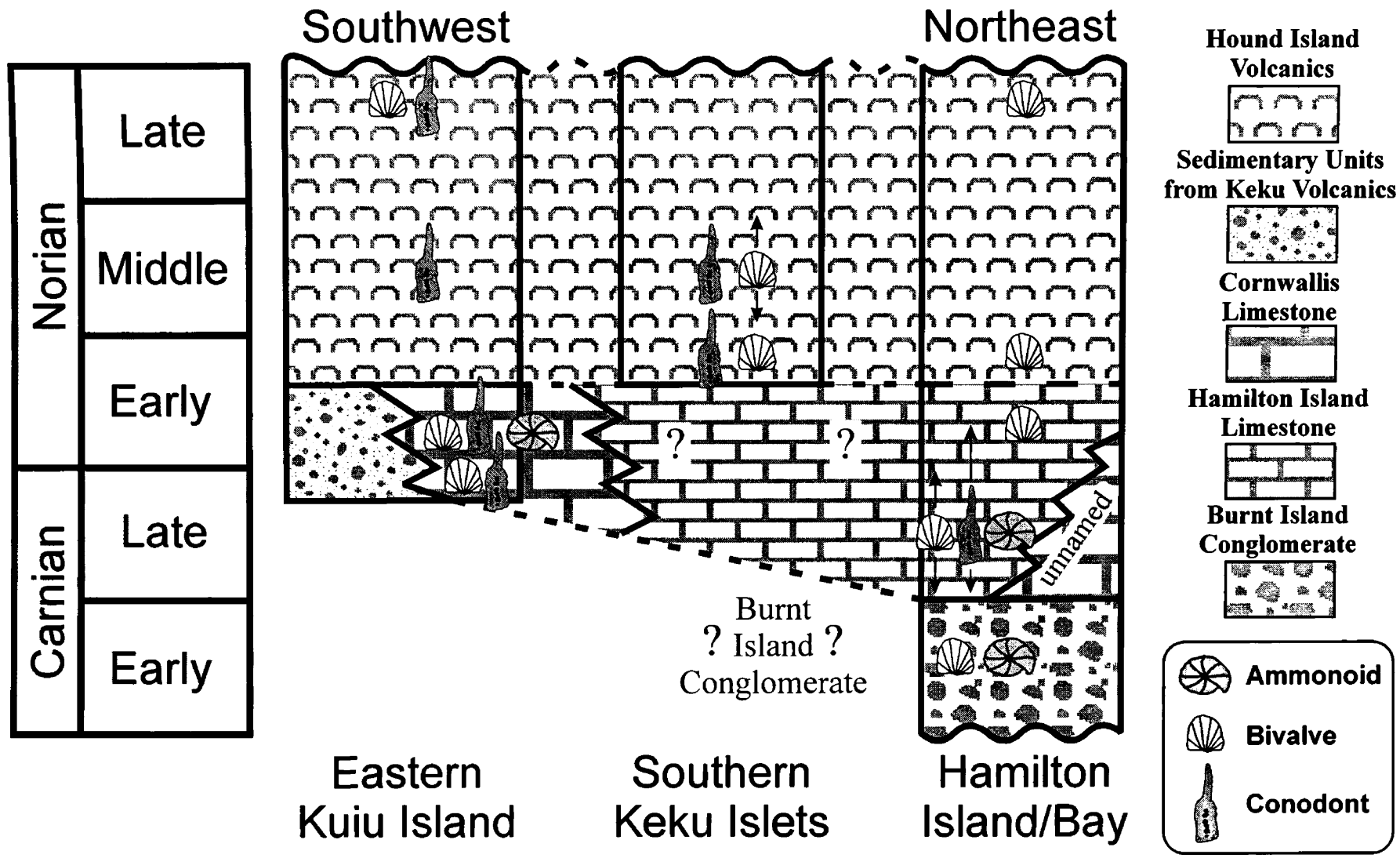


Figure 47. Generalized chronostratigraphic cross-section across the southern end of Keku Strait. Fossil symbols for ammonoids, bivalves, and conodonts indicate biostratigraphic age control with possible ranges indicated by arrows. Specific information on biostratigraphic fossils is in Appendix B.

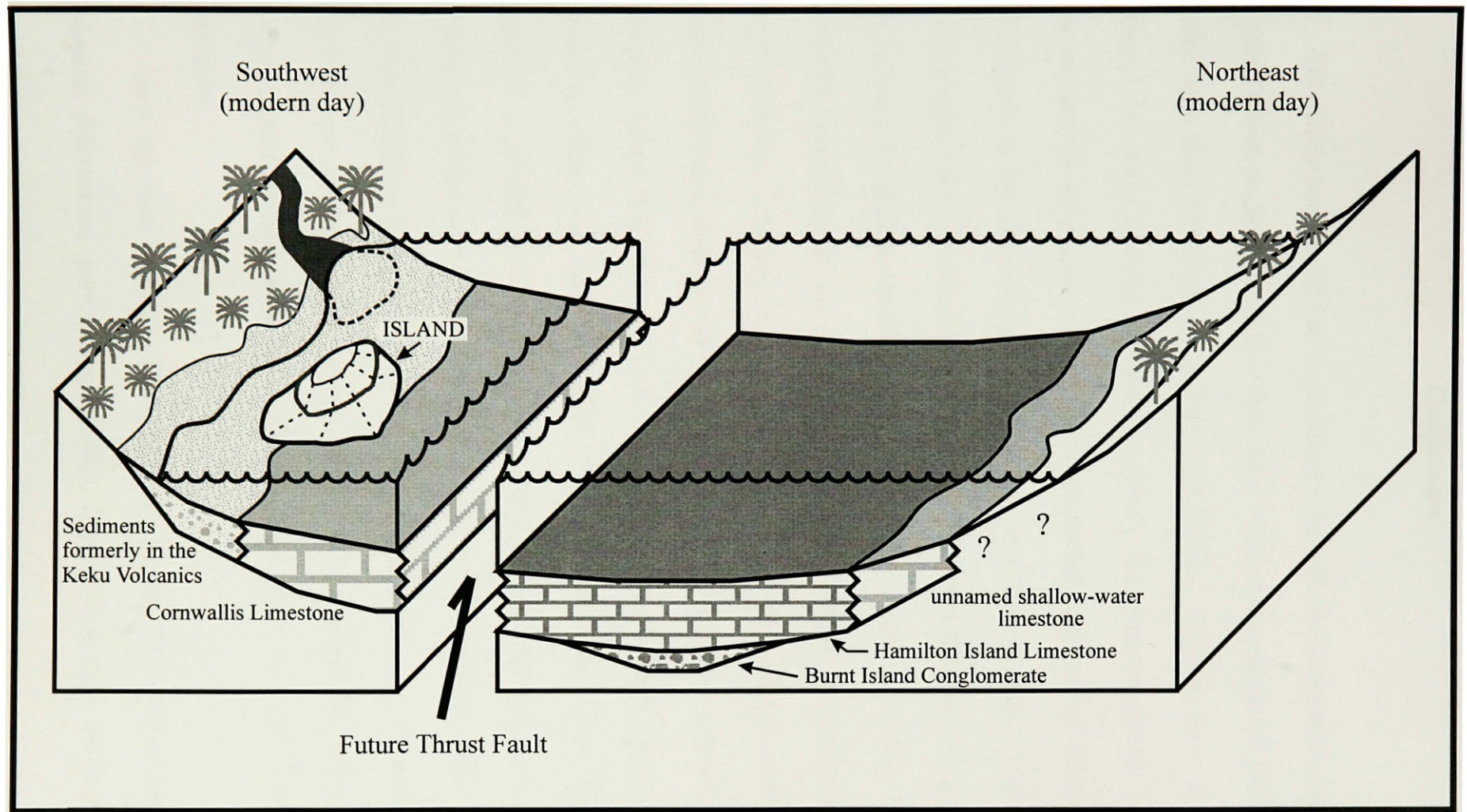


Figure 48. Block diagram depicting Carnian to Early Norian facies correlations and depositional extent for the Burnt Island Conglomerate, sedimentary deposits formerly in the Keku Volcanics, Cornwallis Limestone, and Hamilton Island Limestone. Island on left side of diagram represents a local topographic high. Not to scale.

Conclusions

This study was successful in providing a revised biostratigraphic framework for the Late Triassic rocks in the Keku Strait area. Conodonts, bivalves, and ammonoids revealed ages from Late Carnian through Late Norian. Overall, these ages generally confirmed the dates reported by Muffler (1967), but allowed greater chronological precision over the entire area. Greater precision permitted the precise dating of the onset of volcanism in the Hound Island Volcanics as late Early Norian. Furthermore, the biostratigraphic data allowed greatly improved correlation between the geologic units. This includes the placement of the Keku sedimentary strata as a lateral facies of the Cornwallis Limestone and the correlatable age ranges of the Cornwallis and Hamilton Island limestones. Conodont data from reworked clasts also allowed reinterpretation of the pre-Late Triassic tectonic history. At least two phases of uplift exposed the Paleozoic succession before Late Triassic time. This uplift was probably due to thrusting as opposed to rifting, and the latest phase was after deposition of the Permian Pybus Formation. Identification of possible Carnian-Norian boundary successions will contribute to future work on this elusive interval. Paleontological samplings increased the amount of Triassic macrofossils from Keku Strait by several times and represent the richest Triassic fossil deposit in the Alexander terrane. These fossils will assist in future paleogeographic studies and in facies determination within the Late Triassic carbonate succession.

New age data indicate a Cretaceous age for the felsic intrusions of the Keku Volcanics (Mortenson, pers. comm. 2004). However, several sedimentary deposits

assigned to the Keku Volcanics by Muffler (1967) are of Triassic age based on the presence of Triassic fossils and stratigraphic relationships. This revision requires removal of the Cretaceous Keku Volcanics from the Hyd Group. The remaining Keku sedimentary strata must then be included in the Hyd Group as an informal unit. As the geologic history and outcrop extent of the Keku sedimentary strata are poorly understood, it is inappropriate to give a formal designation at this time. However, based on their close association with the Cornwallis Limestone, similarity to lithoclastic limestone already within the Cornwallis Limestone, and geographic restriction to Cornwallis Peninsula, the Keku sedimentary strata should be associated with the Cornwallis Limestone. A redefined Cornwallis Limestone would also be able to encompass the outcrops of unnamed shallow-water limestone on the east side of Keku Strait. Future work should focus on the rocks of Cornwallis Peninsula.

Overall, the Keku Strait area, with its more extensive exposures and relatively low metamorphism and deformation, proves to have the best exposures of Late Triassic rock in the Alexander terrane. The Burnt Island Conglomerate represents initial infill of the basin, while the Keku sedimentary strata, the Cornwallis Limestone, and the Hamilton Island Limestone represent a proximal to distal facies succession during the Upper Carnian and Early Norian. An absence of volcanism in older deposits is succeeded by extensive basaltic and andesitic volcanism of the ubiquitous Hound Island Volcanics in the late Early Norian. Relative sea level rise was prevalent throughout deposition of the Hyd Group. The wide variety of volcanic and sedimentary facies with rapid facies changes, peri-platform carbonates in the forms of debris flows, slumps, and turbidites, and the presence of terrane-endemic gastropods (Blodgett and Frýda, 2001; Frýda and

Blodgett, 2001), support deposition in an island arc (Soja, 1996). Finally, new ties between different stratigraphic columns on either side of the strait provide a linkage between rocks that might appear unrelated elsewhere in the Alexander Terrane. Thus, the Keku Strait area forms the best standard for comparison when examining the Late Triassic succession in the Alexander terrane.

Taxonomic Notes

Brief descriptions of the Late Triassic conodonts recovered and subsequently applied to the Late Triassic biostratigraphy are included below. Each species description references the plates at the end of the thesis. All conodonts are stored at the University of Montana Museum of Paleontology.

Genus *Epigondolella* Mosher, 1968

A well-differentiated free blade and large, discrete, and sharp anterior platform denticles that at least double the height of the platform characterize species of *Epigondolella*. In profile, the lower surface steps up posterior of the blade-platform junction, but may turn downward, continue straight, or turn upward terminally. Additionally, a basal pit generally lies beneath the central or anterior portion of the platform, the cusp is rarely conspicuous, and element growth proceeds through relatively uniform accretion about the posterior platform expansion. Platform microreticulation is typically subdued and irregular, particularly in younger species. This genus only occurs

in the Norian and differs from ornate species of *Metapolygnathus* based on the anterior platform denticulation; *Metapolygnathus* has no or weak nodes and *Epigondolella* has spine-like nodes. Orchard's (1991b) criterion that *Epigondolella* denticles at least double the overall platform height excludes Upper Carnian and older elements. Early growth stages of similar *Epigondolella* species are often difficult to differentiate. (Kystry, 1980; Orchard, 1983; 1991b)

Epigondolella bidentata Mosher, 1968

Plate 5, Figures 16-18

This epigondolellid is small and slender with a relatively short platform lying posterior of pair of prominent, submedially located denticles. The posterior platform is typically shorter than the anterior blade giving the element a blade-like form. The carina continues to the posterior tip as three to four, rarely five, nodes beyond the lateral denticle pair. Smaller accessory nodes may develop irregularly on the margins. The basal pit is small and lies beneath the lateral denticle pair within a posteriorly tapering basal scar. (Mosher, 1968; Orchard, 1991b)

This species is shorter and wider than *Epigondolella mosheri*, which generally has more carinal nodes posterior of the denticle pair. Rare specimens with five carinal nodes are large and have a wider posterior platform than the laterally reduced platform of *E. mosheri*. *Epigondolella englandi* has a broader platform with strong, symmetrically arranged platform nodes. Small growth stages of various *Epigondolella* species are

difficult to differentiate from *E. bidentata*, but do not attain the same size. (Orchard, 1991b)

Epigondolella englandi Orchard, 1991b

Plate 5, Figures 21-26

This small *Epigondolella* species with an ovoid platform has a pair of unequally developed but very high anterior denticles and additional pairs of smaller, but distinct, symmetrically arranged nodes on the posterior platform. When compared to *E. bidentata* and *E. mosheri*, this species has a broader platform, more prominent anterior denticles, and strong posterior ornamentation. The platform shape differs from the lobate *E. postera*. (Orchard, 1991b)

Epigondolella sp. aff. *E. matthewi* Orchard, 1991b

Plate 5, Figure 9

Epigondolella matthewi has a mostly unornamented, round posterior margin and is characterized by a relatively broad, biconvex platform with two to four large denticles on each anterior platform margin. The blade has relatively few, large denticles that pass into a carina composed of several discrete nodes. The carinal nodes usually do not reach the posterior end of the platform. (Orchard, 1991b)

When compared to *Epigondolella postera*, *E. matthewi* is larger, usually relatively longer, has a more symmetrical posterior platform, and has more anterior nodes (Orchard,

1991b). The specimen from Keku Strait is described as *E. sp. aff. E. matthewi* because it has one large denticle on one margin and three on the other, and its shape is closer to *E. matthewi* than *E. postera*.

Epigondolella sp. aff. E. mosheri Kozur and Mostler, 1971

Plate 5, Figures 31-33

Epigondolella mosheri is a small, typically very slender species with a relatively long, narrow, or incipiently developed platform lying posterior to a pair of prominent denticles, which may be unevenly reduced to a pair of swellings. The carina is prominent, consists of five to ten denticles posterior to the lateral denticle pair, is generally longer than the blade, and is narrower than the anterior end of the platform. A small basal pit lies within a narrow, pointed scar at a point beneath the lateral denticle pair. (Orchard, 1991b)

These specimens from Keku Strait, Alaska are larger, more elongate, and have more denticles on the lateral margins than *Epigondolella bidentata*. They have five carinal nodes posterior of a prominent denticle pair, and are not as elongate nor as narrow posteriorly as *E. mosheri*. Orchard (1991b) noted how small growth stages of *E. mosheri* are very similar to *E. bidentata*, and how transitional forms in the Cordilleranus Zone are larger, have five carinal nodes, and have a broader posterior platform. Thus, these specimens may be variations on the form of *E. mosheri*, or transitional forms between *E. bidentata* and true *E. mosheri*.

Epigondolella sp. cf. *E. postera* Kozur and Mostler, 1971

Plate 5, Figure 10

This relatively short epigondolellid has distinctive anterior denticulation commonly consisting of one prominent denticle on one platform margin and two on the other. The posterior platform is typically unornamented, but the nodes of the carina may be continuous to the posterior end of the platform. The posterior platform margins are often asymmetrical, with one margin being strongly convex. The blade is short and high, and descends relatively abruptly onto the platform. The basal pit is located anterior to the platform midlength. (Orchard, 1991b)

When compared to *Epigondolella elongata*, *E. postera* is much shorter and has a characteristically asymmetrical and lobate posterior platform. While accessory nodes may occur on the platform, specimens of *E. postera* are neither as strongly ornate nor as narrow posteriorly as *E. carinata*. Early growth stages of *E. triangularis* are smaller, have different blade and platform profiles, and do not have a lobate posterior platform. (Orchard, 1991b)

Epigondolella quadrata Orchard, 1991b

Plate 3, Figures 19-23

This species of *Epigondolella* has a flat, mostly unornamented, commonly rectangular posterior platform with variably pointed, posterolaterally extended corners. The blade has 9 to 12 denticles and is up to one-half unit length. In profile, the blade

rises from both the anterior and posterior ends in a low convex crest. Additionally, the lower surface of the platform clearly steps up posterior to the blade and turns down at the posterior end of the platform. The three to five discrete carinal nodes are commonly small except for the posteriormost one, which often dominates the center of the posterior platform, but may have a small node occurring beyond it. The lateral margins of the anterior platform bear several large, discrete and sharp denticles. The lower surface bears a centrally located basal pit with a small surrounding loop, and a basal scar that commonly bifurcates posterior to the pit. Dense microreticulae are largely confined to the posterior platform and are more pronounced peripherally. (Orchard, 1991b)

When compared to *Metapolygnathus primitius*, *Epigondolella quadrata* has a shorter and broader platform and the anterior denticles at least double the height of the platform and are more prominent. Furthermore, the lower surface profile and microreticulation are different from *M. primitius* and the posterolaterally extended corners are rare in *Metapolygnathus*. Specimens of *E. quadrata* may have a medial constriction reminiscent of *Metapolygnathus* ancestors, especially with pronounced posterolateral expansion. *Epigondolella* sp. aff. *E. spatulata* and *E. triangularis* share the profile and lower surface morphology with *E. quadrata*, although these two species show decreased posterior downarching, increased bifurcation of the basal scar, a diminished relative blade length, and distinctive posterior ornamentation. Forms transitional between *E. quadrata* and *E. triangularis* (Plate 3, Figures 23 and 24) display an increased amount of posterior ornamentation on both the lateral and posterior margins. Posteriorly smooth Middle Norian elements lacking a posterior carina have different profiles. (Orchard, 1983; 1991b)

Epigondolella sp. aff. *E. quadrata* (Hayashi, 1968)

Plate 3, Figures 24-25 and Plate 4, Figures 1-3

The Keku Strait specimens designated under this name are forms transitional between *Epigondolella quadrata* and *E. triangularis*. They show the increased posterior ornamentation and slight posterolateral platform expansion, which become prominent in *E. triangularis*.

Epigondolella sp. aff. *E. spatulata* (Hayashi, 1968)

Plate 4, Figures 21-23

Epigondolella spatulata is a relatively short, subcircular species characterized by a strongly expanded posterior platform that constitutes between two-thirds and three-quarters of the unit length. The short anterior platform margins have a pair of large, commonly transversely elongate nodes; posterior of these nodes the platform abruptly and roundly expands. The carina commonly has a series of partially fused nodes which may be followed by a more discrete and noticeable, posterior node. Low nodes occur on all of the platform margins, and may form secondary carinas. On the lower surface, the keel is commonly bifurcated posterior to the pit. Overall, this species is shorter and more expanded than *E. quadrata* or *E. triangularis* (Hayashi, 1968; Orchard, 1991b)

These specimens from Keku Strait, Alaska resemble *Epigondolella spatulata* with their generally shorter platform and blade, and their noticeable posterior expansion. They have less prominent posterior ornamentation than *E. triangularis*, but still have some

posterior ornamentation. They differ in that the unexpanded anterior platforms are relatively longer and the posterior expansion is not as great. These specimens occur with *E. triangularis* and *E. spiculata*.

Epigondolella spiculata Orchard, 1991b

Plate 5, Figures 1-7

This epigondolellid has an asymmetric, subrectangular platform with a pronounced convexity of the outer posterior margin on the upper surface. In profile, the unit has a characteristic flat to convex base and the posterior platform is clearly upturned. The blade is one-quarter to one-third unit length, is commonly composed of five to seven denticles which are highest towards the anterior end, and declines strongly to the posterior where it ends abruptly on the anterior platform. The discrete nodes of the carina are small anteriorly and increase in size toward the posterior where they align and often connect to a node on the posterior margin that is invariably more prominent than the preceding carinal nodes. Several large denticles occur on each anterior platform margin and may be higher on one side. The posterior margin is more ornate with additional sharp nodes that are often unevenly developed. These nodes project beyond the platform margin and give the unit a serrated appearance. In lower view, the basal scar is relatively broad and flat, and has only slightly raised edges. The posterior margin of the scar is often obliquely truncated but may be straight or weakly indented; in rare cases, it may bifurcate but in these examples the indentation does not extend to the pit. The small pit is located slightly to the anterior of the platform midpoint, and a groove extends anteriorly

within the tapered scar, which continues as a broad strip beneath the blade. Platform microreticulae are poorly developed. (Orchard, 1991b)

When compared to the holotype of *Epigondolella spiculata*, the Keku Strait specimens are not as asymmetric, but they do not have the posterior platform expansion typical of *E. triangularis triangularis*. As in *E. spiculata*, the blade is shorter than in *E. triangularis* and the anterior nodes are large, discrete, and sharp. The carina extends to the posterior and a prominent carinal node on the posterior platform projects posteriorly like *E. spiculata*. These specimens are strongly denticulate posteriorly and the denticles project outward from the platform margin. The main differences from *E. spiculata* are on the lower surface and correspond somewhat with *E. triangularis*. In profile, the lower surface is not flat or convex, but is slightly concave anterior of the posteriorly upturned margin. This concavity is not as pronounced as in other Norian epigondolellids, and the posteriorly projecting denticles make the upturned posterior margin appear similar to *E. spiculata*. The asymmetric keel is not straight or obliquely truncated like typical *E. spiculata*, but is instead weakly bifurcated as in rare occurrences documented by Orchard (1991b). Unlike *E. triangularis*, this bifurcation does not extend to the pit. Finally, the loop surrounding the basal pit is more pronounced, as in *E. triangularis*.

Epigondolella tozeri Orchard, 1991b

Plate 5, Figures 19-20, 27-30

Epigondolella tozeri is strongly denticulate with two to four high anterior platform denticles and strong nodes on the tapered to subparallel margins of the pointed

to narrowly truncated posterior platform. It has discrete carinal nodes that extend without significant elevation to the posterior end of the unit. The lower surface has a basal pit beneath the anterior third of the platform and a posteriorly broad basal scar. (Orchard, 1991b)

When compared to *Epigondolella multidentata*, this epigondolellid consistently develops strong posterior nodes and lacks a high posterior carina. When compared to *E. spiculata*, it has a relatively symmetrical posterior platform and a strong continuous carina. *Epigondolella serrulata* is consistently smaller, has a thinner, more biconvex platform with smaller, often outwardly directed nodes, and a relatively shorter blade. Similarly sized elements of *E. triangularis* have posteriorly expanded platforms, broadly truncated platforms, and no posterior carina. (Orchard, 1991b)

Epigondolella sp. aff. *E. transitia* Orchard, 1991b

Plate 4, Figures 19-20

This very ornate epigondolellid has an asymmetric posterior platform due to strong development of one posterolateral lobe. The carina appears continuous to the posterior tip of the platform, but consists of a main anterior carina and one secondary carina on the posteriorly developed lobe. The lower surface has a central to anteriorly shifted pit, and an asymmetric keel that reflects the asymmetry of the platform and carina development. (Orchard, 1991b)

The strong asymmetry of the ornate posterior platform distinguishes this species from other species of *Epigondolella*, particularly the very similar *Epigondolella*

triangularis. *Epigondolella spiculata* also has an asymmetric platform, but differs in ornamentation, profile, and node and carinal formation. The specimens of *E. sp. aff. E. transitia* from Keku Strait are different from *E. transitia* in that they have a strongly bifurcated, less asymmetric keel as in specimens of *E. triangularis*. (Orchard, 1991b)

Epigondolella triangularis (Budurov, 1972) *sensu lato*

Plate 4, Figures 4-12, 15-18

This *Epigondolella* species is strongly ornate with an almost symmetrical platform that is subquadrate to triangular in the posterior half. In profile, the lower surface of the posterior platform steps up posterior of the blade but typically turns down terminally. The blade has about seven to nine denticles and commonly has its maximum height at about midlength, although this is variable in young populations. The blade descends onto the platform and passes into discrete, round carinal nodes that are commonly terminated by a prominent node that lies at the center of the posterior platform, and which rises above adjacent marginal nodes. Lateral nodes on the anterior margins are particularly prominent, as they are upright, sharp, and generally discrete. Secondary nodes on the posterior platform sometimes merge diagonally into secondary carinae. The lower surface bears a basal scar with a distinct edge that surrounds a submedially located pit surrounded by a small, prominent loop. The basal scar commonly bifurcates posteriorly, forming secondary keels extending toward the posterlateral corners and a posterior indentation of the scar that commonly lies close to the pit. (Orchard, 1991b)

Quadrate elements of *Epigondolella triangularis* resemble *E. spiculata*, but the profile, symmetry, node and carinal formation, and basal scar differ. *E. quadrata* is unornamented posteriorly, *E. transitia* has a pronounced posterior asymmetry, and *E. spatulata* and related elements are much shorter and have relatively more expanded subcircular posterior platforms. (Orchard, 1991b)

Orchard (1991b) documented a trend towards increased platform ornamentation, increased posterolateral expansion, and decreased relative blade length in Early Norian populations of *Epigondolella triangularis*. This trend is present within specimens found in this study. While Orchard (1991b) did not report Middle Norian populations of *E. triangularis*, Middle Norian specimens from Keku Strait still display the increased ornamentation, increased posterolateral expansion, and decreased relative blade length. These differences in the posterior platform morphology are most apparent in large specimens and are represented by the following two subspecies.

Epigondolella triangularis triangularis (Budurov, 1972)

Plate 4, Figures 8-9, 15-18

In this subspecies, the posterior half of the platform is bulbous or triangular due to accentuated posterolateral growth and the posterior ornamentation is typically heavier than in *Epigondolella triangularis uniformis*. *Epigondolella triangularis triangularis* originates later in the Early Norian than *E. triangularis uniformis*. (Orchard, 1991b)

Epigondolella triangularis uniformis Orchard, 1991b

Plate 4, Figures 4-7, 10-12

Epigondolella triangularis uniformis exhibits relatively uniform development of the posterior platform, commonly retains subparallel margins throughout growth, and does not become strongly expanded. The posterior ornamentation is commonly weaker than in *E. triangularis triangularis* and this subspecies originates before *E. triangularis triangularis* in the Early Norian. (Orchard, 1991b)

Genus *Metapolygnathus* Hayashi, 1968

This genus comprises gondolellids with a reduced platform anterior of variably pronounced geniculation points and relatively coarse and compact platform microreticulation that covers both the platform margins and nodes in most species. Individual species may be unornamented or show varying degrees of node formation, ranging from subdued to well developed, but never as pronounced as in species of *Epigondolella*. When present, the nodes are relatively small and their maximum amplitude is less than one-half of the total platform height. In lateral profile, the lower surface of *Metapolygnathus* is regularly concave and the platform turns down posteriorly. Growth characteristically proceeds through dual outgrowth of the anterior and, later, posterior portions of the platform which commonly produces a marked submedial to posterior constriction in the early to medium growth stages. The carina is generally low and does not reach the posterior platform margin, which is characteristically rounded or,

in late growth stages, subquadrate. A basal pit is located beneath the posterior half of the platform in most species, though the basal pit migrates to the platform midpoint in advanced forms of the Late Carnian. *Metapolygnathus* ranges throughout the Carnian into the basal Norian. (Orchard, 1983; 1991b)

Metapolygnathus carpathicus (Mock, 1979)

Plate 2, Figures 14-17

The platform of this *Metapolygnathus* species is generally broad with a blunted or broadly rounded posterior margin, and is narrower anteriorly. The low posterior carina has discrete nodes and the pit is located subterminally. In lateral profile, the anterior edge of the platform drops abruptly towards the anterior. Small, anterior facing nodes occur on this geniculation point and distinguish this species from the unornamented *M.* ex. gr. *M. polygnathiformis*. The rest of the platform is unornamented, distinguishing it from *M. nodosus*. In this study, this species co-occurred with *M.* ex. gr. *M. polygnathiformis* and *M. nodosus*. (Mock, 1979)

Metapolygnathus nodosus (Hayashi, 1968)

Plate 2, Figures 12-13, 19-25

Metapolygnathus nodosus has highly variable ornamentation on the platform which ranges from non-nodose (particularly in larger specimens), to weakly nodose (typical), to distinctly but irregularly nodose where the anterior and/or lateral platform

margins are incised. The platform is oval to sub-parallel, generally subsymmetrical, in shape, with a posteriorly downturned platform in profile. Advanced specimens may have discrete, usually irregular anterior nodes, but they are not clearly elevated above the posterior platform margins. The ten or more denticles along the carina are typically highest and commonly fused near the anterior end and the posterior cusp is discrete and node-like. Early growth stages typically have a strong posterior constriction, but in larger specimens, the platform fills out and the once discrete nodes commonly coalesce and become indistinct. This advanced fusion of nodes can make discrimination between nodose and non-nodose species of *Metapolygnathus* difficult. The keel on the lower surface has a groove ending in a pit surrounded by a loop. Large specimens in particular, but also smaller specimens, display great variation in form. The posterior margin can be greatly expanded, creating a strong bifurcation in the keel posterior of the basal pit. Later specimens show anterior migration of the basal pit, denoting transition to later metapolygnathids such as *M. communisti* and *M. primitius*. (Hayashi, 1968; Orchard, 1991b)

This species is similar to *Metapolygnathus primitius*, which has more discrete anterior nodes that clearly rise above the platform margins and are depressed posteriorly. The nodes of *M. nodosus* are more irregular and develop through incision of the platform margins, which otherwise retain a regular height. Nodal fusion creates difficulty in discerning *M. nodosus* from *M. polygnathiformis*. However, most specimens with fusion still have traces of nodes, and since only the largest specimens show well-developed fusion, most specimens are easily differentiated. For example, one specimen (**Plate 2, Figure 27**) has nodes present on one side of the platform margin (partially obscured), but

not on the other. See *M. ex. gr. M. polygnathiformis* for further discussion. (Orchard, 1991a; 1991b)

Metapolygnathus sp. aff. *M. nodosus* (Hayashi, 1968)

Plate 2, Figures 30-33

This species of *Metapolygnathus* is similar to *M. nodosus*, but has a more linguiform shape, a flatter platform which in profile is still slightly raised anteriorly, a higher posterior carina, and a posteriorly located basal pit which is slightly shifted towards the anterior when compared to other *Metapolygnathus* species. Orchard (pers. comm. 2003) believes this species may be an advanced form of *M. nodosus* distinctive of the latest Carnian.

Metapolygnathus ex. gr. *M. polygnathiformis* (Budurov and Stefanov, 1965)

Plate 2, Figures 1-8

For the purpose of this study, *Metapolygnathus polygnathiformis* represents a group of metapolygnathids with subsymmetrical, subquadrate platforms with unornamented margins of uniform height. The platform is generally broadest at or slightly anterior of the midlength and has a strong brim on the posterior platform margin. The anterior carina is high and decreases uniformly into round, discrete carinal nodes. Lateral of the relatively broad adcarinal troughs, the margins of the platform are upturned. The basal keel is broad and terminates posteriorly in a basal pit that, in large

specimens, may bifurcate in a fashion similar to epigondolellids (Hayashi, 1968; Mosher, 1968; Mosher, 1973; Orchard, 1991b)

This definition includes forms that have been called *Metapolygnathus polygnathiformis* and *M. noah* Hayashi 1968, as well as larger forms of *M. nodosus* with fused nodes that appear smooth, and are sometimes hard to distinguish. Figure 7 on Plate 2 may represent a smooth form of *M. nodosus* or a transitional form between nodose and non-nodose species of *Metapolygnathus*. During growth the platforms generally develop more uniformly than *M. nodosus*, do not develop marginal nodes, and develop the broadest part of the platform more anteriorly than in *M. nodosus*. Using these distinctions and the ones discussed with *M. nodosus*, every sample with large, non-nodose *Metapolygnathus* also had smaller, definitive specimens of *M. polygnathiformis*, allowing positive identification of the conodont population. While distinctions between Lower Carnian and Upper Carnian forms may exist, they are not pursued in this study, as *M. polygnathiformis* nearly always co-occurred with *M. carpathicus* and/or *M. nodosus*, indicating the Upper Carnian. (Orchard, 1991b)

Metapolygnathus primitius (Mosher, 1970)

Plate 3, Figures 6-11, 13-18

The anterior half of the platform on this species of *Metapolygnathus* has two to five uniformly developed, discrete, roundly terminated nodes of moderate size on each margin. In lateral view, these nodes project above level of the platform which is relatively flattened and depressed posterior to the nodes. The nodes often coalesce in

very large specimens. The posterior platform is typically broad, subquadrate, and carries no peripheral nodes. Microreticulae cover most of the platform and the nodes and are absent only from the adcarinal area. The high, free blade is well developed, is about one-third unit length, and has a convex upper profile. The blade descends onto the platform and continues as a row of discrete carinal nodes, which terminate in a prominent node that lies well in front of the posterior margin. In profile, the unit is evenly arched with a slight step at the basal pit and downturned posteriorly. The small basal pit has a prominent loop and is typically located under the platform midlength, but well in front of the broad, truncated posterior termination of the keel, which may be posterolaterally expanded in very large specimens. (Mosher, 1970; Orchard, 1983; Orchard, 1991b)

When compared to *Metapolygnathus nodosus*, the pit has distinctly shifted to the anterior and the anterior platform nodes project above the level of the platform margin. When compared to *Epigondolella quadrata*, *M. primitius* has a relatively longer platform, the less prominent anterior denticles are less than double the height of the platform, and the basal pit is still posterior of the platform midlength. Specimens referred to as *M. sp. cf. M. primitius* (**Plate 3, Figures 1-5**) display a similar platform shape and ornamentation as *M. primitius*, but the basal pit has not shifted very far to the anterior of the posterior truncation of the keel. (Orchard, 1991b)

Metapolygnathus sp. cf. *M. reversus* (Mosher, 1973)

Plate 2, Figure 18

Metapolygnathus reversus has an elongate, sub-parallel platform with a medial constriction, a tapered anterior one-quarter platform with indistinct nodes at poorly defined geniculation points, and a rounded posterior one-quarter platform with a distinct brim around the subterminal cusp. The carina is composed of eight or nine low, discrete, ovoid denticles that diminish in size towards the medial constriction, the posterior cusp is not much larger than the other denticles, and, unlike most metapolygnathids, there is no free blade. The grooved keel expands toward the posterior where a pit is surrounded by a prominent oval loop (Mosher, 1973; Orchard, 1991b)

Unlike other neogondolellid-like Upper Triassic species, *Metapolygnathus reversus* has irregular growth of the platform margins, poorly defined but present geniculation points, and a metapolygnathid-like lower surface. The dual outgrowth of the anterior and posterior platform is characteristic of *Metapolygnathus* species. The medially restricted platform in large specimens that is diagnostic of the species is represented by a medially broadened platform in juvenile specimens. *Metapolygnathus* sp. cf. *M. reversus* is similar in platform shape and ornamentation to *M. reversus*, but retains a small free blade. (Mosher, 1973; Orchard, 1991b)

Metapolygnathus sp. aff. *M. zoeae* Orchard, 1991b

Plate 2, Figures 26-29

This relatively elongate species of *Metapolygnathus* is characterized by about four large, well defined, but low, circular nodes on each anterior platform margin. The free blade is about one-third unit length and may have a relatively high convex profile. A prominent loop surrounds the basal pit, which may be slightly shifted anteriorly, and occupies a position near the posterior end of the narrow keel. (Orchard, 1991b)

When compared to *Metapolygnathus nodosus*, this species has much larger, more prominent, and, in upper view, more rounded anterior platform nodes. Additionally, in profile the nodes are much broader, but not significantly higher, than *M. nodosus*. In advanced specimens, the anteriormost nodes may become sharp, as in *M. samueli*, and the blade is often higher than in *M. samueli*. This species can be distinguished from *M. primitius* as the latter has more differentiated and upstanding anterior nodes. The specimens of *M. sp. aff. M. zoeae* presented within have circular nodes, but they are not as well defined as typical *M. zoeae*. (Orchard, 1991a; 1991b)

Genus *Misikella* Kozur and Mock, 1974*Misikella longidentata* Kozur and Mock, 1974

Plate 4, Figure 14

This conodont is very small with a notably widened, deeply incised, cone-shaped basal cavity. The basal cavity extends the length of the unit where it is wide posteriorly and tapered anteriorly. The wide, posterior basal cavity extends beyond the base of the terminal cusp, which is large and strongly points towards the posterior, though a small denticle may occur posterior of the cusp. The three to four denticles anterior to the cusp are much smaller and decrease in size towards the anterior end. The anteriormost denticle, and sometimes the next anteriormost denticle, are vertical or may even point towards the anterior. (Kozur and Mock, 1974)

References

- Atwood, W.W. 1912. Some Triassic Fossils from Southeastern Alaska. *Journal of Geology*, Vol. 20, No. 7, p. 653-655.
- Babcock, L.C. 1976. Conodont Paleocology of the Lamar Limestone (Permian), Delaware Basin, West Texas. *In: Conodont Paleocology*, C.R. Barnes (ed.). Geological Association of Canada, Special Paper 15, p.279-294.
- Behnken, F.H. 1975. Leonardian and Guadalupian (Permian) Conodont Biostratigraphy in Western and Southwestern United States. *Journal of Paleontology*, Vol. 49, No.2, p. 284-315.
- Berg, H.C. 1973. Geology of Gravina Island, Alaska. United States Geological Survey, Bulletin 1373, 44 p.

- Berg, H.C. 1981. Upper Triassic Volcanogenic Massive-Sulfide Metallogenic Province Identified in Southeastern Alaska. *In*: The United States Geological Survey in Alaska; accomplishments during 1979, N.R. Albert and T. Hudson (eds.). United States Geological Survey, Circular 0823-B, p. 104-108.
- Berg, H.C., Jones, D.L., and Coney, P.J. 1978. Map Showing Pre-Cenozoic Tectonostratigraphic Terranes of Southeastern Alaska and Adjacent Areas. United States Geological Survey, Open-File Report 78-1085, 2 sheets.
- Berg, H.C., Jones, D.L., and Richter, D.H. 1972. Gravina-Nutzotin Belt – Tectonic Significance of an Upper Mesozoic Sedimentary and Volcanic Sequence in Southern and Southeastern Alaska. *In*: Geological Survey Research 1972. United States Geological Survey, Professional Paper 800-D, p. 1-24.
- Bittenbender, P.E., Still, J.C., McDonald, M.E. Jr., and Gensler, E.G. 2000. Mineral Investigations in the Stikine Area, Central Southeast Alaska, 1997-1998. Bureau of Land Management – Alaska Open File Report 83, 265 p.
- Blodgett, R.B. and Frýda, J. 2001. On the Occurrence of *Spinidelphinulopsis whaleni* (Gastropoda) in the Late Triassic (Early Norian) Cornwallis Limestone, Kuiu Island, Southeastern Alaska (Alexander Terrane) and its Paleobiogeographic Significance. *Bulletin of the Czech Geological Survey*, Vol. 76, No. 4, p. 235-242.
- Brew, D.A. and Muffler, L.J.P. 1965. Upper Triassic Undevitrified Volcanic Glass from Hound Island, Keku Strait, Southeastern Alaska. *In*: Geological Survey Research 1965. United States Geological Survey, Professional Paper 525-C, p. 38-43.
- Buddington, A.F. and Chapin, T. 1929. Geology and Mineral Deposits of Southeastern Alaska. United States Geological Survey, Bulletin 800, 398 p.
- Budurov, K. 1972. *Ancyrogondolella triangularis* gen. et sp. n. (Conodonta). *Mitteilungen der Gesellschaft der Geologie- und Bergbaustudenten in Oesterreich*, Vol. 21, No. 2, p. 853-860.
- Budurov, K. and Stefanov, S. 1965. Gattung *Gondolella* aus der Trias Bulgariens. *Académie Bulgarien des Sciences, Travaux Géologiques de Bulgare, Série Paléontologie*, Vol. 7, p. 115-127.
- Buryi, G.I. 1997. Evolution of the Platform Elements of the Conodont Genus *Metapolygnathus* and their Distribution in the Upper Triassic of Sikhote-Alin. *In*: Late Paleozoic and Early Mesozoic Circum-Pacific Events and Their Global Correlation, M.J. Dickens, Y. Zunyi, Y. Hongfu, S.G. Lucas, and S.K. Acharyya (eds.). *World and Regional Geology*, Vol. 10, p. 193-197.

- Carey, S.P. 1984. Conodont Biofacies of the Triassic of Northwestern Nevada. In: Conodont Biofacies and Provincialism, D.L. Clark (ed.). Geological Society of America, Special Paper 196, p. 295-305.
- Carlisle, D. 1963. Pillow Breccias and their Aquagene Tuff, Quadra Island, British Columbia. *Journal of Geology*, Vol. 71, No. 1, p. 48-71.
- Carr, T.R., Paull, R.K., and Clark, D.L. 1984. Conodont Paleocology and Biofacies Analysis of the Lower Triassic Thaynes Formation in the Cordilleran Miogeocline. In: Conodont Biofacies and Provincialism, D.L. Clark (ed.). Geological Society of America, Special Paper 196, p. 283-293.
- Carter, E.S. and Orchard, M.J. 2000. Intercalibrated Conodont-Radiolarian Biostratigraphy and Potential Datums for the Carnian-Norian Boundary within the Upper Triassic Peril Formation, Queen Charlotte Islands, British Columbia. Geological Survey of Canada, Current Research 2000-A7, 11 p.
- Channel, J.E.T., Kozur, H.W., Sievers, T., Mock, R., Aubrecht, R., and Sykora, M. 2003. Carnian-Norian Biomagnetostratigraphy at Silická Brezová (Slovakia): Correlation to other Tethyan sections and to the Newark Basin. *Palaeogeography, Palaeoclimatology, Palaeoecology*, Vol. 191, p. 56-109.
- Coney, P.J., Jones, D.L., and Monger, J.W.H. 1980. Cordilleran Suspect Terranes. *Nature (London)*, Vol. 288, p. 329-333.
- Fryda, J. and Blodgett, R.B. 2001. *Chulitnacula*, a New Paleobiogeographically Distinctive Gastropod Genus from Upper Triassic Strata in Accreted Terranes of Southern Alaska. *Journal of the Czech Geological Society*, Vol. 46, No. 3-4, p. 299-306.
- Gehrels, G.E. 1990. Late Proterozoic-Cambrian Metamorphic Basement of the Alexander Terrane on Long and Dall Islands, Southeast Alaska. *Geological Society of America Bulletin*, Vol. 102, p. 760-767.
- Gehrels, G.E. and Berg, H.C. 1984. Geologic Map of Southeastern Alaska. United States Geologic Survey, Open-File Report 84-886.
- Gehrels, G.E. and Berg, H.C. 1994. Geology of Southeastern Alaska. In: The Geology of Alaska, G. Plafker and H.C. Berg (eds.). Geological Society of America, The Geology of North America, Vol. G-1, p. 451-467.
- Gehrels, G.E. and Saleeby, J.B. 1987. Geologic Framework, Tectonic Evolution, and Displacement History of the Alexander Terrane. *Tectonics*, Vol. 6, No. 2, p. 151-173.

- Gehrels, G.E., Saleeby, J.B., and Berg, H.C. 1987. Geology of Anette, Gravina, and Duke Islands, Southeastern Alaska. *Canadian Journal of Earth Sciences*, Vol. 24, p. 866-881.
- Gonzalez, L.C.M., Taylor, D.G., and Stanley, G.D. Jr. 1996. The Antimonio Formation in Sonora, Mexico, and the Triassic-Jurassic boundary. *Canadian Journal of Earth Sciences*, Vol. 33, No. 3, p. 418-428.
- Haeussler, P., Coe, R.S., and Onstott, T.C. 1992. Paleomagnetism of the Triassic Hound Island Volcanics: Revisited. *Journal of Geophysical Research*, Vol. 97, No. B13, p. 19,617-19,639.
- Hayashi, S. 1968. The Permian Conodonts in Chert of the Adoyama Formation, Ashio Mountains, Central Japan. *Earth Science*, Vol. 22, No. 2, p. 63-77.
- Hillhouse, J.W. and Grommé, C.S. 1980. Paleomagnetism of the Triassic Hound Island Volcanics, Alexander Terrane, Southeastern Alaska. *Journal of Geophysical Research*, Vol. 85, No. B5, p. 2,594-2,602.
- Hoover, P.R. 1991. Late Triassic Cyrtinoid Spiriferinacean Brachiopods from Western North America and Their Biostratigraphic and Biogeographic Implications. *Bulletins of American Paleontology*, Vol. 100, No. 337, p. 63-109.
- Jones, D.L., Berg, H.C., Coney, P., and Harris, A. 1981. Structural and Stratigraphic Significance of Upper Devonian and Mississippian Fossils from the Cannery Formation, Kupreanof Island, Southeastern Alaska. *In: The United States Geological Survey in Alaska; accomplishments during 1979*, N.R. Albert and T. Hudson (eds.). United States Geological Survey, Circular 0823-B, p. 109-112.
- Jones, D.L., Howell, D.G., Coney, P.J., and Monger, J.W.H. 1983. Recognition, Character, and Analysis of Tectonostratigraphic Terranes in Western North America. *In: Accretion tectonics in the Circum-Pacific Regions; Proceedings, Oji International Seminar on Accretion Tectonics*, M. Hashimoto and S. Uyeda (eds.), p. 21-35.
- Jones, D.L., Irwin, W.P., and Owenshine A.T. 1972. Southeastern Alaska – A Displaced Continental Fragment? *In: Geological Survey Research 1972*. United States Geological Survey, Professional Paper 800-B, p. 211-217.
- Karl, S.M., Haeussler, P.J., and McCafferty, A.E. 1999. Reconnaissance Geologic Map of the Duncan Canal/Zarembo Area, Southeastern Alaska. United States Geological Survey, Open-File Report 99-168, 29 p.
- Kozur, H. and Mock, R. 1974. Zwei Neue Conodonten-Arten aus der Trias des Slowakischen Karstes. *Casopis pro Mineralogii a Geologii*, Vol. 19, No. 2, p. 135-139.

- Kozur, H. and Mostler, H. 1971. Probleme der Conodontenforschung in der Trias. Geologisch - Palaeontologische Mitteilungen Innsbruck, Vol. 1, No. 4, p. 1-19.
- Kozur, H. 1980. Revision der Conodontenzonierung der Mittel- und Obertrias des Tethyalen Faunenreichs. Geologisch – Paläontologische Mitteilungen Innsbruck, Vol. 10, p. 79-172.
- Krystyn, L. 1980. Field Trip B – Triassic Conodont Localities of the Salzkammergut Region (Northern Calcareous Alps). In: Second European Conodont Symposium, H.P. Schönlaub (ed.). Abhandlungen der Geologischen Bundesanstalt, Vol. 35, p. 61-98.
- Krystyn, L. and Wiedmann, J. 1986. Ein *Choristoceras*- Vorläufer (Ceratitina, Ammonoidea), aus dem Nor von Timor. Neues Jahrbuch für Geologie und Paläontologie, Monatshefte, Vol. 1, p. 27-37.
- Loney, R.A. 1964. Stratigraphy and Petrography of the Pybus-Gambier Area, Admiralty Island, Alaska. United States Geological Survey, Bulletin 1178, 103 p.
- Martin, G.C. 1916. Triassic Rocks of Alaska. Geological Society of America, Bulletin, Vol. 27, p. 685-718.
- McDonald, M.E. Jr., Still, J.C., Bittenbender, P.E., and Coldwell, J.R. 1998. Mineral Investigations in the Stikine Area, Southeast Alaska, 1997. Bureau of Land Management – Alaska, Open File Report 72, 29 p.
- McRoberts, C.A. 1993. Systematics and Biostratigraphy of Halobiid Bivalves from the Martin Bridge Formation (Upper Triassic), Northeast Oregon. Journal of Paleontology, Vol. 67, p. 198-210.
- McRoberts, C.A. 1997. Late Triassic North American Halobiid Bivalves: Diversity Trends and Circum-Pacific Correlations. In: Late Paleozoic and Early Mesozoic Circum-Pacific Events and Their Global Correlation, M.J. Dickens, Y. Zuyi, Y. Hongfu, S.G. Lucas, and S.K. Acharyya (eds.). World and Regional Geology, Vol. 10, p. 198-208.
- McRoberts, C.A. and Blodgett, R.B. 2000. Late Triassic (Norian) Mollusks from the Taylor Mountains Quadrangle, Southwest Alaska. In: Studies by the United States Geological Survey in Alaska, 2000. United States Geological Survey, Professional Paper 62, p. 55-67.
- Mercantel, E.L. 1973. Upper Permian Conodont Biostratigraphy of Northeast Nevada and West-Central Utah. Geological Society of America, Abstracts with Programs, Vol. 5, No. 4, p. 334.

- Mock, R. 1979. *Gondolella carpathica* n. sp., eine wichtige tuvalische Conodontenart. Geologisch - Palaeontologische Mitteilungen Innsbruck Vol. 9, No. 4, p. 171-174.
- Monger, J.W.H. and Ross, C.A. 1971. Distribution of Fusulinaceans in the Western Canadian Cordillera. Canadian Journal of Earth Sciences, Vol. 8, No. 2, p. 259-278.
- Monger, J.W.H., Souther, J.G., Gabrielse, H. 1972. Evolution of the Canadian Cordillera; a Plate-Tectonic Model. American Journal of Science, Vol. 272, No. 7, p. 15-39.
- Montanaro-Gallitelli, E., Russo, A., and Ferrari, P. 1979. Upper Triassic Coelenterates of Western North America. Bolletino della Societa Paleontologica Italiana, Vol. 18, No. 1, p. 133-156.
- Mosher, L.C. 1968. Triassic Conodonts from Western North America and Europe and their Correlation. Journal of Paleontology, Vol. 42, No. 4, p. 895-946.
- Mosher, L.C. 1970. New Conodont Species as Triassic Guide Fossils. Journal of Paleontology, Vol. 44, No. 4, p. 737-742.
- Mosher, L.C. 1973. Triassic Conodonts from British Columbia and the Northern Arctic Islands. Geological Survey of Canada, Bulletin 222, p. 141-193.
- Muffler, L.J.P. 1967. Stratigraphy of the Keku Islets and Neighboring Parts of Kuiu and Kupreanof Island Southeastern Alaska. United States Geological Survey, Bulletin 1241-C, 52 p.
- Muffler, L.J.P., Short, J.M., Keith, T.E.C., and Smith, V.C. 1969. Chemistry of Fresh and Altered Basaltic Glass from the Upper Triassic Hound Island Volcanics, Southeastern Alaska. American Journal of Science, Vol. 267, p. 196-209.
- Newton, C.R. 1983. Paleozoogeographic Affinities of Norian Bivalves from the Wrangellian, Peninsular, and Alexander Terranes, Western North America. In: Pre-Jurassic Rocks in Western North American Suspect Terranes, C.H. Stevens (ed.), Pacific Section, Society of Economic Paleontologists and Mineralogists, Los Angeles, p. 37-48.
- Orchard, M.J. 1983. *Epigondolella* Populations and their Phylogeny and Zonation in the Norian (Upper Triassic). Fossils and Strata, Vol. 15, p. 177-192.
- Orchard, M.J. 1991a. Late Triassic Conodont Biochronology and Biostratigraphy of the Kunga Group, Queen Charlotte Islands, British Columbia. In: Evolution and Hydrocarbon Potential of the Queen Charlotte Basin, British Columbia, G.J. Woodsworth (ed.). Geological Survey of Canada, Paper 90-10, p. 173-193.

- Orchard, M.J. 1991b. Upper Triassic Conodont Biochronology and New Index Species from the Canadian Cordillera. In: Ordovician to Triassic Conodont Paleontology of the Canadian Cordillera, M.J. Orchard and A.D. McCracken (eds.). Geological Survey of Canada, Bulletin 417, p. 299-335.
- Orchard, M.J., and Tozer, E.T. 1997. Triassic Conodont Biochronology, its Calibration with the Ammonoid Standard, and a Biostratigraphic Summary for the Western Canada Sedimentary Basin. Bulletin of Canadian Petroleum Geology, Vol. 45, No. 4, p. 675-692.
- Orchard, M.J., Cordey, F., Rui, L., Bamber, E.W., Mamet, B., Struik, L.C., Sano, H., and Taylor, H.J. 2001. Biostratigraphic and Biogeographic Constraints on the Carboniferous to Jurassic Cache Creek Terrane in Central British Columbia. Canadian Journal of Earth Sciences, Vol. 38, No. 4, p. 551-578.
- Rubin, C.M. and Saleeby, J.B. 1991. The Gravina Sequence: Remnants of a Mid-Mesozoic Oceanic Arc in Southern Southeast Alaska. Journal of Geophysical Research, Vol. 96, No. B9, p. 14,551-14,568.
- Saleeby, J.B. 1983. Accretionary Tectonics of the North American Cordillera. Annual Review of Earth and Planetary Sciences, Vol. 11, p. 45-73.
- Silberling, N.J. and Tozer, E.T. 1968. Biostratigraphic Classification of the Marine Triassic in North America. Geological Society of America, Special Paper 110, 63 p.
- Silberling, N.J., Grant-Mackie, J.A., and Nichols, K.M. 1997. The Late Triassic Bivalve *Monotis* in Accreted Terranes of Alaska. United States Geological Survey, Bulletin 2151, 21 p.
- Smith, J.P. 1927. Upper Triassic Marine Invertebrate Faunas of North America. United States Geological Survey, Professional Paper 141, 262 p.
- Soja, C.M. 1996. Island-Arc Carbonates: Characterization and Recognition in the Ancient Geologic Record. Earth Science Reviews, Vol. 41, p. 31-65.
- Stanley, G.D., González-León, C., Sandy, M.R., Senowbari-Daryan, B., Doyle, P., Tamura, M., and Erwin, D.H. 1994. Upper Triassic Invertebrates from the Antimonio Formation, Sonora, Mexico. Journal of Paleontology, Vol. 68, Supplement to No. 4, The Paleontological Society Memoir 36, 33p.
- Still, J.C., Bittenbender, P.E., Bean, K.W., and Gensler, E.G. 2002. Mineral Assessment of the Stikine Area, Central Southeast Alaska. Bureau of Land Management – Alaska Technical Report 51, 560 p.

- Tatzreiter, F. 1975. Zur Stellung der *Himavatites columbianus* Zone (Höheres Mittelnor) in der Tethys. In: Beitrage zur Biostratigraphie der Tethys-Trias, H. Zapfe (ed.). Schriftenreihe der Erdwissenschaftlichen Kommissionen, Vol. 4, p. 105-139.
- Taylor C., Philpotts J.A., Sutley S.J., Gent C.A., Harlan S.S., Premo W.R., Tatsumoto M. Emsbo P., and Meier A.L. 1995. Geochemistry of Late Triassic Volcanic Host Rocks and Age of Alteration Associated with Volcanogenic Massive Sulfide Occurrences, Alexander Terrane, Southeast Alaska. In: Geology and Ore Deposits of the American Cordillera; a Symposium, p. 74.
- Tozer, E.T. 1967. A Standard for Triassic Time. Geological Survey of Canada, Bulletin 156, 103 p.
- Tozer, E.T. 1984. The Trias and its Ammonoids: The Evolution of a Time Scale. Geological Survey of Canada, Miscellaneous Report 35, 171 p.
- Tozer, E.T. 1994. Canadian Triassic Ammonoid Faunas. Geological Survey of Canada, Bulletin 467, 663 p.
- Van Nieuwenhuyse, U.E. 1984. Geology and Geochemistry of the Pyrola Massive Sulfide Deposit Admiralty Island, Southeast Alaska. University of Arizona, Unpublished Master's Thesis, 170 p.
- Wardlaw, B.T. 1982. Report on Referred Fossils, 1982 (1220). Unpublished United States Geological Survey E&R Report, USGS Mesozoic locality 32771.
- Wilson, J.T. 1968. Static or Mobile Earth; the Current Scientific Revolution. Proceedings of the American Philosophical Society, Vol. 112, No. 5, p. 309-320.
- Wright, F.E. and Wright, C.W. 1908. The Ketchikan and Wrangell Mining Districts, Alaska. United States Geological Survey, Bulletin 347, 210 p.

APPENDIX A: Locality table with University of Montana Museum of Paleontology locality numbers

Locality #	USGS #	Formation	Locality Name	N Latitude	W Longitude	Age
MI 0040	--	Cannery	Watershed Rocks - Sample 1	56°58.812'	133°55.591'	Permian?
MI 0041	--	Cannery	Watershed Rocks - Sample 2	56°58.991'	133°53.455'	Permian?
MI 0042	--	Cannery	Watershed Rocks - Sample 3	56°59.547'	133°52.395'	Permian?
MI 0043	--	Cannery	Watershed Rocks - Sample 4	57°00.678'	133°51.515'	Permian?
MI 0044	--	Cannery	Watershed Rocks - Sample 5	57°01.796'	133°51.384'	Permian?
MI 0045		Keku Volcanics	Cornwallis Peninsula East, Keku/Cornwallis Transition - site 1	56°55.069'	134°11.039'	Cretaceous?
MI 0046	--	Hound Island Volcanics	Black and Tan	56°49.372'	133°57.859'	Late Triassic
MI 0047	--	Burnt Island Conglomerate	Island East of Burnt Island	56°56.898'	133°55.959'	Late Triassic
MI 0050	--	Saginaw Bay	Trickling Cave	56°53.172'	134°03.480'	Carboniferous
MI 0051	--	Saginaw Bay	Samtron Monitor Island	56°55.399'	134°08.546'	Carboniferous
MI 0052	--	Muffler's Crinoidal limestone	Cornwallis Peninsula East, east of the Elephant's Head	56°54.908'	134°09.886'	Carboniferous?
MI 0053	--	Cannery	Hamilton Island Northeast, Cannery Formation	56°56.572'	133°55.104'	Permian?
MI 0054	--	Pybus	White Rock Road Pit	56°54.534'	133°44.010'	Permian
MI 0055	1918	Keku Volcanics / Cornwallis Limestone	Neptunian Dike and M1918	56°53.347'	134°04.380'	Late Triassic
MI 0056	2135	Keku Volcanics / Cornwallis Limestone	Big Spruce Island	56°55.400'	134°09.217'	Late Triassic
MI 0057	--	Burnt Island Conglomerate	Hamilton Island Northeast, Burnt Island Conglomerate	56°56.671'	133°55.435'	Late Triassic
MI 0058	--	Burnt Island Conglomerate	Portage Pass, Burnt Island Conglomerate site 3	56°55.031'	133°51.963'	Late Triassic
MI 0059	--	Burnt Island Conglomerate / unnamed shallow water limestone	Portage Pass, Burnt Island Conglomerate site 4	56°54.875'	133°51.545'	Late Triassic
MI 0060	1882-4	Hamilton Island Limestone	Hamilton Island Northeast NE Shore	56°56.630'	133°55.437'	Late Triassic
MI 0061	1924	Hamilton Island Limestone	Payne Island North, M1924	56°56.571'	134°08.675'	Late Triassic
MI 0062	1904	Burnt Island Conglomerate / Hamilton Island Limestone	Payne Island Southwest	56°56.339'	134°06.832'	Late Triassic

MI 0063	--	Hamilton Island Limestone	Small Island south of Payne Island Southwest	56°56.207'	134°06.809'	Late Triassic
MI 0064	1903	Hamilton Island Limestone	Payne Island Southwest, M1903	56°56.336'	134°07.454'	Late Triassic
MI 0065	2126?	Hamilton Island Limestone	Top Cathedral Falls	56°54.103'	133°43.281'	Late Triassic
MI 0066	1932	Hamilton Island Limestone	Portage Pass	56°55.218'	133°52.491'	Late Triassic
MI 0067	1889	Hamilton Island Limestone	Hamilton Island Southeast	56°54.559'	133°51.118'	Late Triassic
MI 0068	--	Cornwallis Limestone	Floating Unknown	56°52.838'	134°02.406'	Late Triassic
MI 0069	--	Cornwallis Limestone	Cornwallis Peninsula East june 22	56°56.215'	134°15.180'	Late Triassic
MI 0070	1906	Cornwallis Limestone	Cornwallis Peninsula East, M1906	56°56.099'	134°14.534'	Late Triassic
MI 0071	--	Cornwallis Limestone	Kuiu Island East	56°52.922'	134°01.397'	Late Triassic
MI 0072	--	Cornwallis Limestone	Kuiu Island East-A	56°52.726'	134°01.336'	Late Triassic
MI 0073	--	Cornwallis Limestone	K(?) and K(not)	56°52.770'	134°02.203'	Late Triassic
MI 0074	2136	Cornwallis Limestone	Southwest of Kousk Island	56°53.690'	134°00.508'	Late Triassic
MI 0075	--	Hound Island Volcanics	Hamilton Island West - site 3	56°55.653'	133°54.135'	Late Triassic
MI 0076	--	Hound Island Volcanics	Hamilton Island West - site 4	56°55.885'	133°54.636'	Late Triassic
MI 0077	--	Hound Island Volcanics	Hamilton Island West - site 5	56°55.920'	133°54.644'	Late Triassic
MI 0078	1886-7	Hound Island Volcanics	Hamilton Island West - site 6	56°56.260'	133°55.125'	Late Triassic
MI 0079	1899	Hound Island Volcanics	Hound Island West, M1899	56°52.798'	133°56.805'	Late Triassic
MI 0080	1923	Hound Island Volcanics	Hound Island West, M1923	56°52.323'	133°56.447'	Late Triassic
MI 0081	1921	Hound Island Volcanics	Hound Island West, M1921	56°52.017'	133°56.075'	Late Triassic
MI 0082	--	Hound Island Volcanics	Hound Island North	56°53.132'	133°56.848'	Late Triassic
MI 0083	1913	unnamed shallow water limestone	Cape Bendel Day 2	57°04.176'	134°00.905'	Late Triassic
MI 0084	--	Hamilton Island Limestone	Cape Bendel Day 2-A	57°04.155'	134°00.907'	Late Triassic
MI 0085	1890/ 1921	Hound Island Volcanics	Hamilton Island Southwest	56°54.696'	133°52.330'	Late Triassic
MI 0086	1900-1	Hound Island Volcanics	Hound Island East	56°52.635'	133°56.011'	Late Triassic
MI 0087	1912	Hound Island Volcanics	Gil Harbor	56°50.050'	134°00.717'	Late Triassic
MI 0088	--	Cannery	Cape Bendel Day 1 - site 1	57°02.147'	134°00.697'	Permian?
MI 0089	--	Pybus	Cape Bendel Day 1 - site 2	57°02.296'	134°00.652'	Permian
MI 0090	--	Burnt Island Conglomerate	Cape Bendel Day 1 - site 3	57°02.448'	134°00.729'	Late Triassic

MI 0091	--	Cannery? / Hamilton Island Limestone	Cape Bendel Day 1 - site 4	57°02.599'	134°00.805'	Permian? / Late Triassic
MI 0092	--	Hound Island Volcanics	Cape Bendel Day 1 - site 5	57°02.893'	134°00.878'	Late Triassic
MI 0093	--	Cannery?	Cape Bendel Day 1 - site 6	57°03.763'	133°59.112'	Permian?
MI 0094	--	Hound Island Volcanics	Cape Bendel Day 1 - site 9	57°02.682'	134°01.154'	Late Triassic
MI 0095	--	Cornwallis Limestone	Cornwallis Peninsula East, Keku/Cornwallis Transition - site 3	56°55.040'	134°11.011'	Late Triassic
MI 0096	--	Cornwallis Limestone	Cornwallis Peninsula East, Keku/Cornwallis Transition - site 2	56°55.058'	134°11.038'	Late Triassic
MI 0097	--	Pybus / Burnt Island Conglomerate / Hamilton Island Limestone	Squawking Crow	56°55.744'	134°05.260'	Permian / Late Triassic
MI 0098	1928	Hamilton Island Limestone / Hound Island Volcanics	Hamilton Island Southwest, Hamilton/Hound Transition	56°55.021'	133°52.468'	Late Triassic
MI 0099	1910- 11	Keku Volcanics / Cornwallis Limestone	Flounder Cove	56°51.643'	134°00.661'	Late Triassic
MI 0100	--	Burnt Island Conglomerate?	Metamorphic 2002: Metaconglomerate rock pit	56°55.223'	133°38.259'	Late Triassic?
MI 0101	--	Cannery?	Metamorphic 2002: phyllite A	56°52.940'	133°37.379'	Permian?
MI 0102	--	Keku Volcanics?	Metamorphic 2002: Rhyolite	56°55.756'	133°32.875'	Cretaceous?
MI 0103	--	Cannery?	Metamorphic 2002: phyllite B	56°55.665'	133°29.122'	Permian?

APPENDIX B: Biostratigraphically significant fossils recovered from the Keku Strait area

Locality # is as in Appendix A; Biozone is the applicable ammonoid or conodont biozone as presented in Figure 48; Type is the fossil used to determine the biozone with A for ammonoid, B for bivalve, C for conodont, and H for *Heterastridium*; and Fm is Formation as in Table 1.

Late Carnian

Locality #	Sample	Biozone	Type	Fossil Names	Fm
60	HMNE-C1	"upper" <i>nodosus</i>	C	<i>Metapolygnathus nodosus</i> , <i>M. polygnathiformis</i> , <i>M. carpathicus</i>	HL
60	HMNE-C3	upper <i>nodosus</i>	C	<i>Metapolygnathus nodosus</i> , <i>M. polygnathiformis</i> , <i>M. carpathicus</i> , <i>M. sp. aff. M. zoeae</i>	HL
60	HMNE-C6	upper <i>nodosus</i>	C	<i>Metapolygnathus nodosus</i> , <i>M. polygnathiformis</i>	HL
60	HMNE 34.4	--	A	Tropitid	HL
60	HMNE-C8	Dilleri	A	<i>Shastitas sp.</i> , <i>Hannoceras sp.</i> , <i>Shastitas? sp.</i>	HL
60	HMNE-C8	Dilleri-Welleri	A	<i>Paratropites?</i>	HL
60	HMNE-C9F2	Welleri	A	<i>Discotropites? sp.</i>	HL
60	HMNE-C10	upper <i>nodosus</i>	C	<i>Metapolygnathus polygnathiformis</i>	HL
60	HMNE-C13	upper <i>nodosus</i>	C	<i>Metapolygnathus carpathicus</i>	HL
60	HMNE-C15	upper <i>nodosus</i>	C	<i>Metapolygnathus nodosus</i> , <i>M. sp. aff. M. zoeae</i>	HL
60	HMNE-C16	upper <i>nodosus</i>	C	<i>Metapolygnathus nodosus</i> , <i>M. carpathicus</i>	HL
60	HMNE-C17	upper <i>nodosus</i>	C	<i>Metapolygnathus nodosus</i> , <i>M. polygnathiformis</i> , <i>M. carpathicus</i>	HL
60	HMNE 69.1	Welleri	A	<i>Hannoceras sp.</i>	HL
61	M1924-F	--	A	Tropitid	HL
61	M1924-F	--	B	<i>Halobia sp. cf. H. superba</i> , <i>H. sp. cf. H. ornatissima</i>	HL
62	PISW-C2L2	middle <i>nodosus</i>	C	<i>Metapolygnathus nodosus</i> , <i>M. polygnathiformis</i> , <i>M. sp. cf. M. reversus</i>	HL
62	PISW-C3L3	<i>nodosus</i>	C	<i>Metapolygnathus polygnathiformis?</i> , <i>M. sp.</i> , <i>Neogondolella? sp.</i>	HL
62	PISW-C7	<i>nodosus</i>	C	<i>Metapolygnathus nodosus</i>	HL
66	PP-C2F2	<i>nodosus</i>	C	<i>Metapolygnathus polygnathiformis</i> , <i>M. carpathicus</i>	HL
66	M1932 (photo)	--	B	<i>Halobia ornatissima</i> (silicified)	HL
67	HMSE-C1	uppermost <i>nodosus</i>	C	<i>Metapolygnathus sp. aff. M. nodosus</i>	HL
67	HMSE-C2	uppermost <i>nodosus</i>	C	<i>Metapolygnathus sp. aff. M. nodosus</i> , <i>M. sp. aff. M. zoeae</i>	HL
67	HMSE A5.6-5.7	--	B	<i>Halobia sp. cf. H. superba</i>	HL
67	HMSE A10.75m	Welleri	A	<i>Discotropites? sp.</i>	HL
83	CB2-C2	uppermost <i>nodosus</i>	C	<i>Metapolygnathus sp. aff. M. nodosus</i> , <i>M. polygnathiformis</i>	un
83	CB2-C3	uppermost <i>nodosus</i>	C	<i>Metapolygnathus sp. aff. M. nodosus</i> , <i>M. polygnathiformis</i>	un
84	CB2-C1A	lower <i>nodosus</i>	C	<i>Metapolygnathus sp. cf. M. nodosus</i>	HL

Late Carnian (continued)

Locality #	Sample	Biozone	Type	Fossil Names	Fm
84	CB2-C2A	<i>lower nodosus</i>	C	<i>Metapolygnathus polygnathiformis</i> , <i>M. sp. cf. M. reversus</i> , <i>M. reversus?</i>	HL
97	SC-C4	<i>upper nodosus</i>	C	<i>Metapolygnathus nodosus</i> , <i>M. polygnathiformis</i>	HL
97	SC-F4	--	A,B	Tropitids, <i>Halobia ornatissima?</i>	HL
99	FL-C2	<i>nodosus</i>	C	<i>Metapolygnathus sp. cf. M. nodosus</i>	C
99	FL-C3	<i>nodosus-primitius</i>	C	<i>Metapolygnathus sp. cf. M. primitius</i>	C
99	FC2-C1	<i>nodosus-primitius</i>	C	<i>Metapolygnathus sp. cf. M. primitius</i>	C
99	FC2-C2	<i>nodosus-primitius</i>	C	<i>Metapolygnathus nodosus</i> , <i>M. sp. aff. M. zoeae</i> , <i>M. sp. cf. M. primitius</i>	C

Late Carnian or Early Norian

Locality #	Sample	Biozone	Type	Fossil Names	Fm
55	SM-C1	<i>nodosus-primitius</i>	C	<i>Metapolygnathus sp. cf. M. primitius</i>	C
56	BS-C2	--	C	Metapolygnathid or Epigondolellid	C
64	PISW-F3	--	B	<i>Halobia radiata</i> , <i>H. sp. cf. H. austriaca</i>	HL
65	TCF-F	--	B	<i>Halobia radiata</i>	HL
70	CP-C2	<i>nodosus-primitius</i>	C	<i>Metapolygnathus sp. cf. M. primitius</i> , <i>Neogondolella sp.</i>	C
70	CPE-F2	<i>primitius</i>	C	<i>Metapolygnathus primitius</i> , <i>M. sp. aff. M. primitius</i>	C
70	CPE-C3	<i>primitius</i>	C	<i>Metapolygnathus primitius</i>	C
74	SWK 1	<i>primitius</i>	C	<i>Metapolygnathus primitius</i>	C
95	CPE-C4	<i>primitius?</i>	C	<i>Metapolygnathus primitius?</i>	C
96	CPE-C5	<i>primitius</i>	C	<i>Metapolygnathus primitius</i>	C

Early Norian

Locality #	Sample	Biozone	Type	Fossil Names	Fm
56	BS-C5	<i>quadrata</i>	C	<i>Epigondolella sp. cf. E. quadrata</i>	C
66	PP-C1F1	--	B	<i>Halobia beyrichi</i> , <i>H. sp. cf. H. cordillerana</i> , <i>H. sp. cf. H. lineata</i>	HL
66	PP-C2F2	--	B	<i>Halobia sp. cf. H. beyrichi</i> , <i>H. cordillerana</i>	HL
68	FU-C1	<i>quadrata?</i>	C	<i>Epigondolella sp. cf. E. quadrata</i> , <i>Metapolygnathus sp.</i>	C
69	CPE-C2	<i>triangularis</i>	C	<i>Epigondolella triangularis uniformis</i> , <i>E. quadrata</i> , <i>E. sp. aff. E. quadrata</i> , <i>Metapolygnathus primitius</i>	C
70	CP-C1	<i>primitius-quadrata</i>	C	<i>Epigondolella sp. cf. E. quadrata</i> , <i>Metapolygnathus sp. cf. M. primitius</i>	C
72	KUW-F3A	<i>Kerri</i>	A	<i>Guembelites clavatus</i>	C
73	K(not)-C	--	C	<i>Epigondolella sp.</i>	C

Early Norian (continued)

Locality #	Sample	Biozone	Type	Fossil Names	Fm
74	SWK 2	<i>primitius-quadrata</i>	C	<i>Epigondolella</i> sp. cf. <i>E. quadrata</i> , <i>Metapolygnathus primitius</i>	C
74	SWK 2	<i>primitius-quadrata</i>	C	<i>Epigondolella</i> sp. cf. <i>E. quadrata</i> , <i>Metapolygnathus primitius</i>	C
79	HIW-C2	<i>triangularis</i>	C	<i>Epigondolella triangularis uniformis</i> , <i>E. triangularis triangularis</i> , <i>E. quadrata</i>	HV
79	HIW-F1	--	B	<i>Halobia</i> sp. cf. <i>H. beyrichi</i> , <i>H. sp. cf. H. lineata</i>	HV
80	HIW-F2	--	B	<i>Halobia beyrichi</i> ?	HV
81	HIW-C5	<i>triangularis</i>	C	<i>Epigondolella</i> sp. cf. <i>E. triangularis</i>	HV
82	HIN-C2	<i>triangularis?</i>	C	<i>Epigondolella triangularis?</i> , <i>E?</i> sp., <i>Metapolygnathus?</i> sp., <i>Neogondolella?</i> sp.	HV
85	HMSW-C1F1	--	B	<i>Halobia</i> sp. cf. <i>H. beyrichi</i> , <i>H. sp. cf. H. fallax</i>	HV
97	SC-F1	--	B	<i>Halobia cordillerana</i> , <i>H. lineata</i>	HL
99	FL-C6	<i>primitius</i>	C	<i>Metapolygnathus primitius</i>	C
99	FL-C11	<i>primitius</i>	C	<i>Metapolygnathus</i> sp. aff. <i>M. primitius</i>	C
99	FL-C12	<i>primitius</i>	C	<i>Metapolygnathus</i> sp. aff. <i>M. primitius</i>	C
99	FL-C16	<i>triangularis</i>	C	<i>Epigondolella triangularis uniformis</i> , <i>E. triangularis triangularis</i> , <i>E. quadrata</i> , <i>E. sp. aff. E. quadrata</i> , REWORKED unknown older conodont	C
99	FL-C17	<i>triangularis</i>	C	<i>Epigondolella triangularis uniformis</i> , <i>E. triangularis triangularis</i> , <i>E. quadrata</i> , <i>E. sp. aff. E. quadrata</i> , <i>Misikella longidentata</i>	C
99	FL	Kerri	A	<i>Stikinoceras kerri</i> , <i>Greisbachites?</i> sp.	C
99	FC2-F3	Kerri	A,B	<i>Stikinoceras kerri</i> , <i>Halobia beyrichi</i>	C
99	FC2-F7	Kerri	B	<i>Halobia cordillerana</i>	C
99	FC2-F6	Kerri	A	<i>Stikinoceras kerri</i>	C

Middle Norian

Locality #	Sample	Biozone	Type	Fossil Names	Fm
46	BT-C2	<i>spiculata</i>	C	<i>Epigondolella triangularis triangularis</i> , <i>E. spiculata</i>	HV
86	HIE-C2	--	C	<i>Neogondolella</i> sp. cf. <i>N. steinbergensis</i> , <i>N. sp.</i>	HV
86	HIE-C3	<i>postera</i>	C	<i>Epigondolella</i> sp. cf. <i>E. postera</i> , <i>Neogondolella</i> sp.	HV
86	HL-C1	--	C	<i>Neogondolella</i> sp.	HV
86	HL-C2	--	C	<i>Metapolygnathus?</i> sp.	HV
86	HL-C6	<i>spiculata</i>	C	<i>Epigondolella spiculata</i> , <i>Neogondolella</i> sp.	HV
86	HIE-F1	--	B	<i>Halobia fallax</i>	HV
86	HIE-F4	--	B	<i>Halobia fallax</i>	HV

Middle Norian (continued)

Locality #	Sample	Biozone	Type	Fossil Names	Fm
87	GH-C1	<i>spiculata</i>	C	<i>Epigondolella spiculata</i> , <i>E. sp. aff. E. matthewi</i> , <i>E. sp. aff. E. spatulata</i> , <i>E. triangularis triangularis</i>	HV
87	GH-C2	<i>spiculata</i>	C	<i>Epigondolella spiculata</i>	HV

Late Norian

Locality #	Sample	Biozone	Type	Fossil Names	Fm
87	GH-C6	<i>bidentata</i>	C	<i>Epigondolella tozeri</i> , <i>E. sp. aff. E. mosheri</i> , <i>E. bidentata</i>	HV
87	=GH-C6	<i>bidentata</i>	C	<i>Epigondolella tozeri</i> , <i>E. englandi</i> , <i>E. sp. aff. E. mosheri</i> , <i>E. bidentata</i>	HV
87	GBC	Cordilleranus	H	<i>Heterastridium conglobatum</i>	HV
87	GHBC-1	Cordilleranus	H	<i>Heterastridium conglobatum</i>	HV
87	GHBC-1	Columbianus III	A	<i>Hellerites sp. or Parajuvavites sp.</i>	HV

Reworked Paleozoic Conodonts

Locality #	Sample	Age	Type	Fossil Names	Fm
62	PISW-C1L1	Early Permian	C	<i>Mesogondolella sp.</i>	HL
68	FU-C1	Devonian	C	<i>Polygnathus linguiformis</i> , <i>P. sp.</i>	C
68	FU-C2	middle Devonian	C	<i>Belodella triangularis</i> , <i>Panderodus sp.</i> , <i>Palmatolepis sp. (juvenile)</i> , <i>Polygnathus sp.</i> , Unknown?	C
97	SC-C2	Early Permian	C	<i>Mesogondolella sp.</i> , <i>Sweetognathus sp.</i>	HL

Appendix C: Methods

Field Work

I visited Triassic rocks of the Hyd Group in the Keku Strait area during five days in the summer of 2001 and thirty days in the summer of 2002. During these field seasons, I collected paleontologic and lithologic samples, and measured several stratigraphic sections. Hyd Group outcrops are well-exposed within island tidal zones throughout the area and are less well-exposed inland in areas of steep relief or road construction. Accordingly, small boats of all kinds can access island outcrops, while automobiles can access areas inland on Kupreanof Island via an extensive road system. Overall, I attempted to visit a variety of units, lithologies, and ages throughout the field area in order to construct a robust data set. In the field, I used a hand-held Garmin III Plus GPS (Global Positioning System) unit to assist site location and record site coordinates. This unit was especially useful for boat navigation.

During both field seasons, I collected conodont samples from every carbonate rock available, focusing on higher carbonate contents from every calcareous lithology. If enough continuous outcrop was present, I took samples approximately every 5 meters. If the outcrop was small, then I took between one and three representative samples from the outcrop available. Conodont samples averaged between two and four kilograms. I collected macrofossils whenever I found them, and photographed ones that were unobtainable, in order to fully represent the fossil diversity and preservation. At many macrofossil-rich localities, I collected limestone blocks for acid etching and further fossil recovery in the laboratory. I also collected lithologic samples from every major unit and each conodont sample. All of the fossils are curated at the University of Montana Museum of Paleontology, and the lithology samples are stored in the Department of Geology at the University of Montana. The few places with successions over ten meters in thickness were measured using a 1.5-meter stick divided into one decimeter units by alternating red and white stripes. These sites were at Northeastern Hamilton Island, Flounder Cove, and Big Spruce Island (University of Montana, Museum of Paleontology Localities 60, 99 and 56 respectively).

Laboratory Work

To extract the conodonts, I used the techniques of acetic acid dissolution, wet-sieving, and heavy liquid separation in sodium polytungstate. Sample preparation and conodont extraction were carried out in the University of Montana rock preparation lab and paleontology lab respectively. First, I crushed the limestone and other calcareous samples in a Braun Chipmunk to make pieces of rock from one to four centimeters in size. One to one-and-a-half kilogram portions of the crushed samples were measured into ten-liter plastic buckets, which were subsequently filled with ten-percent acetic acid solution. After the samples sat in acid for two days under ventilation, I decanted six to seven liters of the solution, leaving behind the remaining sample and some calcium acetate solution. Then, I refilled the buckets proportionally to create a ten-percent acetic acid solution around the samples. The calcium acetate solution acts as a buffer to maintain the pH of the reaction and prevent damage to exposed conodonts. Because the buffered reaction is slower, the samples were left in the fume hood for three days.

The resulting insoluble residues from the dissolution procedure were wet-sieved and washed through a two-sieve stack consisting of 20 (0.841 mm) and 200 (0.075 mm) mesh standard 21cm diameter sieves. If the material in the 200-mesh sieve was high in organic content, I treated it with bleach and then washed it through the 200-mesh sieve again. All the material from the 200-mesh sieve was air dried in an oven at about 75 degrees Celsius to remove excess water. I then placed the dried samples in separatory funnels, with about 200 ml of sample per funnel. Each funnel contained sodium polytungstate solution at a specific gravity of 2.85. I stirred the solution in each funnel every half-hour for three hours to ensure that the heavy grains fell through the viscous fluid. After allowing the fluid to settle for one hour, I collected the heavy and light fractions separately in paper filters and washed them with water. I collected the water-washed and diluted sodium polytungstate solution in beakers and allowed it to evaporate, leaving behind sodium polytungstate solution for reuse. After the washed heavy fraction dried, I picked the conodonts from it using a very fine brush and a binocular dissecting microscope.

Of the 80 samples processed for conodonts, 63 were productive. By comparing the pre-dissolution weight to the coarse sieve fraction remaining after dissolution, a percentage of the remaining sample roughly indicates sample breakdown. The average breakdown for these samples was 67%. After picking out the conodonts, I identified them under the binocular microscope. M. Orchard of the Geological Survey of Canada in Vancouver assisted in conodont identifications. I selected and mounted some of the identified conodonts on aluminum SEM stubs with two-sided tape and coated them with about 30 nm of gold in a PELCO Model 3 Sputter Coater 91000 before viewing them on a Hitachi S-4700 Scanning Electron Microscope (SEM). The SEM allowed me to examine the conodonts in more detail, thereby facilitating and improving identification, and allowed me to take digital photographs.

As a NSF grant associated with this project was focused on corals and reef faunas from various terranes, many limestone blocks were processed for macrofossils to supplement field collections. This involved etching of the limestone blocks in various concentrations of acetic and hydrochloric acid. When I needed conodonts from a limestone block with abundant macrofossils, it was only processed in acetic acid as hydrochloric acid rapidly dissolves conodonts. This saved time and money, as we avoided processing two different limestone blocks separately for conodonts and macrofossils. When processing macrofossil samples, the limestone blocks were not crushed before acid dissolution. Overall, this technique more than tripled the amount of macrofossils collected in the field.

Many of the lithologic samples used in this thesis were cut to produce fresh surfaces for examination, and some of these were polished. Most lithologic observations were based on these rough or cut, occasionally polished, hand samples. Some rocks were made into thin sections, though petrographic analysis was not a focus of this study and only one is figured in the preceding work.

Appendix D: Future Work

Despite the amount of new data this project produced, it raised even more questions about the Triassic units in the Keku Strait area. These include new mapping of examined and unexamined Triassic outcrop, additional paleontologic sampling, improved stratigraphic correlations with sedimentary, volcanic, and metamorphic units, and improved structural and tectonic interpretations.

Because of the reliance on past localities for sample collection and the limited time available for fieldwork, much of the Triassic outcrop in Keku Strait is unexamined. Additionally, many unstudied and undiscovered sites of Triassic outcrop exist inland on Kupreanof and Kuiu islands. The development of road systems, mainly from resource production, has greatly improved access to the inland regions. The only two maps available for Triassic outcrops in the Keku Strait area (Muffler, 1967) and the Duncan Canal-Zarembo map area to the east (Karl *et al.*, 1999) are reconnaissance maps. These maps are well-drafted, but for a more complete understanding of the region's geologic history, more geologic mapping is required. Augmented and improved geologic maps contribute to all other geologic interpretations with the region. Cornwallis Peninsula is a specific example of an area that needs revised mapping. Many repercussions result from the fact that the felsic igneous rock of the Keku Volcanics is probably Cretaceous (Mortenson, pers. comm. 2004) rather than Triassic in age. First, all of the geologic relationships on Cornwallis Peninsula with the previously mapped Keku Volcanics are suspect; this includes most of the contacts on the Peninsula. Second, as mineral deposits associated with the Keku Volcanics are common, reinterpretation of their formation and reassessment of their locations are possible. Finally, if it is Cretaceous in age, than this unit represents a previously unknown Cretaceous magmatic province, the presence of which alters many of the Triassic and Cretaceous tectonic interpretations for the Alexander terrane. The Puppets Formation on Gravina Island appears similar to the Keku Volcanics (Berg, 1973; Berg *et al.*, 1978; Gehrels *et al.*, 1987), but zircons from rhyolite of the Puppets Formation had an overall age of 225 Ma (± 3 at 95%) (Gehrels *et al.*, 1987). A small outcrop of felsic volcanic rock (**Appendix 2, site 102**) and additional reports of felsic tuff (Karl *et al.*, 1999) on Kupreanof Island may indicate correlative

units, though the stratigraphic context of these recent discoveries is not well understood. Overall, the ages of these units and their outcrop extent need close examination.

In regards to paleontologic sampling, even the known sites have many undiscovered fossils. Because microfossils are retrieved after fieldwork, gaps in the data due to unproductive or poorly productive samples are common. Thus, new sampling can fill in these gaps or improve individual sample information. Macrofossils suffer some of the same sample problems as microfossils. Collecting macrofossils requires a lot of time in the field, especially if a relatively complete data set is desired. Since enough time is rarely available to examine every site completely, many gaps in the data exist for macrofossils as well. For example, on the third trip to the Flounder Cove locality (Figure 6b, site 99), we still found previously undescribed and/or unreported fossils. Additionally, macrofossil deposits are sporadic due to variable preservation. Thus, finding more macrofossil sites and previously undiscovered biofacies requires more field work than microfossils. Overall, fossil information can improve our understanding of where boundaries might be located, the extent of deposition for a given time period, as well as yield insight on facies relationships and geologic contacts. Since a Carnian-Norian boundary is tentatively identified by this project, there are likely more in the field area that can help our understanding of this time interval. Finally, biostratigraphic and paleogeographic data sets both require relatively complete and sufficiently large data sets to be fully effective.

Updated stratigraphic data from the area would also improve correlations within the entire region. Specifically, the Triassic stratigraphy includes both sedimentary and volcanic units, and metamorphosed equivalents exist east of Keku Strait. Very few measured sections exist, but an increased number would permit comparisons that are more reliable. Since the stratigraphic sections available in terranes are often small, the measurements must be more detailed. The units most in need are the clastic rocks formerly included in the Keku Volcanics and the rocks of the Hound Island Volcanics. Reports of clastic units inland on Kuiu Island (R. Blodgett and A. Caruthers, pers. comm. 2003) and the association of these clastic units with the Cornwallis Limestone suggests that many more clastic sedimentary deposits lie inland on Cornwallis Peninsula. The possible presence of these clastic units and their relation to the Cornwallis Limestone

needs examination in order to understand more clearly the facies relationships and whether they should be combined into one geologic unit. Because these clastic units contain eroded clasts from older rock, they also contribute to the geologic history. Specifically, they reveal the spatial and temporal extent of exposure of Paleozoic units during Triassic time. They also contribute to our understanding of sedimentology in ancient island arc systems.

The potential for volcanic and sedimentologic studies is also present in the Hound Island Volcanics. The variety of volcanic, volcanoclastic, and lithoclastic units in this unit has led to an incomplete understanding of their stratigraphy. Collaboration between sedimentology, volcanology, and paleontology is necessary to gain a complete stratigraphic understanding of this unit. The many different lithofacies also presents potential for understanding their deposition in ancient island arc environments.

The metamorphosed equivalents of the Hyd Group east of Keku Strait also deserve attention. While some of this metamorphic rock has been identified on Kupreanof Island, it is likely that more unidentified Triassic units also exist due to the sparse mapping of interior Kupreanof Island. Some of these units are not heavily metamorphosed, permitting stratigraphic studies. Besides understanding the relationship between the Hyd Group in Keku Strait and its metamorphosed equivalents to the east, these units contribute information on the full depositional extent of the Hyd Group. This is important for tectonic interpretations. The discovery of Triassic outcrop east of central Kupreanof Island necessitated revision of tectonic interpretations based on the eastern edge of Triassic deposition (Karl *et al.*, 1999).

Finally, there have been no published attempts to understand fully the structural geology in the Keku Strait area since Muffler (1967). Additional data since Muffler's (1967) work have tremendous impact on these interpretations. For example, if the felsic volcanic rock in the Keku Volcanics is Cretaceous instead of Triassic, this reinterpretation greatly alters many of the past structural and tectonic interpretations. Structural interpretations directly affect tectonic interpretations, so they are also important in the regional history. The abundance of Triassic exposure facilitates study of post-Triassic structure and tectonic events. Structural data is present in the sedimentary, volcanic, and metamorphic units while the diagenetic features in Keku Strait and

metamorphism east of Keku Strait are probably due to relatively unstudied intrusive events. Renewed mapping and improved stratigraphy have considerable potential to remedy these deficiencies in the geologic understanding.

Plate 1

Late Devonian and Early Permian conodonts reworked into Hyd Group units. All figures are scanning electron micrographs at x82 magnification except Figure 12. Illustrated specimens are upper surface views of Pa elements unless otherwise indicated

Figures 1-3. *Belodella triangularis*

1. FU-C2 UMIP# 302712
2. FU-C2 UMIP# 302714
3. FU-C2 UMIP# 302718

Figures 4-5. *Panderodus* sp.

4. FU-C2 UMIP# 302717
5. FU-C2 UMIP# 302713

Figure 6. Pb element

6. FU-C2 UMIP# 302715

Figure 7. *Polygnathus linguiformis*

7. FU-C1 UMIP# 302724

Figures 8-9. *Palmatolepis* sp.

8. FU-C2 UMIP# 302721
9. FU-C2 UMIP# 302720

Figures 10-11. *Polygnathus* sp.

10. FU-C2 UMIP# 302719
11. FU-C1 UMIP# 302723

Figure 12. Pb element

12. x60 FU-C2 UMIP# 302716

Figure 13. *Sweetognathus?* sp.

13. SC-C2 UMIP# 302725

Figures 14-17. *Mesogondolella* sp.

14. SC-C2 UMIP# 302726
15. SC-C2 UMIP# 302727
16. SC-C2 UMIP# 302728
17. SC-C2 UMIP# 302729



Plate 2

Late Carnian conodonts from the Hyd Group. All figures are scanning electron micrographs at x82 magnification. Illustrated specimens are upper surface views of Pa elements unless otherwise indicated

Figures 1-8. *Metapolygnathus polygnathiformis* (Hayashi, 1968)

1. PP-C2F2 UMIP# 302675
2. lower view PP-C2F2 UMIP# 302676
3. lateral view PP-C2F2 UMIP# 302677
4. CB2-C3 UMIP# 302711
5. HMNE-C6 UMIP# 302688
6. lateral view PISW-C2L2 UMIP# 302660
7. PISW-C2L2 UMIP# 302665
8. PISW-C2L2 UMIP# 302666

Figures 9-11. juvenile *Metapolygnathus* sp. Hayashi, 1968

9. HMNE-C6 UMIP# 302689
10. HMNE-C15 UMIP# 302696
11. HMNE-C15 UMIP# 302695

Figures 12-13. juvenile *Metapolygnathus nodosus* (Hayashi, 1968)

12. HMNE-C16 UMIP# 302699
13. HMNE-C15 UMIP# 302697

Figures 14-17. *Metapolygnathus carpathicus* (Mock, 1969)

14. PP-C2F2 UMIP# 302679
15. lower view PP-C2F2 UMIP# 302680
16. HMNE-C3 UMIP# 302686
17. lateral view PP-C2F2 UMIP# 302678

Figures 18. *Metapolygnathus* sp. cf. *M. reversus* (Mosher, 1973)

18. PISW-C2L2 UMIP# 302671

Figures 19-25. *Metapolygnathus nodosus* (Hayashi, 1968)

19. HMNE-C6 UMIP# 302691
20. HMNE-C6 UMIP# 302690
21. lateral view HMNE-C1 UMIP# 302685
22. lower view HMNE-C1 UMIP# 302684
23. lateral view PISW-C2L2 UMIP# 302667
24. HMNE-C1 UMIP# 302682
25. HMNE-C1 UMIP# 302683

Figures 26-29. *Metapolygnathus* sp. aff. *M. zoeae* Orchard, 1991b

- 26. HMNE-C3 UMIP# 302687
- 27. HMNE-C1 UMIP# 302681
- 28. HMNE-C15 UMIP# 302693
- 29. HMSE-C2 UMIP# 302708

Figures 30-33. *Metapolygnathus* sp. aff. *M. nodosus* (Hayashi, 1968)

- 30. CB2-C2 UMIP# 302709
- 31. lower view HMSE-C2 UMIP# 302706
- 32. HMSE-C1 UMIP# 302703
- 33. lateral view HMSE-C2 UMIP# 302707

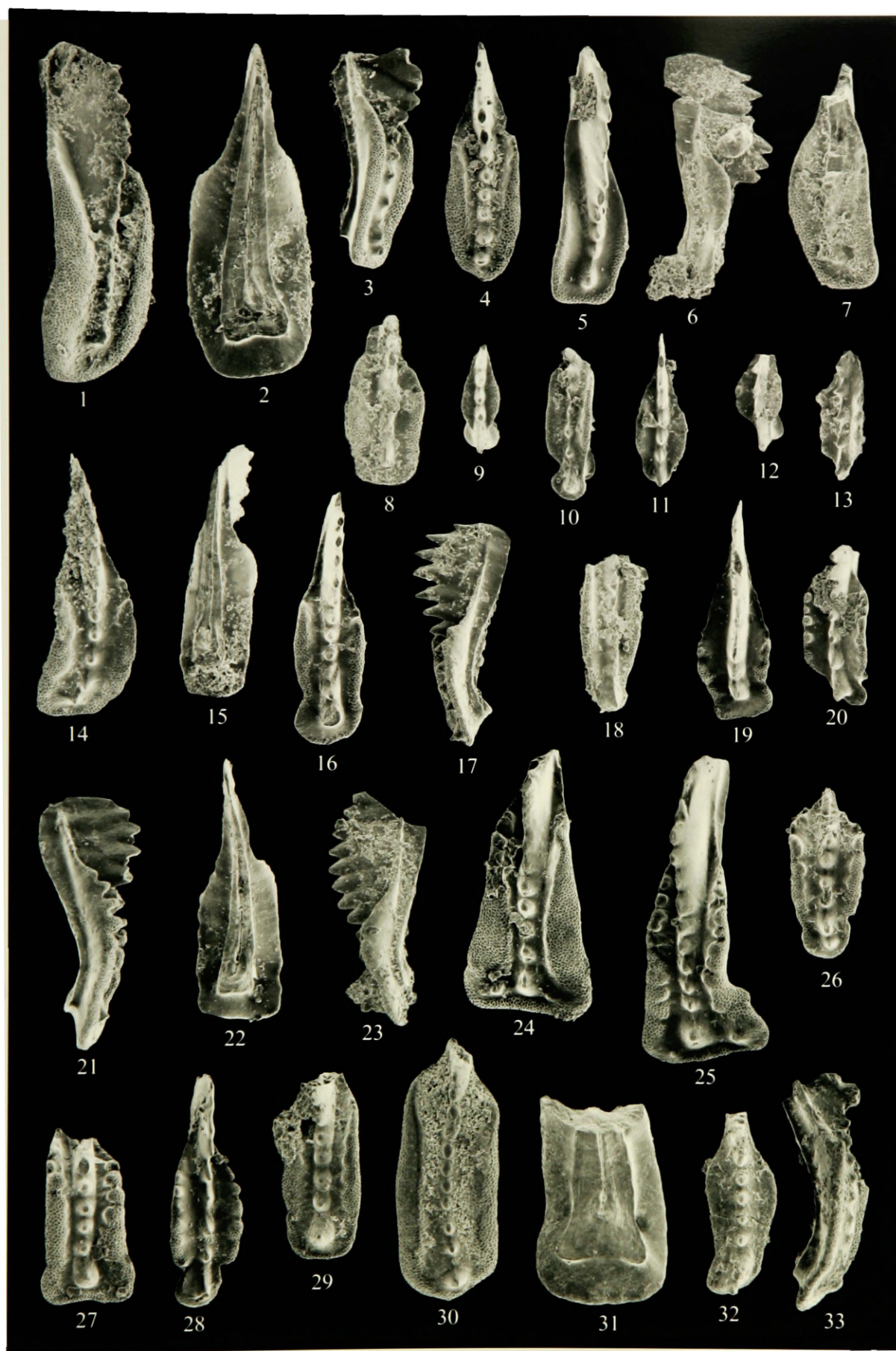


Plate 3

Late Carnian through Early Norian conodonts from the Hyd Group. All figures are scanning electron micrographs at x82 magnification. Illustrated specimens are upper surface views of Pa elements unless otherwise indicated

Figures 1-5. *Metapolygnathus* sp. cf. *M. primitius* (Mosher, 1970)

1. FL-C3 UMIP# 302652
2. FC2-C2 UMIP# 302655
3. lateral view FC2-C2 UMIP# 302659
4. FC2-C2 UMIP# 302656
5. FC2-C2 UMIP# 302658

Figures 6-11, 13-18. *Metapolygnathus primitius* (Mosher, 1970)

6. lateral view FL-C6 UMIP# 302615
7. lower view CPE-F2 UMIP# 302648
8. FL-C6 UMIP# 302617
9. CPE-C2 UMIP# 302613
10. CPE-F2 UMIP# 302645
11. lower view CPE-C2 UMIP# 302612
13. (Early Norian) FL-C6 UMIP# 302614
14. lateral view CPE-F2 UMIP# 302649
15. subadult CPE-C2 UMIP# 302604
16. CPE-C5 UMIP# 302638
17. CPE-C3 UMIP# 302641
18. CPE-F2 UMIP# 302642

Figure 12. *Neogondolella* sp. Bender and Stoppel, 1965

12. CP-C2 UMIP# 302650

Figures 19-23. *Epigondolella quadrata* Orchard, 1991b

19. SWK-2 UMIP# 302599
20. FL-C17 UMIP# 302631
21. HIW-C2 UMIP# 302633
22. lateral view CPE-C2 UMIP# 302607
23. lower view FL-C17 UMIP# 302625

Figures 24-25. *Epigondolella* sp. aff. *E. quadrata* Orchard, 1991b

24. FL-C16 UMIP# 302620
25. FL-C17 UMIP# 302622



Plate 4

Early through Middle Norian conodonts from the Hyd Group. All figures are scanning electron micrographs at x82 magnification. Illustrated specimens are upper surface views of Pa elements unless otherwise indicated

Figures 1-3. *Epigondolella* sp. aff. *E. quadrata* Orchard, 1991b

1. CPE-C2 UMIP# 302606
2. FL-C17 UMIP# 302627
3. lateral view FL-C17 UMIP# 302630

Figures 4-7, 10-12. *Epigondolella triangularis uniformis* Orchard, 1991b

4. CPE-C2 UMIP# 302609
5. HIW-C2 UMIP# 302634
6. lower view FL-C17 UMIP# 302628
7. lower view CPE-C2 UMIP# 302608
10. FL-C16 UMIP# 302621
11. FL-C17 UMIP# 302623
12. FL-C16 UMIP# 302619

Figures 8-9, 15-18. *Epigondolella triangularis triangularis* (Budurov, 1972)

8. FL-C17 UMIP# 302629
9. HIW-C2 UMIP# 302635
15. lateral view GH-C1 UMIP# 302579
16. GH-C1 UMIP# 302572
17. BT-C2 UMIP# 302586
18. GH-C1 UMIP# 302581

Figure 13. juvenile *Epigondolella* sp. Mosher, 1968

13. (*triangularis* Zone) FL-C17 UMIP# 302632

Figure 14. *Misikella longidentata* Kozur and Mock, 1974

14. FL-C17 UMIP# 302636

Figures 19-20. *Epigondolella* sp. aff. *E. transitia* Orchard, 1991b

19. GH-C1 UMIP# 302573
20. lower view GH-C1 UMIP# 302574

Figures 21-23. *Epigondolella* sp. aff. *E. spatulata* (Hayashi, 1968)

21. GH-C1 UMIP# 302571
22. GH-C1 UMIP# 302575
23. lateral view GH-C1 UMIP# 302583

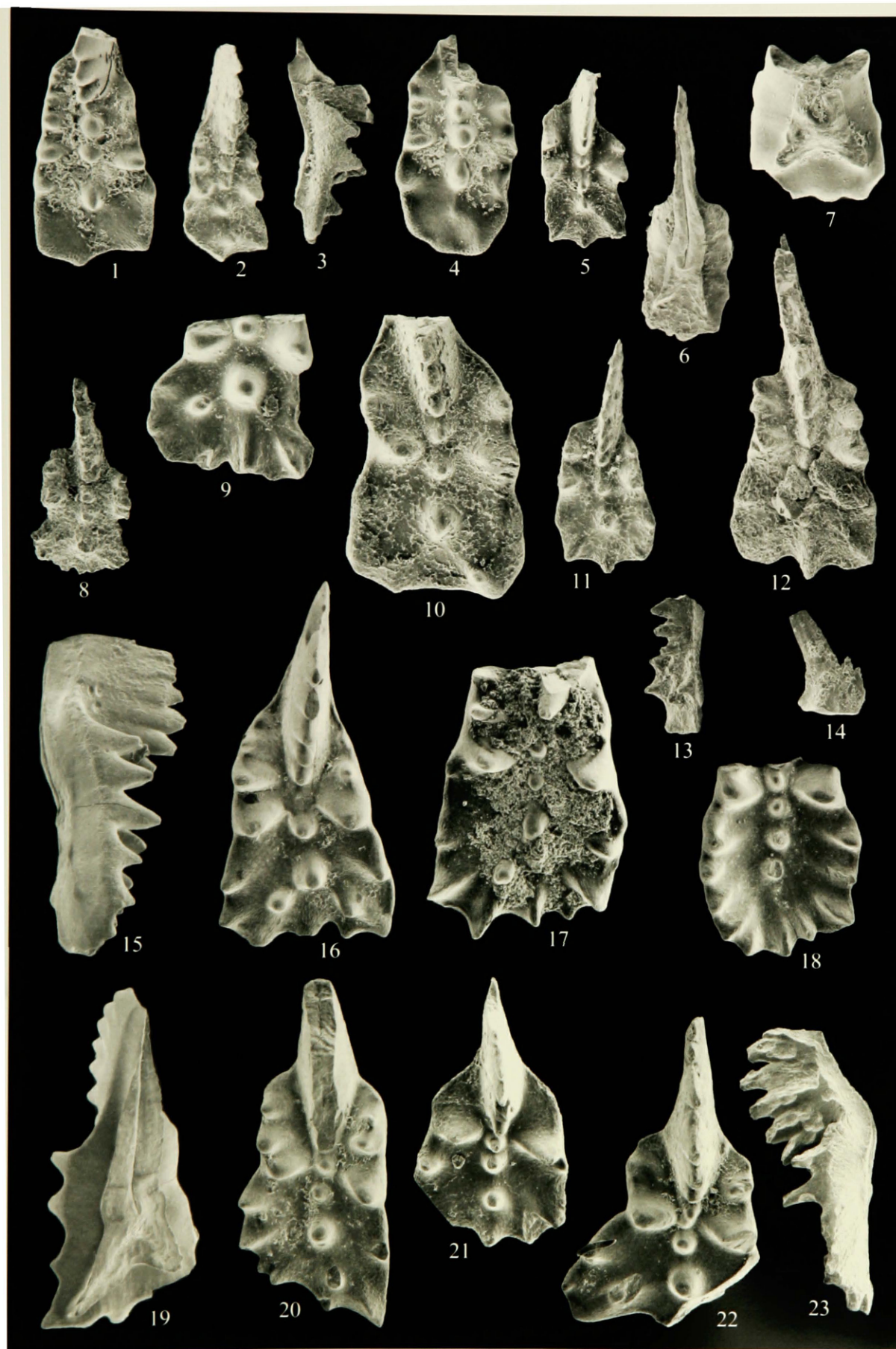


Plate 5

Middle through Late Norian conodonts from the Hyd Group. All figures are scanning electron micrographs at x82 magnification. Illustrated specimens are upper surface views of Pa elements unless otherwise indicated

Figures 1-7 *Epigondolella spiculata* Orchard, 1991b

1. lateral view GH-C1 UMIP# 302582
2. GH-C1 UMIP# 302578
3. lower view GH-C1 UMIP# 302576
4. BT-C2 UMIP# 302587
5. GH-C2 UMIP# 302570
6. GH-C1 UMIP# 302580
7. HL-C6 UMIP# 302588

Figure 8. subadult *Epigondolella* sp. Mosher, 1968

8. (*spiculata* Zone) GH-C1 UMIP# 302585

Figure 9. *Epigondolella* sp. aff. *E. matthewi* Orchard, 1991b

9. GH-C1 UMIP# 302577

Figure 10. *Epigondolella* sp. cf. *E. postera* Kozur and Mostler, 1971

10. HIE-C3 UMIP# 302596

Figures 11. *Neogondolella* sp. cf. *N. steinbergensis* (Mosher, 1968)

11. HIE-C2 UMIP# 302592

Figures 12-13, 15. *Neogondolella* sp. Bender and Stoppel, 1965

12. HL-C6 UMIP# 302589
13. HIE-C3 UMIP# 302595
15. lower view HL-C1 UMIP# 302591

Figure 14. juvenile *Neogondolella* sp. Bender and Stoppel, 1965

14. (Middle Norian) lateral view HIE-C2 UMIP# 302593

Figures 16-18. *Epigondolella bidentata* Mosher, 1968

16. GH-C6 UMIP# 302557
17. lower view GH-C6 UMIP# 302555
18. GH-C6 UMIP# 302556

Figures 19-20, 27-30. *Epigondolella tozeri* Orchard, 1991b

19. GH-C6 UMIP# 302552
20. GH-C6 UMIP# 302553
27. GH-C6 UMIP# 302554
28. =GH6 UMIP# 302565

29. lower view =GH6 UMIP# 302566

30. lateral view =GH6 UMIP# 302567

Figures 21-26. *Epigondolella englandi* Orchard, 1991b

21. =GH6 UMIP# 302564

22. lateral view =GH6 UMIP# 302568

23. lower view =GH6 UMIP# 302569

24. lateral view GH-C6 UMIP# 302558

25. GH-C6 UMIP# 302560

26. =GH6 UMIP# 302563

Figures 31-33. *Epigondolella* sp. aff. *E. mosheri* Kozur and Mostler, 1971

31. GH-C6 UMIP# 302551

32. lateral view GH-C6 UMIP# 302561

33. GH-C6 UMIP# 302562

Figure 34. juvenile Late Norian *Epigondolella* sp. Mosher, 1968

34. GH-C6 UMIP# 302559

